Experimental Study for the Improvement of Vision Through Side Window of a Car During Rain

Dissertation

Submitted for the requirement of course of

Master of Engineering

in

CAD/CAM Engineering

Submitted by:

Mukesh Verma

Regn. No. 801281014

Under the supervision

of

Mr. Devender Kumar

Assistant Professor, MED

MECHANICAL ENGINEERING DEPARTMENT

THAPAR UNIVERSITY, PATIALA-147004, PUNJAB

December, 2014

(Established under the section 3 of UGC Act, 1956)

Certificate

This is to certify that the dissertation entitled **"Experimental Study for the Improvement of Vision Through Side Window of a Car During Rain"**, is an authentic record of my own work carried out as requirements for the award of degree of Master of Engineering in CAD/CAM from Thapar University, Patiala, under the guidance of Mr. Devender Kumar (Assistant Professor, Mechanical Engineering Department).

18/12/14

Date: 18/12/14

(Mukesh Verma)
(Regn. No: 801281014)

It is certified that the above statement made by the student is correct to the best of our knowledge and belief.

18/12/14

(Mr. Devender Kumar)
Assistant Professor
Department of Mechanical Engineering

Countersigned by:

(Dr. S. K. Mohapatra)
Sr. Professor & Head
Department of Mechanical Engineering

(Dr. S. S. Bhatia)
Prof. & Dean of Academic Affairs
Thapar University, Patiala

Acknowledgement

I am highly grateful to the authorities of Thapar University, Patiala for providing this opportunity to carry out the thesis work.

I would like to express a deep sense of gratitude and thank profusely to my thesis guide **Mr. Devender Kumar** for their sincere & invaluable guidance and suggestions which inspired me to submit thesis report in the present form. I am highly thankful to **Dr. S. K. Mohapatra**, H.O.D. Mechanical Engineering Department for his invaluable guidance & permission to carry out work in his department.

18/12/14

(Mukesh Verma)

Abstract

Road visibility in passenger vehicle is of major concern for the car manufacturers and safety design engineers. Water film (fog) that forms on the windshield during winter times would reduce and disturb the driver's visibility. Extreme weather conditions can make a difference while driving. One may experience the wide range of challenges during driving. The factors which mostly affect the visibility can be rain, fog, ice, snow, dust etc. Due to such factors, it becomes very tough for the driver to have a clear view of both sides of the vehicle. Rear view is possible with the help of left and right rear view mirrors fitted outside the front doors. Visibility of rear view mirror depends upon the visibility of the front side window glasses. Driving through rain, produces more challenging situation when water droplets on outside surface of side window glass obstruct the vision through rear view mirrors as well as the left and right side vision at cross roads. This problem becomes more dangerous when light gets scattered through water droplets and obstruct the vision during rainy night.

The main objective of this work is to find the possible solution for removing the rain water droplets and fog from a specific area of side window to have a clear view of the side view mirror to avoid the accidents. In the present work, compressed air utilised as a working fluid to impinge on the side glasses with the help of converging nozzles. The various combinations of nozzle design, air velocity and impinging angle are studied for obtaining maximum clearing area. Computer simulated results are verified with the help of experimental results.

Contents

List of Tables

List of Figures

Chapter 1 Introduction

Visibility in the automotive industry is a major source of concern for the car manufacturers and safety design engineers. Water film (fog) that forms on the windshield during winter times would reduce and disturb the driver's visibility. Extreme weather conditions can make a difference while driving. One may experience the wide range of challenges during driving. The factors which mostly affect the visibility can be rain, fog, ice, snow, dust etc. Due to such factors, it becomes very tough for the driver to have a view of rare of side of the vehicle. This is because to have a view of the rare side use of side view mirror is must which can be seen only through the side windows of the driver becomes difficult for the driver which causes accidents.

Fig. 1.1: Side Window Glass

1.1. Background and Motivation

Rain reduces driver perception in several ways and is especially debilitating at night. It both directly affects perception but also produces visibility changes through its action on headlamps, windshields, the road itself and road markings. We normally see an object when light from a source, the sun, streetlamps, our headlights, reflects from the object back to the eye. Rain affects ability to see through the car windshield. Rain also affects visibility by changing the amount of light reflected from the road back to the driver's eye. Rain water acts

like a lens which disperses the lights, so that much of it is reflected in different directions which greatly affect the visibility.

Fig. 1.2: Visibility Through Windshield During Rain

Fog also affects the visibility to a greater extent. Fog promotes accidents by means of "aerial perspective," a visual effect which causes people to misjudge distance. People automatically perceive objects which are low contrast and indistinct as being farther away. Fog produces accidents because a driver cannot see as far ahead. Fog affects perceptual judgments of speed and distance.

Fig. 1.3 : Visibility Through Windshield During Fog

So, the main objective of this work is to find the solution for removing the rain water droplets and fog from the side window to have a clear view of the side view mirror to avoid the

mishappenings with the help of an air nozzle which will which will impinge the air with certain velocity on the side view mirror to remove the rain water droplets and fog. Before going ahead let us discuss some defogging techniques.

1.2. Formation of Fog

Fog is a thick cloud of tiny water droplets suspended in the atmosphere at or near the earth's surface which obscures or restricts visibility. Fog is actually water droplets that have condensed from the air. The same as clouds. When air has been warm and humid during the day, evaporated water molecules are spread throughout it. Then, when the temperature drops, the cooling air causes the water molecules to turn from a vapour (a gas) into liquid droplets. These droplets are so small they can hang in the air. But they are heavy enough to lie low near the ground.

Fogging on the windshield occurs when the glass temperature falls below the dew point of air. This can take place either due to the rise of humidity in the passenger compartment, which increases the dew point, or due to fall of windshield glass temperature. The following are some of the common fogging scenarios found in a vehicle:

- Fogging that occurs below the start of engine due to trapped moisture in the passenger compartment and external temperature drop.
- Flash fogging at the start of the engine due to pre-existing evaporator condensate from AC operation.
- Fogging that occurs after engine start due to excess moisture introduction by the passengers who have just showered, got rained on, stepped through snow, etc.
- Sudden windshield temperature drop using driving, such as caused by a heavy rainfall during warm day.
- Fogging due to steady vapour stream generation by passengers of the vehicles during driving in cold ambient conditions.
- Highly humid tropical conditions with air saturated at 100% humidity.

With the increased use of air recirculation, fogging is becoming more of a concern. Air recirculation prevents the discharging of moisture out of the passenger compartment and accentuates fogging through the accumulation of moisture from various sources such as perspiration, respiration, wet clothing, melting of deposited snow on floor mats, etc.

1.3. General View about Installing Defog Techniques

Vehicle fogging is a recognised safety concern. The presence of fog on the windshield glass reduces or blocks the field of vision for the driver. It can be dangerous to drive a vehicle with fogged up side view mirrors and/or side windows because the driver has an obstructed view of the traffic and can accidentally drove his/her vehicle in a manner to cause an accident. Therefore it would be a benefit to have a system that would provide a defrosting mechanism in the form of an air stream directed against the side view mirror of the vehicle as well as an air stream directed against the side window of the vehicle adjacent to the side view mirror. As different weather conditions can require different defogging air streams to achieve a maximum defogging effect. It would be further desirable to have a side view mirror and side window defogger system for vehicles that further included one or more adjustment mechanisms to allow the user to optimise the defogging air streams directed towards the side view mirror and the side window.

In today's competitive world once new technique is being installed by one automobile company then the other companies will also try to implement the same idea with some improvement to raise their sale. That is why this system needs to be risen up to improve the features of the vehicle.

Improving the defogging techniques in vehicles will increase the work for the Research and Development department which will raise the scope in the same department.

1.4. Driving Problems Due to Scattering of Light

Driving at night can be a dangerous task for new or even experienced drivers. The highest crash rates occur at night time and traffic rates are three to four times higher at night than during the daytime. The danger arises from the fact that vision is severely limited and glare from the headlights of other vehicles can temporarily blind you due to the additional effect of fog and water droplets at night. Fog distorts what you can see by making it difficult to assess speed and distance. When we view through a window or a windshield, usually the image consist of two linear superposition of images, a real image of the scene beyond the window observed through a glass and a virtual image of the scene reflected by the window on it. In

such cases reflected image cause many problem. This arise a problem for the driver to detect the original view and causes the accidents.

Fig. 1.4 : Visibility Through Windshield During Night

1.5. Problem Due to Water Droplets

Water droplets on windshields of vehicles can degrade the performance of the vehicle. When driving in light or moderate rainy conditions, raindrops appear as small circlets on the windshield. This is why the water droplets removal has become a challenging task as it maximises the risk of accidents. Since most weather-related accidents arise due to rainy weather conditions, reliable assistance in such situations is desirable.

Fig. 1.5 : Water droplet on windshield

1.6. Fluid Nozzles

Air nozzles are used for dispersing air or steam in a concentrated and straight fan. Some recent designs have resulted in air nozzles that can operate over a wide range of operating pressure. Generally, air nozzles have a flat fan or solid stream spray pattern. When using conventional air nozzles, air is blown through a single hole.

1.6.1 Type of Nozzles

- **Hollow Cone Nozzle**

The hollow cone nozzle spray pattern is essentially a circular ring of liquid. This pattern is generally formed by use of an inlet tangential to a whirl chamber or by an internal grooved vane immediately upstream from the orifice. The whirling liquid result in a hollow cone configuration as it leaves the orifice. Standard hollow cone nozzles feature a large and unobstructed flow passage which minimizes or eliminates clogging. Spiral nozzles produce a hollow cone spray pattern with spray angles ranging from 50^{o} to 180^{o}.

Fig. 1.6 : Hollow Cone Nozzle

- **Full Cone Nozzle**

Full cone nozzles have a spray pattern that is round, square or oval. The spray pattern is completely filled with drops. Using an internal vane, which imparts controlled turbulence to the liquid prior to the orifice, forms this pattern. Standard full cone nozzles produce a round cone-shaped spray pattern completely filled with drops. Using an internal vane this pattern

can be formed. Spiral nozzles have a round surface which produces a cone shaped spray and allows maximum liquid throughput.

Fig. 1.7 : Full Cone Nozzle

- **Flat Spray Nozzle**

A flat spray nozzle pattern distributes the liquid as a flat fan or sheet type of spray. In the elliptical orifice design, the axis of the spray pattern is a continuation of the axis of the inlet pipe connection. In the deflector design, the deflection surface diverts the spray pattern away from the axis of the inlet pipe connection. The tapering edges of the flat spray nozzles are useful in establishing overlapping patterns between adjacent sprays on a multiple nozzle header. The resulting distribution across the entire sprayed surface can therefore be uniform. Standard flat spray nozzles feature an elliptical orifice design with the axis of the spray pattern as a continuation of the axis of the inlet pipe connection. Deflector flat spray nozzles divert the spray pattern away from the axis of the inlet pipe connection.

Fig. 1.8 : Flat Spray Nozzle

- **Fine Spray Nozzle**

These low capacity nozzles are available in standard, wide angle and narrow angle, and produce very small drops. Air friction and current affect the full cone and hollow cone spray patterns. Several feet from the nozzle, depending on pressure and nozzle capacity, the fine spray pattern disappears as the drops become suspended in air, they have uniform distribution, which often allows them to achieve misting performance. Fine spray nozzles can be used for evaporating cooling, moistening and humidifying. The standard fine spray nozzle use liquid pressure alone to produce very fine atomized drop. These spray tips have a core body and orifice insert and are applicable with the unijet nozzle system. The wide angle fine spray nozzle use liquid pressure alone to produce very finely atomised drops in a hollow cone spray pattern. The narrow angle fine spray nozzle throw a fogging spray of small sized drops and produce a dense full cone pattern with large flow rates.

Fig. 1.9 : Fine Spray Nozzle

- **Solid Stream Nozzle**

A solid stream spray nozzle pattern is a uniform stream of liquid. By using proper inlet chamber proportions and contours ahead of the orifice or by the addition of internal flow stabilising vanes, these nozzles provide prolonged solid stream integrity and delay breakup and drop formation after leaving the nozzle orifice. Solid stream spray nozzles provide a high impact at lower pressures.

Fig. 1.10 : Solid Stream Nozzle

1.7 Organisation of Thesis

Five chapters are included in this Thesis. Overview of the information included in the various chapters is as follows:

First chapter includes the introduction part which includes the problems during driving in rain, fog and during light, nozzles and their patterns.

Literature review related to the various developments till now for defogging and removing of rain water droplets from the windshield of the vehicle. Literature summary and problem formulation is also included in this second chapter.

Third chapter includes the Velocity Distribution of the different shapes of the nozzles with different parameters to obtain the best possible nozzle for the experiments.

Fourth chapter includes the experimental set up consists of an arrangement made of wood on which side window glass of the vehicle is mounted which is equivalent to the side window of the car to perform the experiment.

Results obtained after the experiments are discussed in the fifth chapter. It includes the best possible results of the finalised nozzle.

Conclusion and future scope is presented in sixth chapter.

Alphonse J. Vandale [1] ***et. al.*** proposed the exterior side view mirror and side window defogger system which is subjected to many different variations in structure, design, application and methodology.

A defrosting mechanism is made in which an air stream is directed against the side view mirror of the vehicle as well as against the side window of the vehicle adjacent to the side view mirror. This defogger system also includes one or more adjustment mechanisms to allow the user to optimise the defogging air streams directed towards the side view mirror and the side window.

The defogger system is provided to a exterior side view mirror and side window defogger system which also includes a side view mirror assembly and a mirror air supply ducting system. The side view mirror assembly is attached to a vehicle door assembly. It also includes a mirror housing portion that defines a mirror receiving cavity with in which a mirror is adjustably mounted. An air cavity is created between a back surface of the mirror and the interior surface of the mirror housing portion for defrosting and also the required designing is done. Accordingly, a exterior side view mirror and side window defogger system is provided which include a side view mirror assembly and a mirror air supply ducting system.

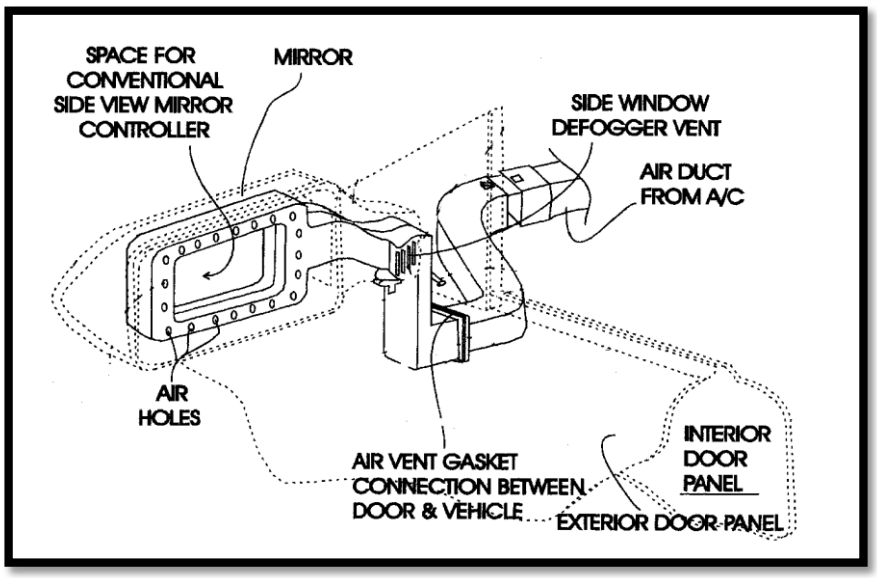

Fig. 2.1 : Side view mirror defogger system

Mingyu Wang [2] ***et. al.*** proposed the system design for the clear vision auto defog system and the improvements made to the Integrate Dew Point and Glass Temperature (IDGT) sensors. The present work describes the design considerations of the auto defog system and the general system design **Urbank T. M. [3]** ***et. al.***. Design improvements to the IDGT sensor are reviewed in some detail.

Different sensors were used under different conditions for the proper functioning of the clear vision automatic windshield defogging system **Peters A. R. [4]** ***et. al.***. Through improved design of the IDGT fog sensor and a fundamentally sound auto defog system design, the Clear Vision auto defog system achieved the objective of defogging the windshield when it is fogged and preventing fogging when it is not already fogged. The system performance is satisfactory even under extreme fogging conditions **Cole J. [5]** ***et. al.***.

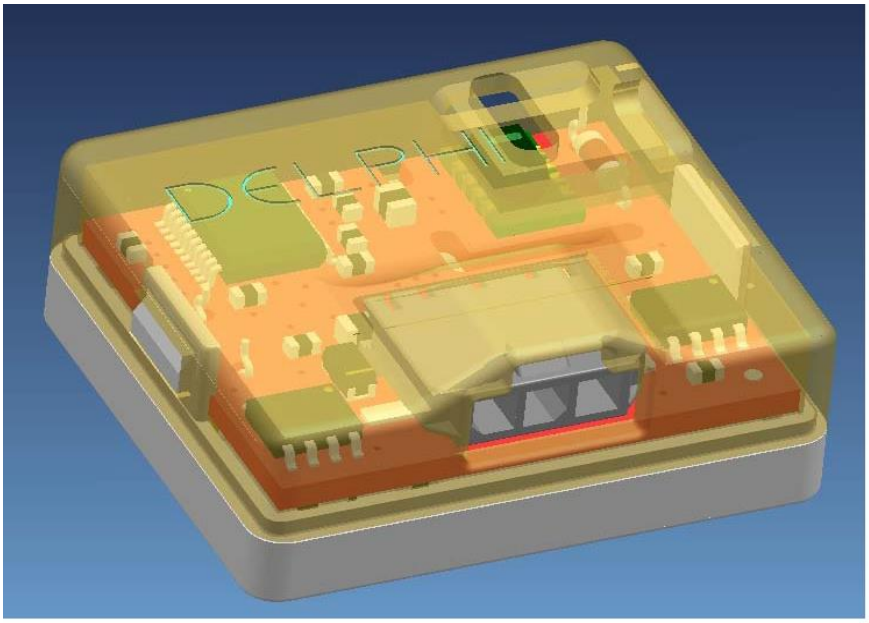

Fig. 2.2 : IGDT Sensor

Bobby J. Jefferson [6] ***et. al.*** proposed the invention which relates to vehicle window defogging and defrosting systems. A vehicle glass clearing system includes an installed portion and an auxiliary heating element system having a control and drive circuit which have mechanisms for detecting the moisture level and the temperature which provides a higher drive current to the heating element when threshold temperature and moisture levels are detected.

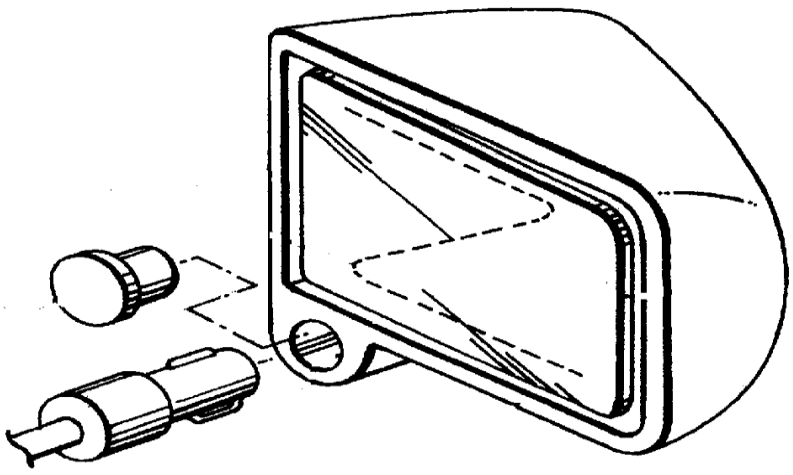

Fig. 2.3 : Power plug of heating element assembly

Leonid Berzin [7] ***et. al.*** proposed a clearing system for external mirrors and side windows of a vehicle. It relates to a system for cleaning and clearing windows and external rear view mirrors of a vehicle and provides conditioned ventilation to the exterior mirrors and windows of a motor vehicle.

It provides a flow of compressed warm air to an air distribution unit equipped with a number of openings to direct the flow of air towards the surface of mirror or a side window. Many ideas were invented according to one of which the air compressor, the air heater and an optional air filter are located in the housing of the external mirror. In other idea a supplemental air distribution unit is provided to be mounted along the door of the vehicle to increase the coverage area of the side window. In another invention the system is made adjustable for allowing the most appropriate angle for the air openings towards the mirror and the side window.

Troy [8] ***et. al.*** relates to an air-conditioning system that is capable of de-icing a side view mirror and side glass. This system is vehicle heating system which employs a vehicle rear view mirror outer case that defines a cavity with in which a mirror resides. A rear view mirror inlet tube may pass through the outer case and the inner case and permit the air to enter the rear view mirror inner case. A rear view mirror outlet tube that passes through the outer case and the inner case may permit air to exit the rear view mirror inner case. An HVAC unit is also attached to the rearview mirror inlet tube to blow air into the rear view mirror outer case or inner case.

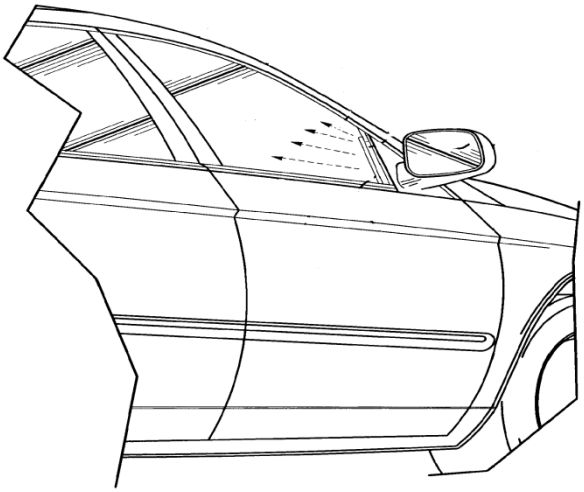

Fig. 2.4 : Exterior view of rear view mirror

Jeong-Hoon Lee [9] ***et. al.*** describes the development and validation of an automatic defogging system control. The auto defog system enhances windshield visibility by decreasing the occurrence of window fogging. This system consists of an auto defog sensor, an independent actuated defrost door flap toward windshield glass and a control head. This system allows drivers to keep their eyes on the road through the clear window and improves the overall comfort for passengers by a moderate humidity level **L. I. Davis [10]** ***et. al.***. It was considered as key technologies to predict misting conditions before mist is visible and to be compatible with overall comfort during auto defogging.

This study defines the unique requirement of auto defog sensor and the fog probability model was presented to define anti-fog actions more accurately. In addition, the auto defog control was developed and validated through the field tests including the worst case – the quick fog situation.

Fig. 2.5 : Auto Defog Sensor

2.1 Literature Summary and Problem Formulation

A very little work was published related to the removal of fog and the water droplets to make the drive easy and comfortable to minimise the risk of accidents. There is lot of work still needed in the previous studies.

Through improved design of the IDGT fog sensor and a fundamentally sound auto defog system design, the Clear Vision auto defog system achieved the objective of defogging the windshield when it is fogged and preventing fogging when it is not already fogged. The improvement in the IDGT sensor through recalibration and digitization ensures that accurate fogging condition is reported to the auto defog algorithm while the auto defog algorithm provides measured and effective response under all conditions. The system performance is satisfactory even under extreme fogging conditions. Certain mechanisms have beed made for detecting the moisture level and the temperature that provides a higher drive current to the heating element when threshold temperature and moisture levels are detected. The unique requirement of auto defog sensor and the fog probability model was presented to define anti-fog actions more accurately. The auto defog control was developed and validated through the field tests including the worst case.

The limitation is the amount of electricity that is consumed by resistance-type electrical heaters to warm specific surfaces that places an electrical burden on an on-board battery and or an on-board alternator. The additional wiring, circuit breakers and associated costs with such necessary components and their installation. The assumption of unique design elements with the on-board air-system of a vehicle and can not be easily adapted to be used for a variety of different vehicles. In some inventions the air flow is often organised. A narrow long passage is present in these devices and the air is emitted there through does not provide for optimal coverage of the surface of the mirror or a side window. Therefore there is a need for a universal system for maximum clearing of the rear view external mirrors and the side windows of a vehicle which is free from the above mentioned drawbacks. The main components of the clearing system should be small enough to be capable of fitting inside the cavity awarded by the external mirror housing. All the systems proposed by various researchers in past was concerned only about the cleaning of rear view mirror but they are not considering the cleaning of the window glass through which a driver can see the rear view mirror. Present day rear view mirror are designed in such a way that the mirror assembly is placed in a plastic crowl which covers the mirror from top and protect it from the vertical

falling droplets. But the side window glass is not vertical. The curved glass is fitted at an angle to match with the aerodynamics body design and style.

Aim of the present study is to clean the water droplets from a area which is necessary to see the rear view mirror and the crossing roads at the corners. From all the possible alternates to perform this operation, the use of compressed air jet is more economical, simple in design, easy to fit in small area and offers no obstruction in normal operation of window glass.

Chapter 3 Modelling and Simulation

3.1 Modelling

Modelling is the representation of a real world object or system in a mathematical framework. It uses software tools to imitate the operation of the real world system over time so that inferences can be drawn about potential future outcomes.

Modelling is an indispensable problem-solving methodology which can be used to describe and analyse the behaviour of a system, to ask what-if questions and to provide information to aid in the design and development of the real system.

The CFD solver Fluent was used to find the velocity distribution of an air jet impinged on the window glass. Fluent software contains the broad physical modelling capabilities needed to predict the impact of every fluid particle on the product. Fluent delivers benefits that include the ability to:

- Quickly prepare product/process geometry for flow Velocity Distribution without tedious rework.
- Avoid duplication through a common data model that is persistently shared across physics beyond basic fluid flow.
- Easily define a series of parametric variations in geometry, mesh, physics and post-processing, enabling automatic new CFD results for that series with a single mouse click.
- Improve product/process quality by increasing the understanding of variability and design sensitivity.
- Easily set up and perform multiphysics simulations.

3.2 Nozzle

Nozzle with different outlet diameter, different inlet diameter, different throat length and different converging section length are modelled to perform the Velocity Distribution to obtain the optimised results for the selection of a nozzle.

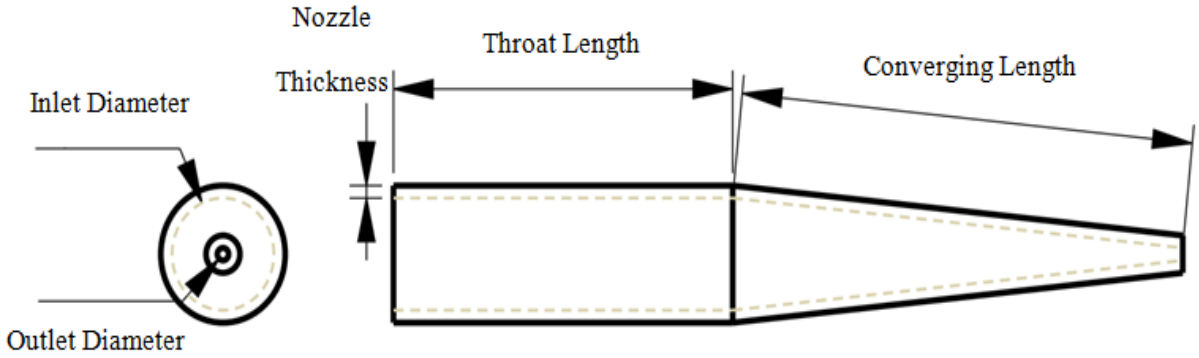

Fig. 3.1 : Labelled Nozzle

3.3 Side Window Glass

Modelling of side window glass is also done at the corner of which nozzles of different parameters are mounted to obtain the results.

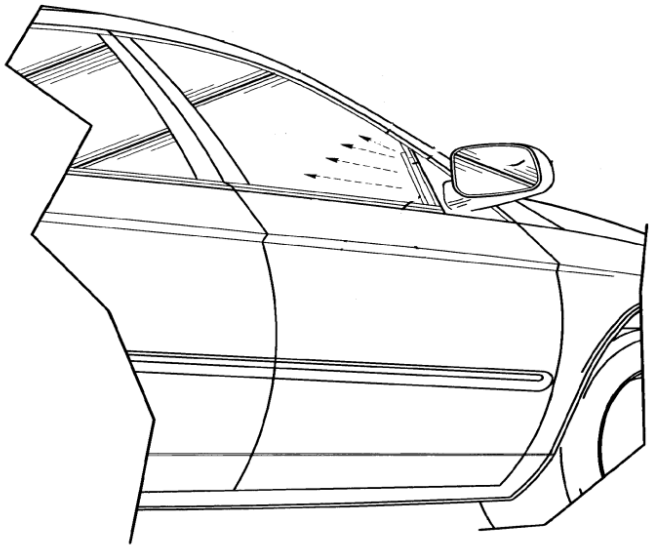

Fig. 3.2 : Side Window Glass [8]

3.4 Boundary Conditions and Velocity Distribution of Set up

Before applying the boundary conditions, the proper area that must be cleared to view the rear view mirror from the side window should be known. The approximate area that should me unspotted is about at the radius of 170 mm if corner of the side window is considered as the centre. Figure 3.3 below clears the view.

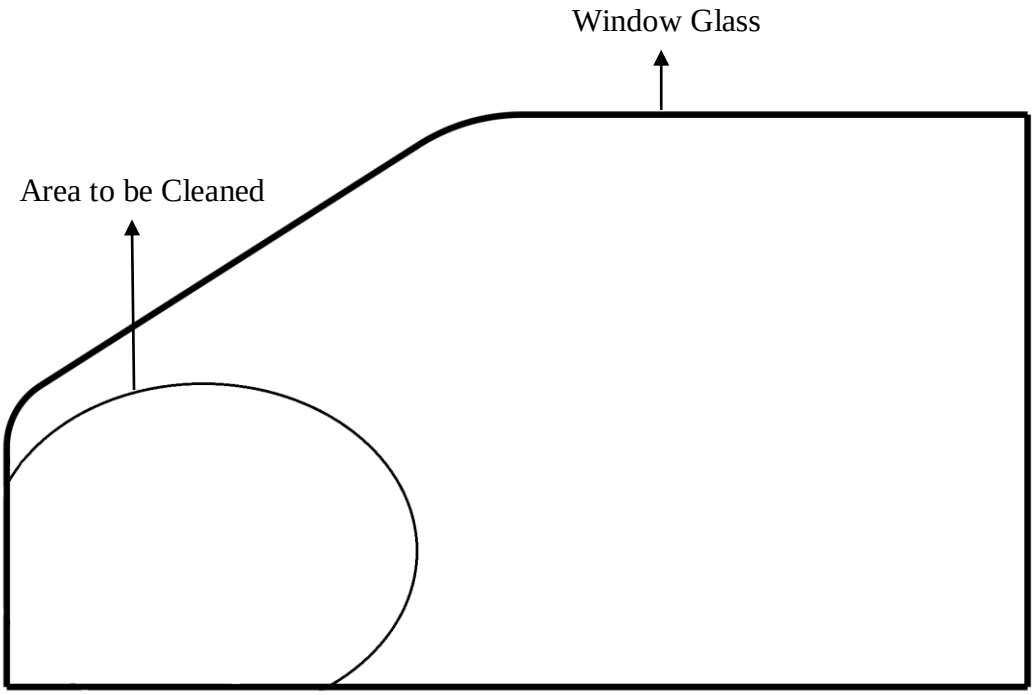

Fig. 3.3 : Area to be kept Unspotted

The velocity that with which the air must be impinged on the window glass that should be known.

Some of the boundary conditions that were applied on the model are:

- The walls are made at no slip condition.
- Atmospheric conditions are applied at the outlet boundaries.
- The temperature of the air released from the nozzle is maintained as 25^{o} C.
- The flow of the air is kept at high intensity.
- The air released from the nozzle is uniformly distributed on the side window glass.

The CFD solver that was used to perform the simulation was Fluent. Fluent is a commercial CFD solver. Fluent software contains the broad physical modelling capabilities needed to predict the impact of every fluid behaviour on the product. Fluent delivers benefits that include the ability to:

- Quickly prepare product/process geometry for flow Velocity Distribution without tedious rework.
- Avoid duplication through a common data model that is persistently shared across physics beyond basic fluid flow.
- Easily define a series of parametric variations in geometry, mesh, physics and post-processing, enabling automatic new CFD results for that series with a single mouse click.
- Improve product/process quality by increasing the understanding of variability and design sensitivity.
- Easily set up and perform multiphysics simulations.

3.5 Velocity Distributions of Single Nozzle

Before going further the concept of impinging angle must be clear which can be explained with the help of figures shown below:

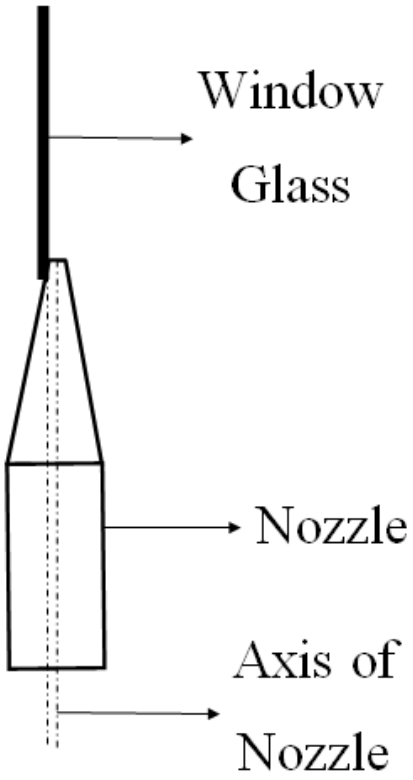

Fig. 3.4 : Nozzle with 0° Impinging Angle

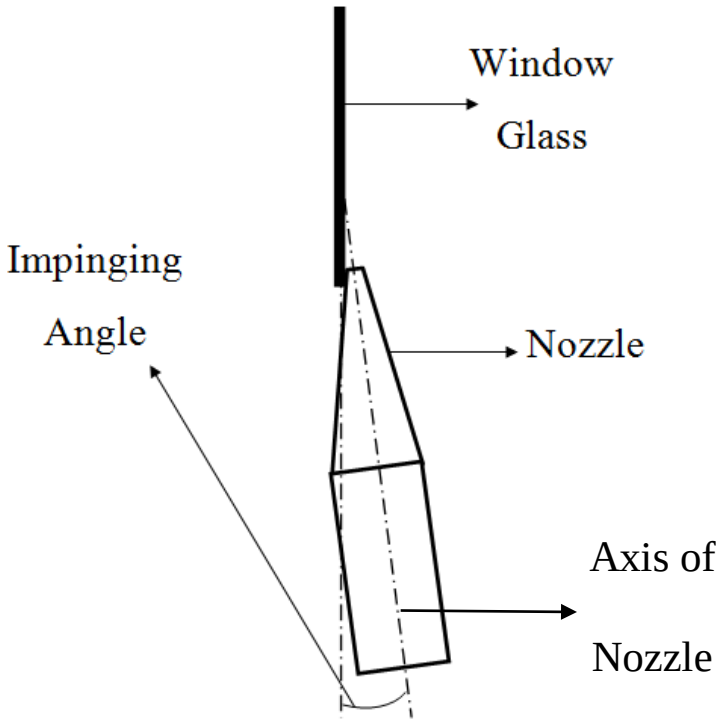

Fig. 3.5 : Nozzle with 5° Impinging Angle

Impinging angle is the angle between the axis of the nozzle and the window glass of the vehicle. It was to be set up in such a way so as to have the proper flow of air from the nozzle so that the maximum area should be cleared of the window glass to have a proper vision on the rear view mirror.

Parameters for the Velocity Distribution:

3.5.1 Varying the impinging angle of the nozzle for outlet diameter of 1 mm:

Table 3.1: Varying the impinging angle for outlet diameter of 1 mm

Experiment No.	Throat Length (mm)	Converging Section Length(mm)	Inlet Diameter (mm)	Outlet Diameter (mm)	Impinging Angle (degree)	Figure No.
1.	40	30	9	1	0	3.6
2.	40	30	9	1	1	3.7
3.	40	30	9	1	3	3.8
4.	40	30	9	1	4	3.9
5.	40	30	9	1	5	3.10

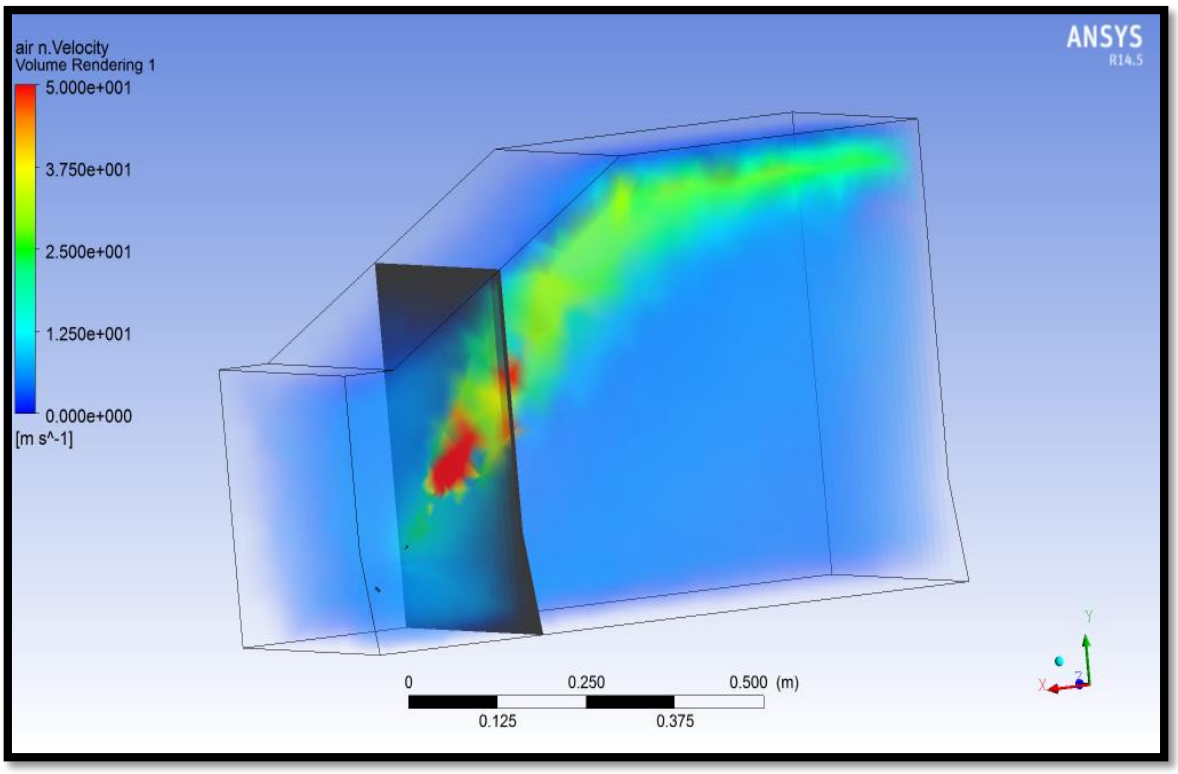

Fig. 3.6 : Velocity Distribution for Impinging Angle = 0^{o} & Outlet Dia. = 1 mm

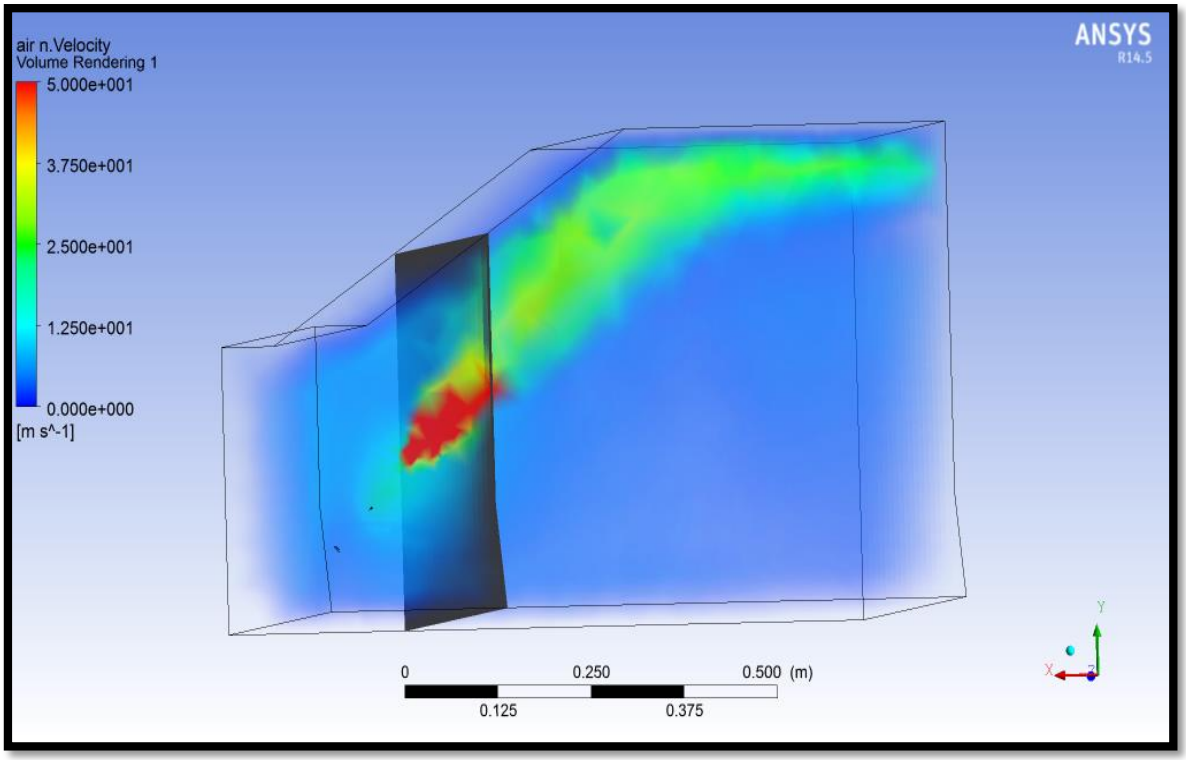

Fig. 3.7 : Velocity Distribution for Impinging Angle = 1^{o} & Outlet Dia. = 1 mm

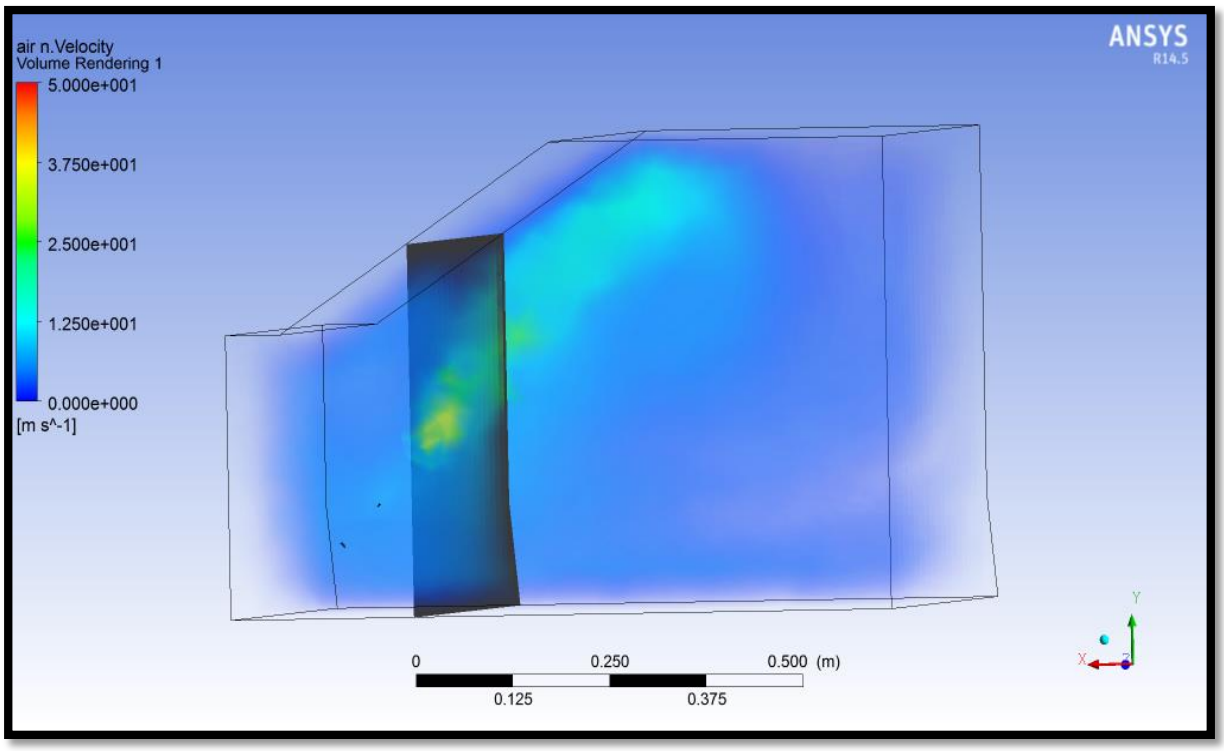

Fig. 3.8 : Velocity Distribution for Impinging Angle = 3° & Outlet Dia. = 1 mm

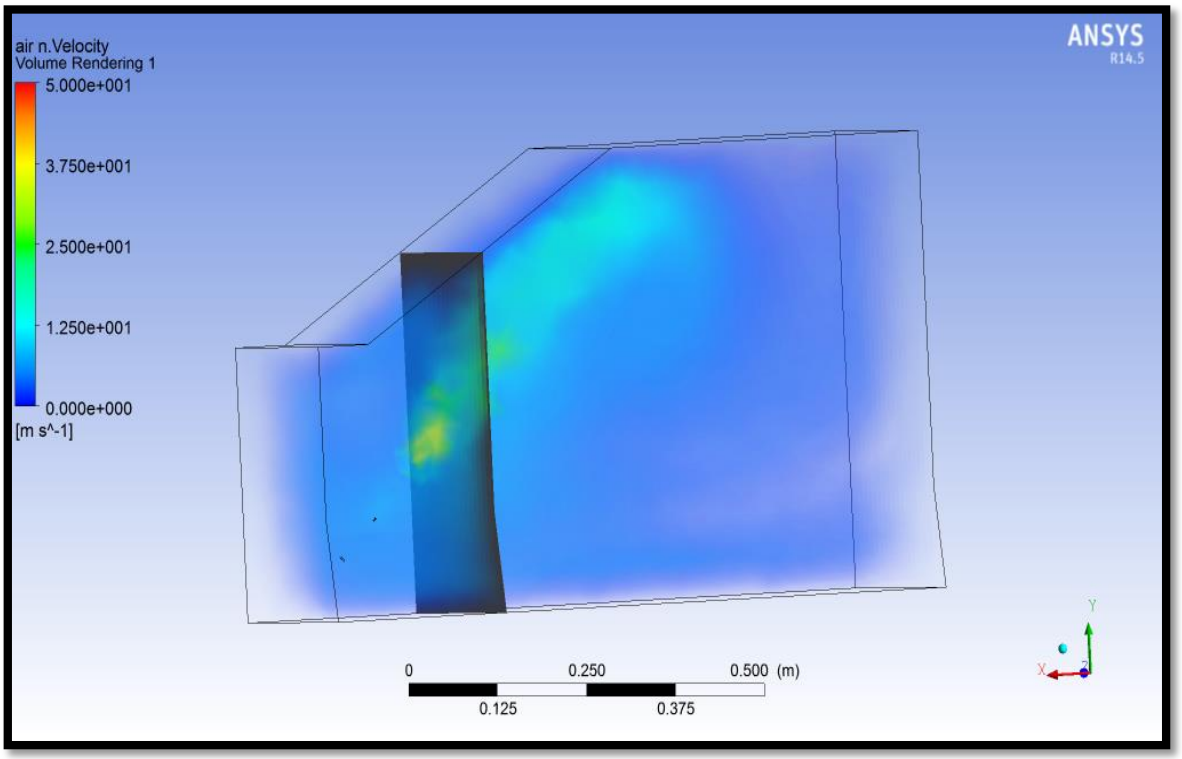

Fig. 3.9 : Velocity Distribution for Impinging Angle = 4° & Outlet Dia. = 1 mm

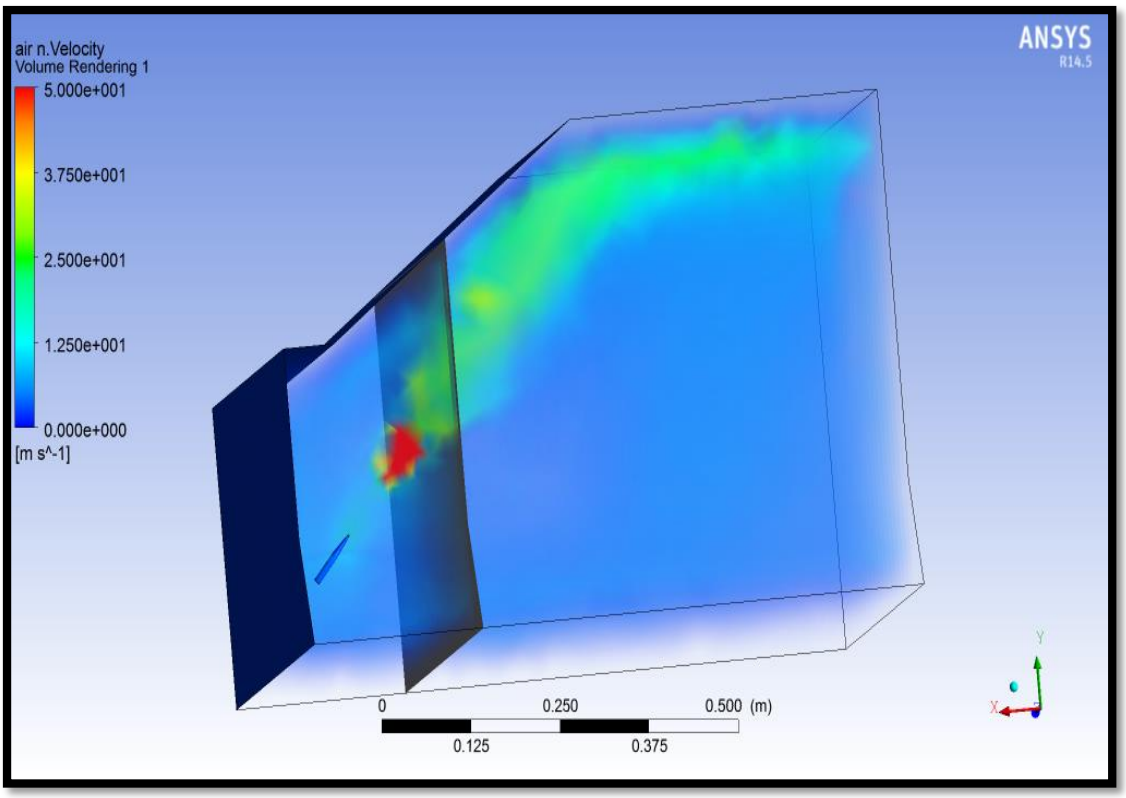

Fig. 3.10 : Velocity Distribution for Impinging Angle = 5^{o} & Outlet Dia. = 1 mm

3.5.2 Velocity Distribution by varying the impinging angle of the nozzle for outlet diameter of 2 mm:

Table 3.2 : Varying the impinging angle for outlet diameter of 2 mm

Experiment No.	Throat Length (mm)	Converging Section Length(mm)	Inlet Diameter (mm)	Outlet Diameter (mm)	Impinging Angle (degree)	Figure No.
1.	40	30	9	2	0	3.11
2.	40	30	9	2	2	3.12
3.	40	30	9	2	3	3.13
4.	40	30	9	2	5	3.14
5.	40	30	9	2	7	3.15
6.	40	30	9	2	10	3.16
7.	40	30	9	2	12	3.17
8.	40	30	9	2	15	3.18

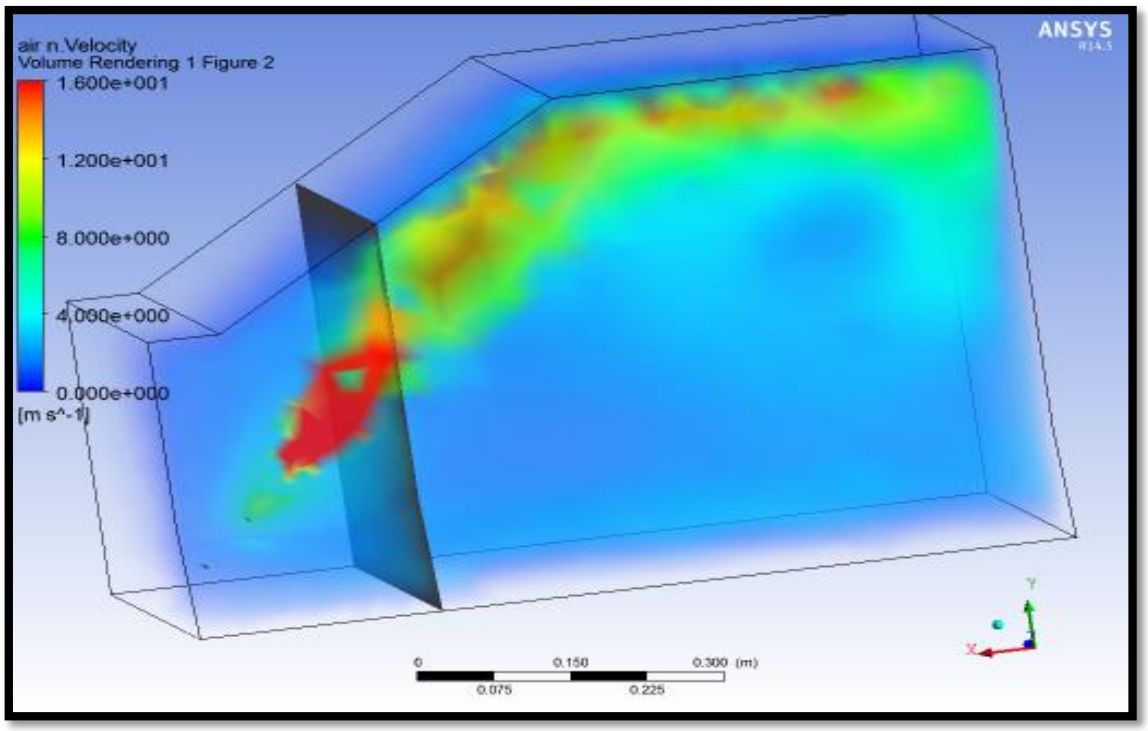

Fig. 3.11 : Velocity Distribution for Impinging Angle = 0^{o} & Outlet Dia. = 2 mm

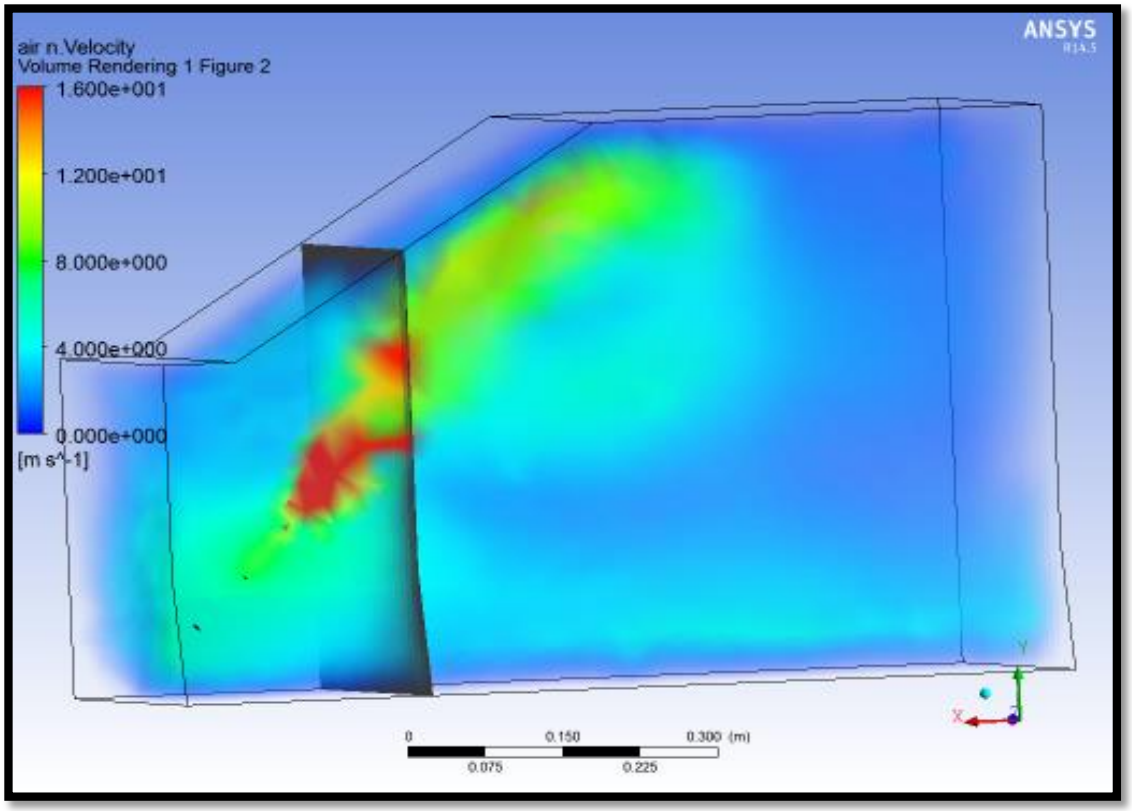

Fig. 3.12 : Velocity Distribution for Impinging Angle = 2^{o} & Outlet Dia. = 2 mm

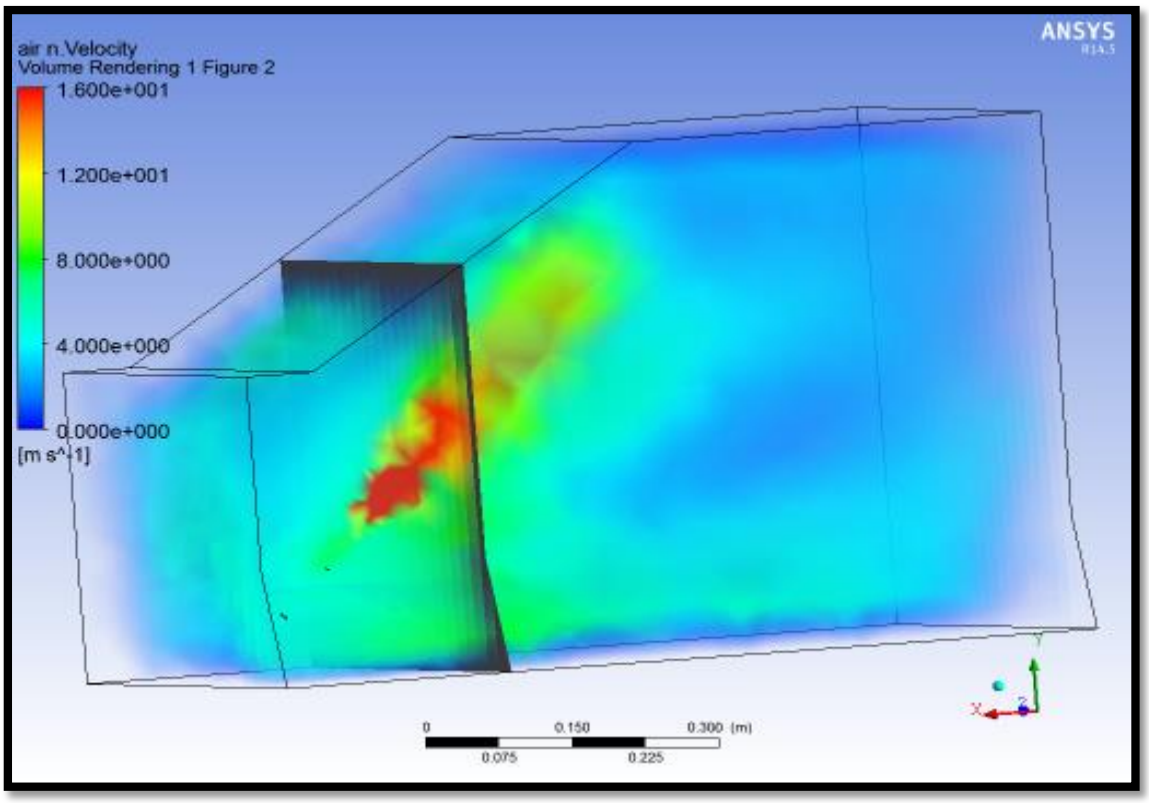

Fig. 3.13 : Velocity Distribution for Impinging Angle = 3° & Outlet Dia. = 2 mm

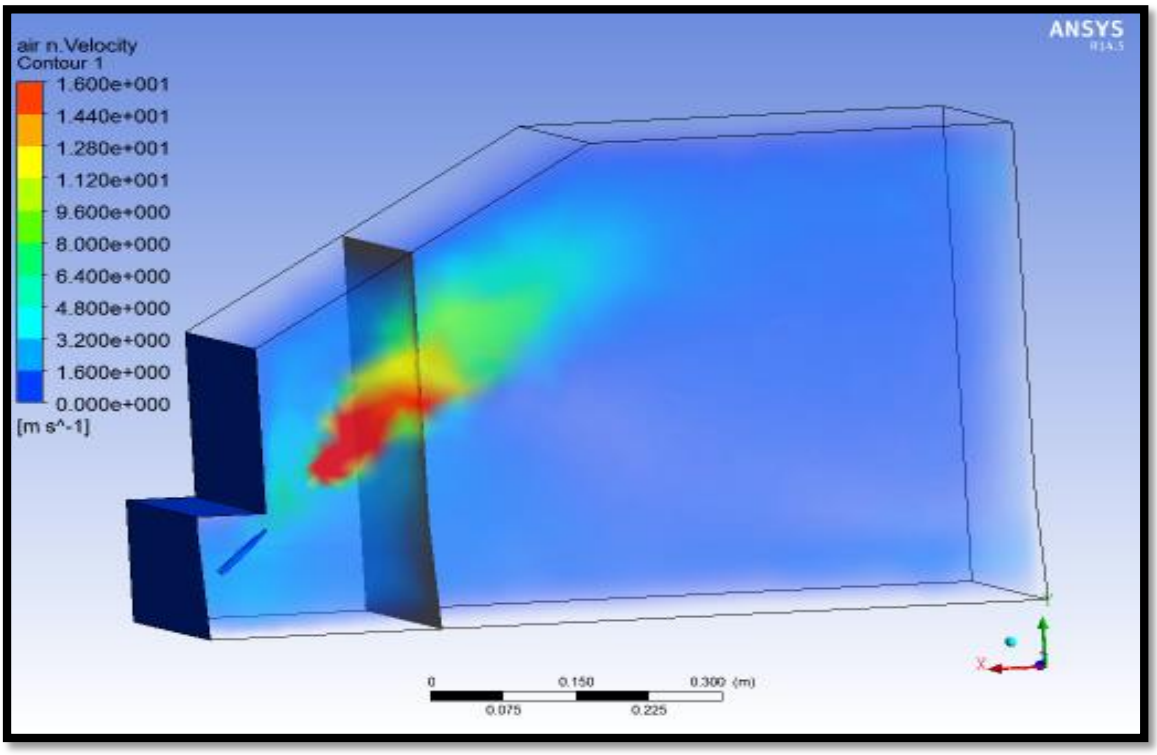

Fig. 3.14 : Velocity Distribution for Impinging Angle = 5° & Outlet Dia. = 2 mm

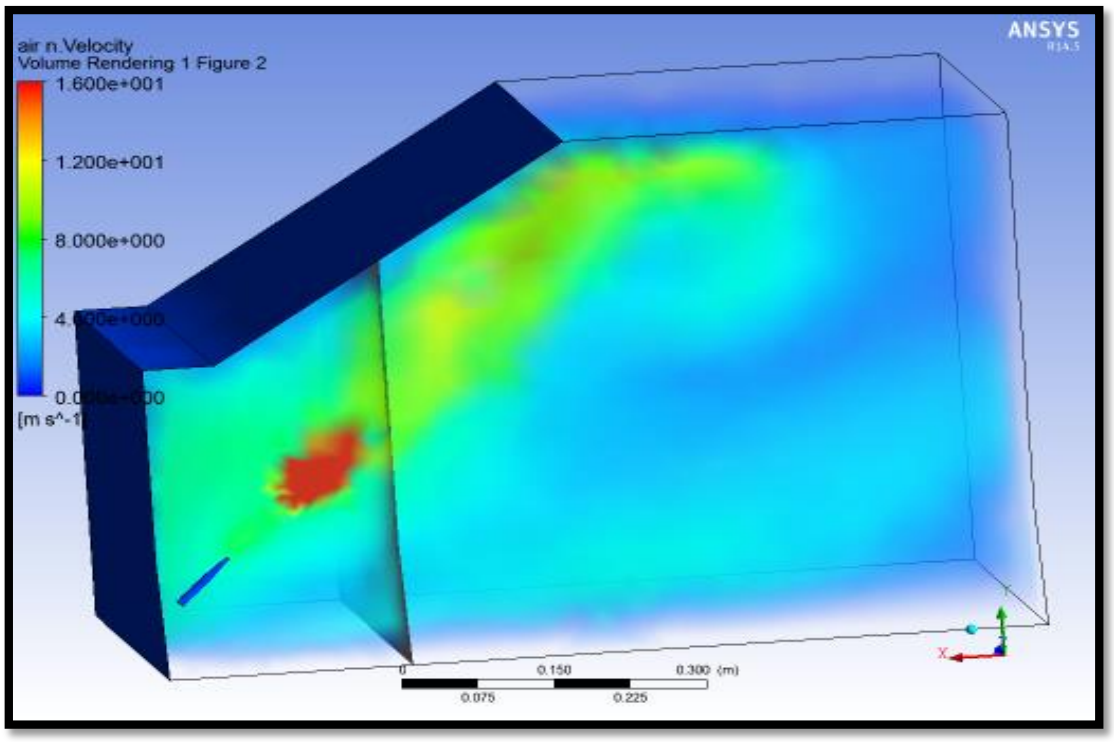

Fig. 3.15 : Velocity Distribution for Impinging Angle = 7^{o} & Outlet Dia. = 2 mm

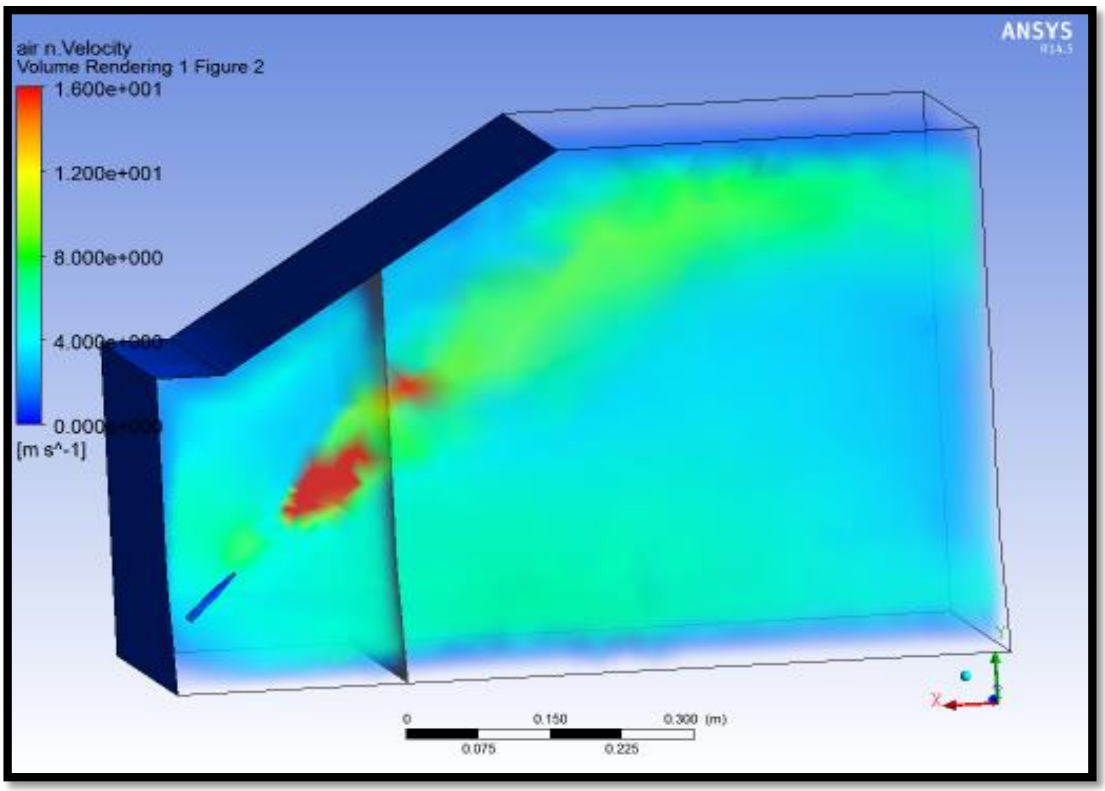

Fig. 3.16 : Velocity Distribution for Impinging Angle = 10^{o} & Outlet Dia. = 2 mm

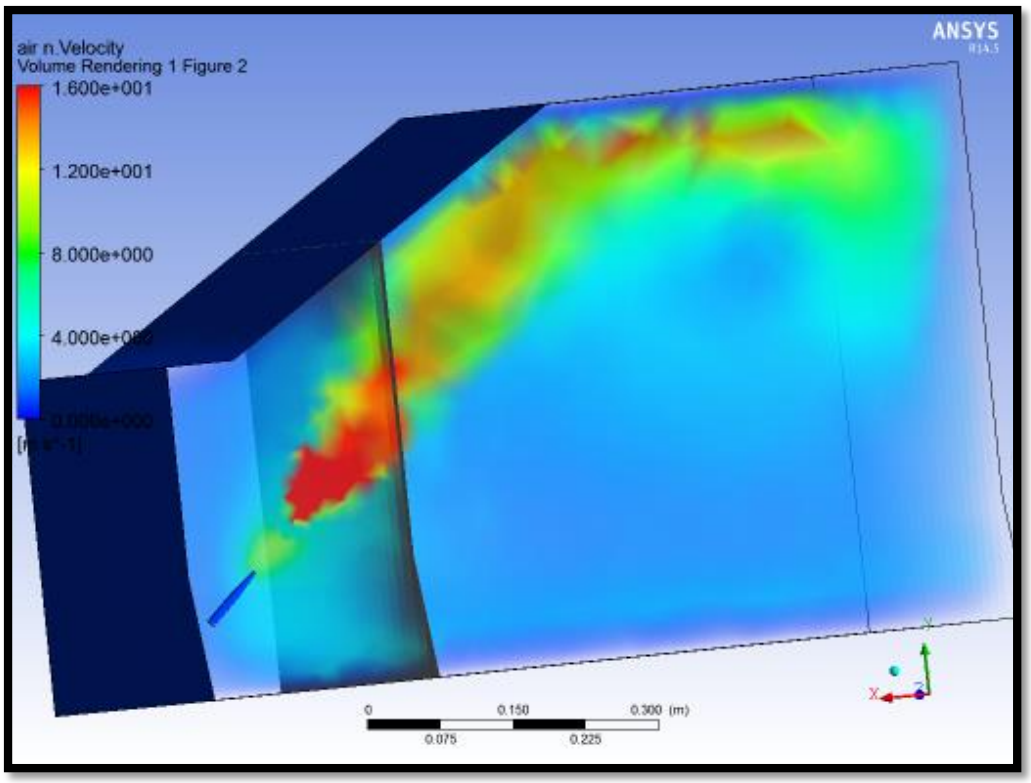

Fig. 3.17 : Velocity Distribution for Impinging Angle = 12° & Outlet Dia. = 2 mm

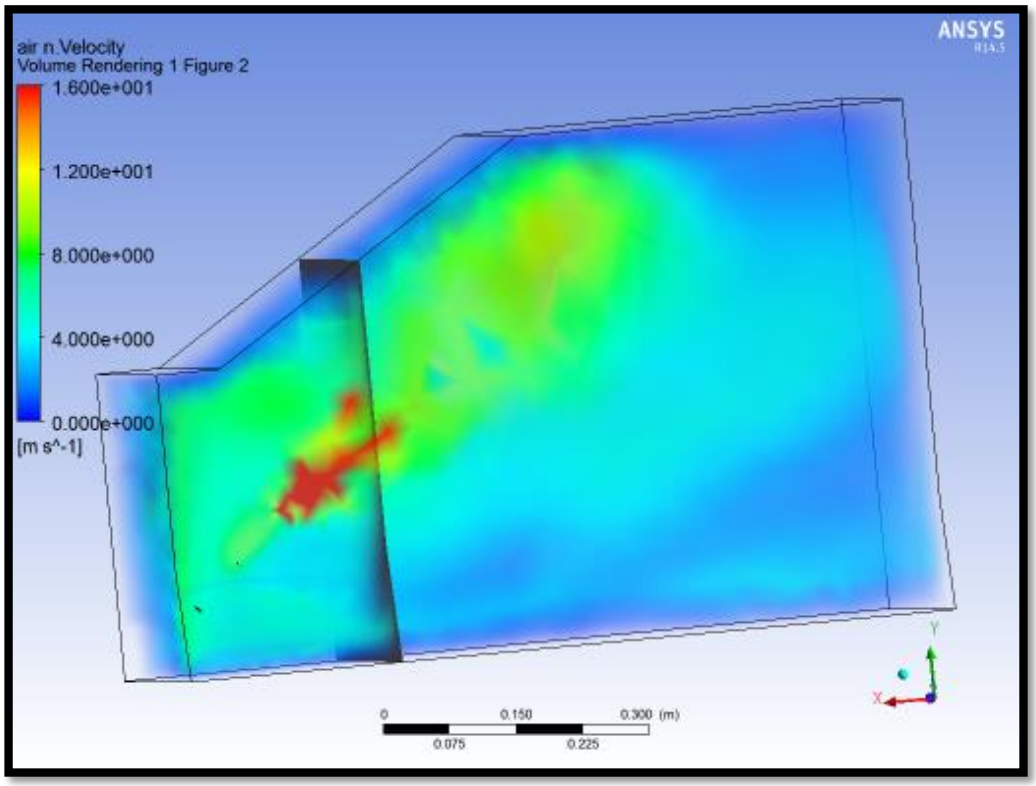

Fig. 3.18 : Velocity Distribution for Impinging Angle = 15° & Outlet Dia. = 2 mm

3.5.3 Varying the impinging angle of the nozzle for outlet diameter of 3 mm:

Table 3.3 : Varying the impinging angle for outlet diameter of 3 mm

Experiment No.	Throat Length (mm)	Converging Section Length(mm)	Inlet Diameter (mm)	Outlet Diameter (mm)	Impinging Angle (degree)	Figure No.
1.	40	30	9	3	0	3.19
2.	40	30	9	3	1	3.20
3.	40	30	9	3	2	3.21
4.	40	30	9	3	3	3.22
5.	40	30	9	3	4	3.23
6.	40	30	9	3	5	3.24

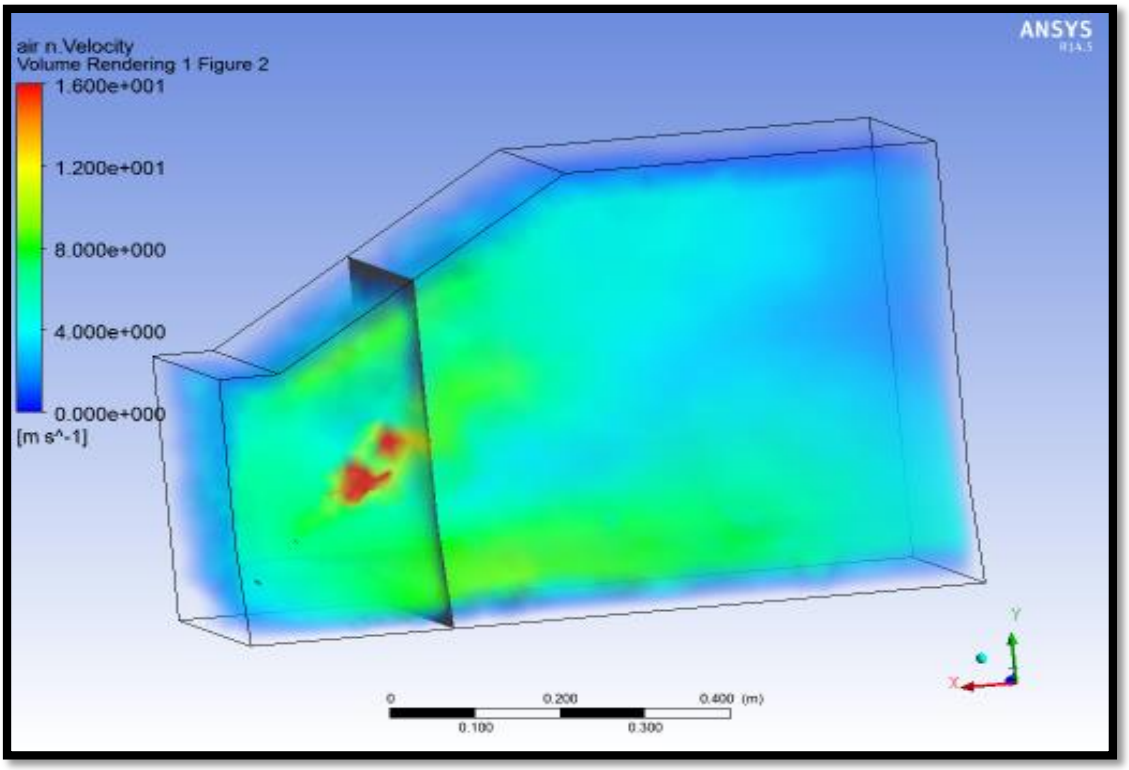

Fig. 3.19 : Velocity Distribution for Impinging Angle = 0^{o} & Outlet Dia. = 3 mm

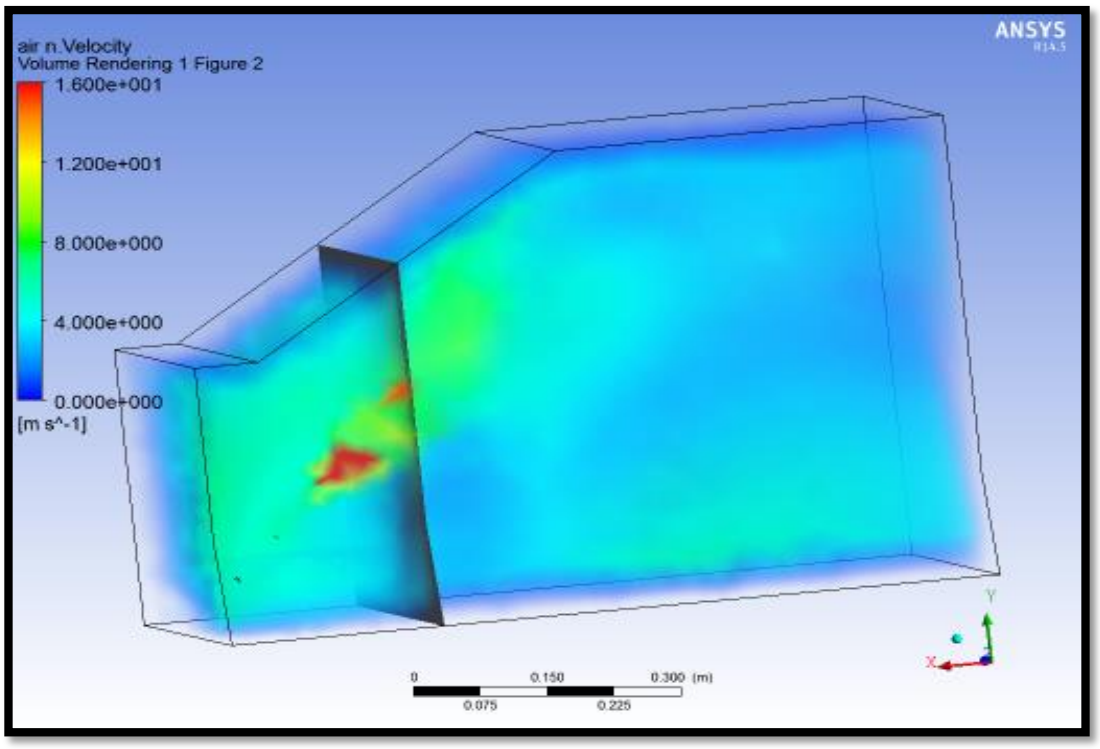

Fig. 3.20 : Velocity Distribution for Impinging Angle = 1^{o} & Outlet Dia. = 3 mm

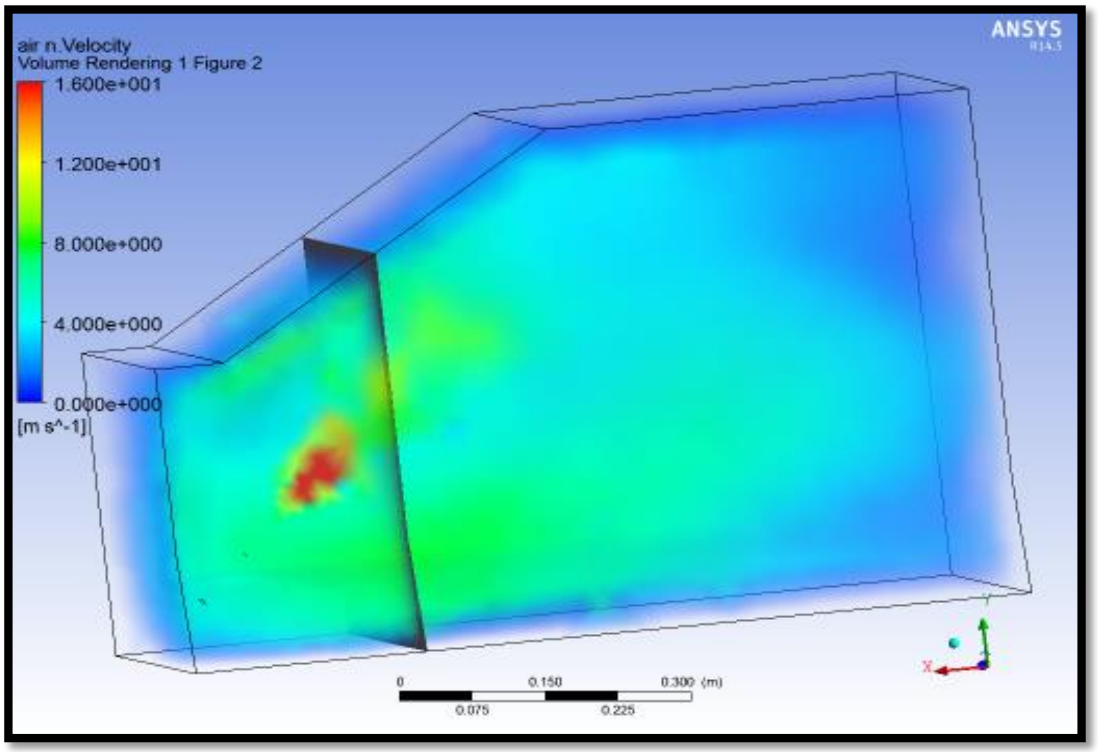

Fig. 3.21 : Velocity Distribution for Impinging Angle = 2^{o} & Outlet Dia. = 3 mm

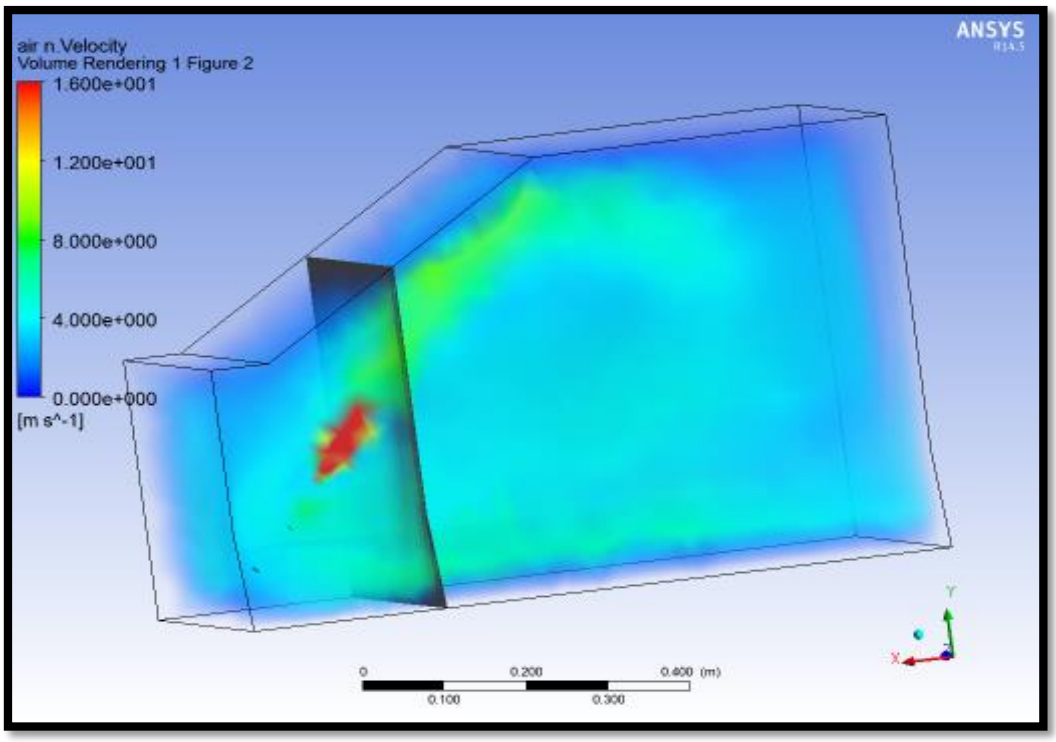

Fig. 3.22 : Velocity Distribution for Impinging Angle = 3^{o} & Outlet Dia. = 3 mm

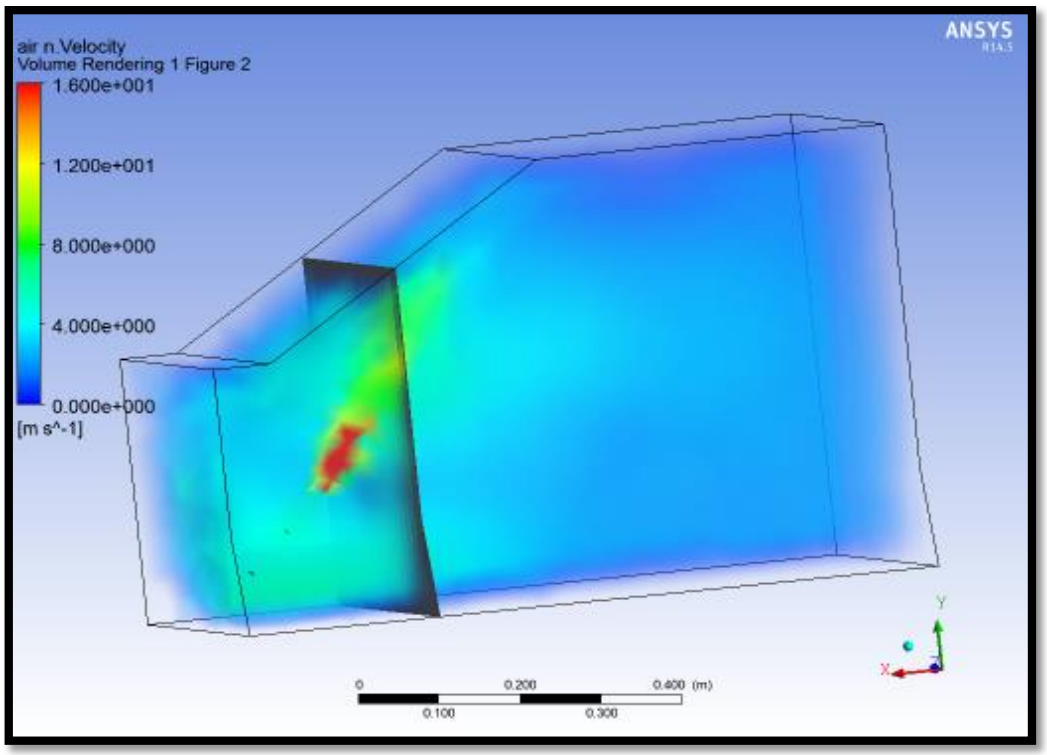

Fig. 3.23 : Velocity Distribution for Impinging Angle = 4^{o} & Outlet Dia. = 3 mm

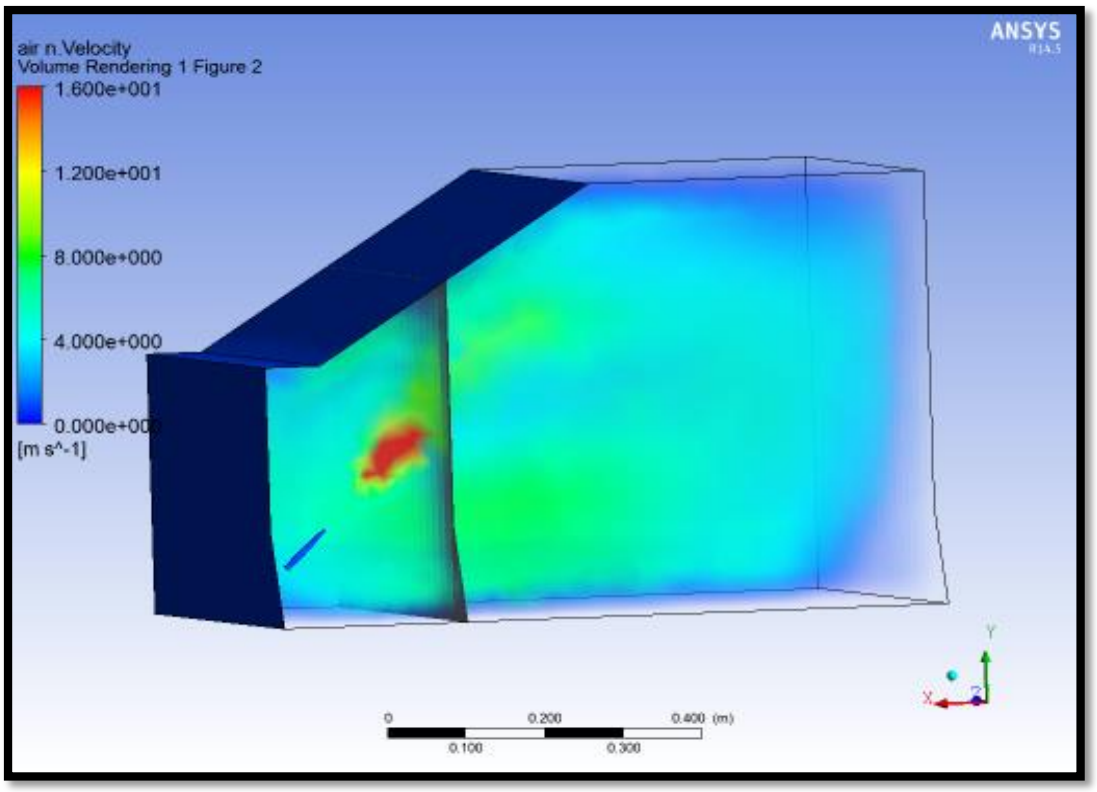

Fig. 3.24 : Velocity Distribution for Impinging Angle = 5^{o} & Outlet Dia. = 3 mm

3.5.4 Varying the impinging angle of the nozzle for outlet Diameter of 4 mm:

Table 3.4 : Varying the impinging angle for outlet Diameter of 4 mm:

Experiment No.	Throat Length (mm)	Converging Section Length(mm)	Inlet Diameter (mm)	Outlet Diameter(mm)	Impinging Angle (degree)	Figure No.
1.	40	30	9	4	0	3.25
2.	40	30	9	4	1	3.26
3.	40	30	9	4	2	3.27
4.	40	30	9	4	3	3.28
5.	40	30	9	4	4	3.29
6.	40	30	9	4	5	3.30

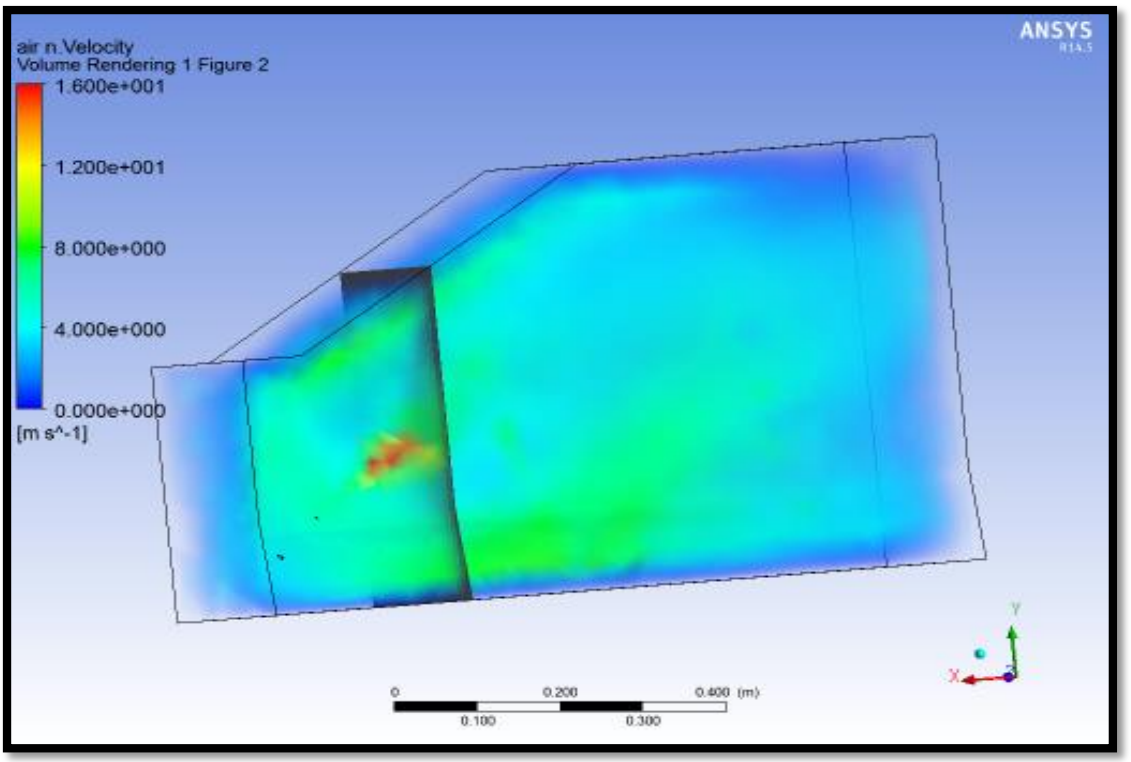

Fig. 3.25 : Velocity Distribution for Impinging Angle = 0^{o} & Outlet Dia. = 4 mm

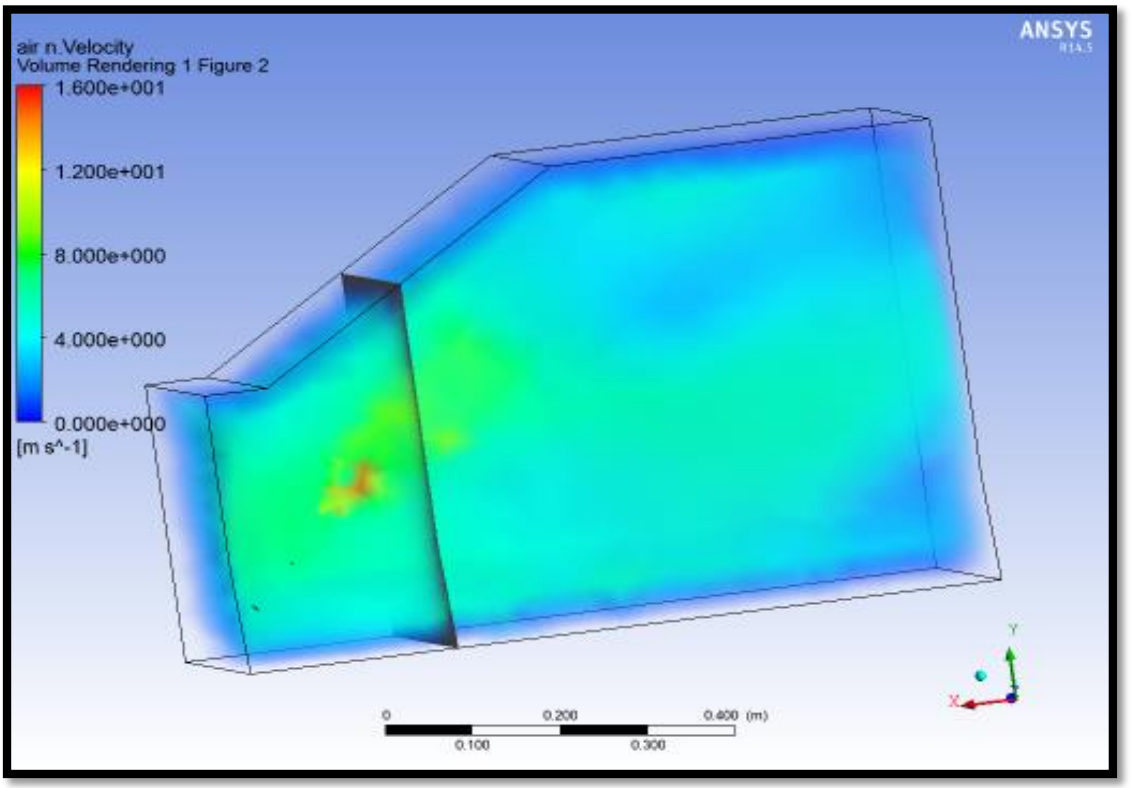

Fig. 3.26 : Velocity Distribution for Impinging Angle = 1^{o} & Outlet Dia. = 4 mm

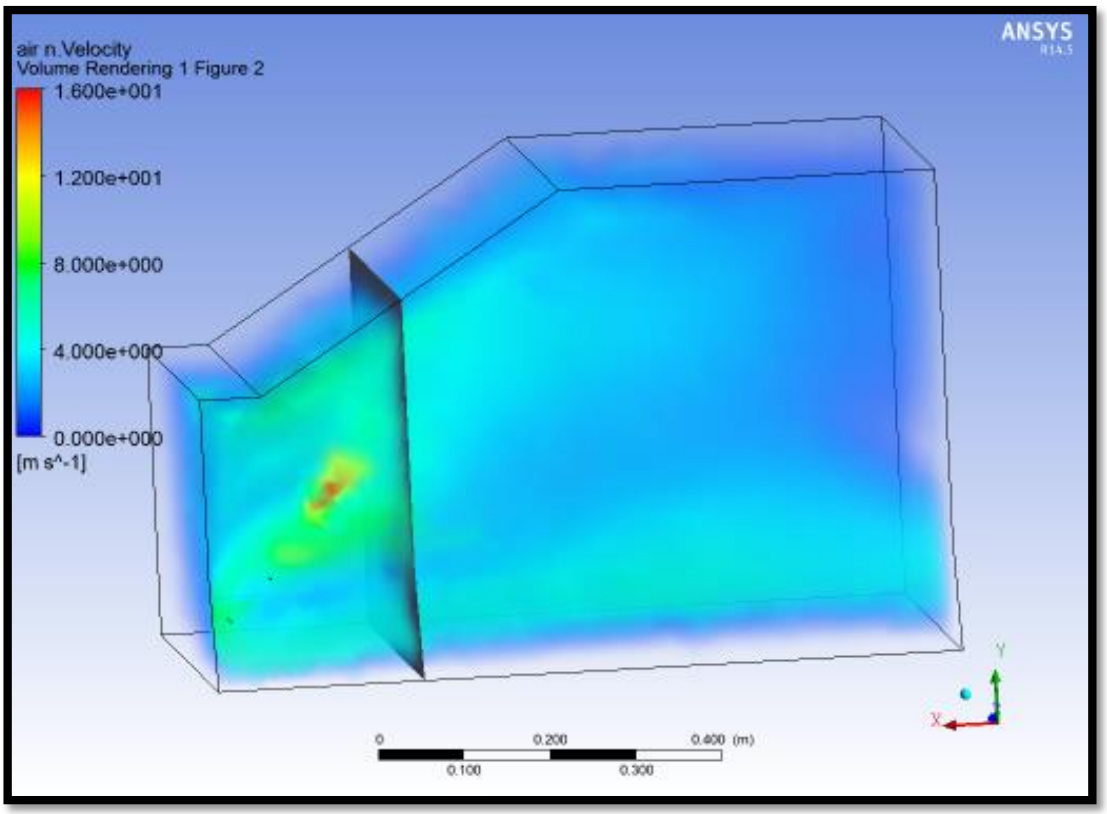

Fig. 3.27 : Velocity Distribution for Impinging Angle = 2^{o} & Outlet Dia. = 4 mm

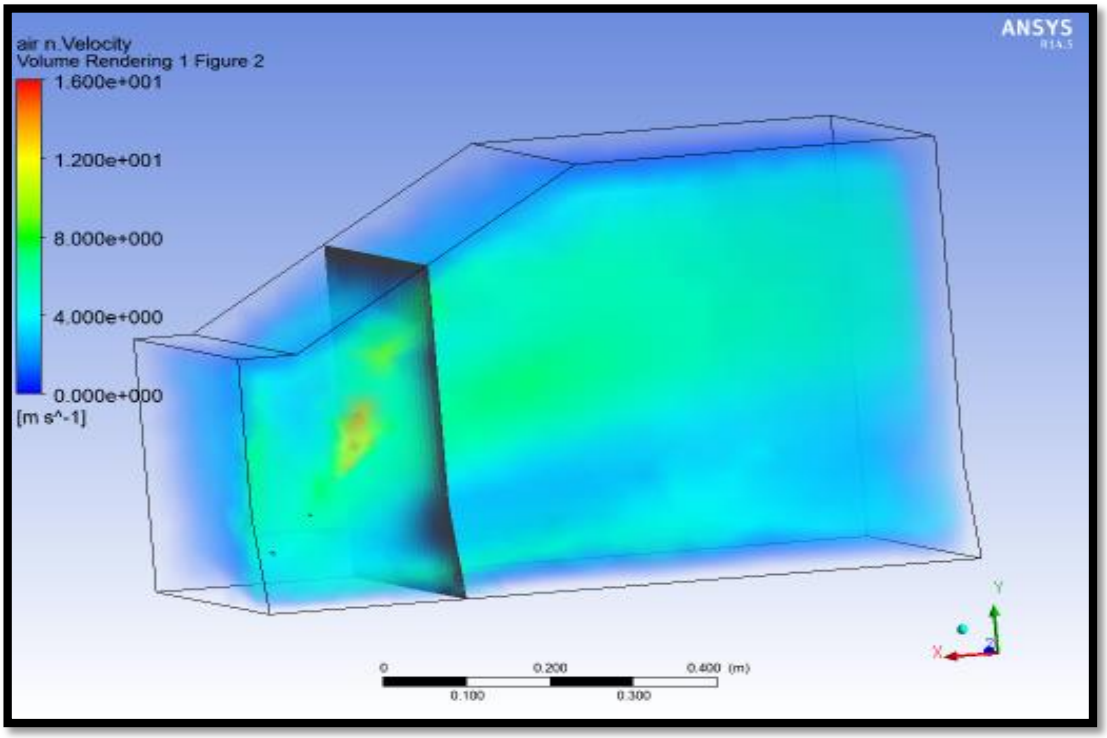

Fig. 3.28 : Velocity Distribution for Impinging Angle = 3^{o} & Outlet Dia. = 4 mm

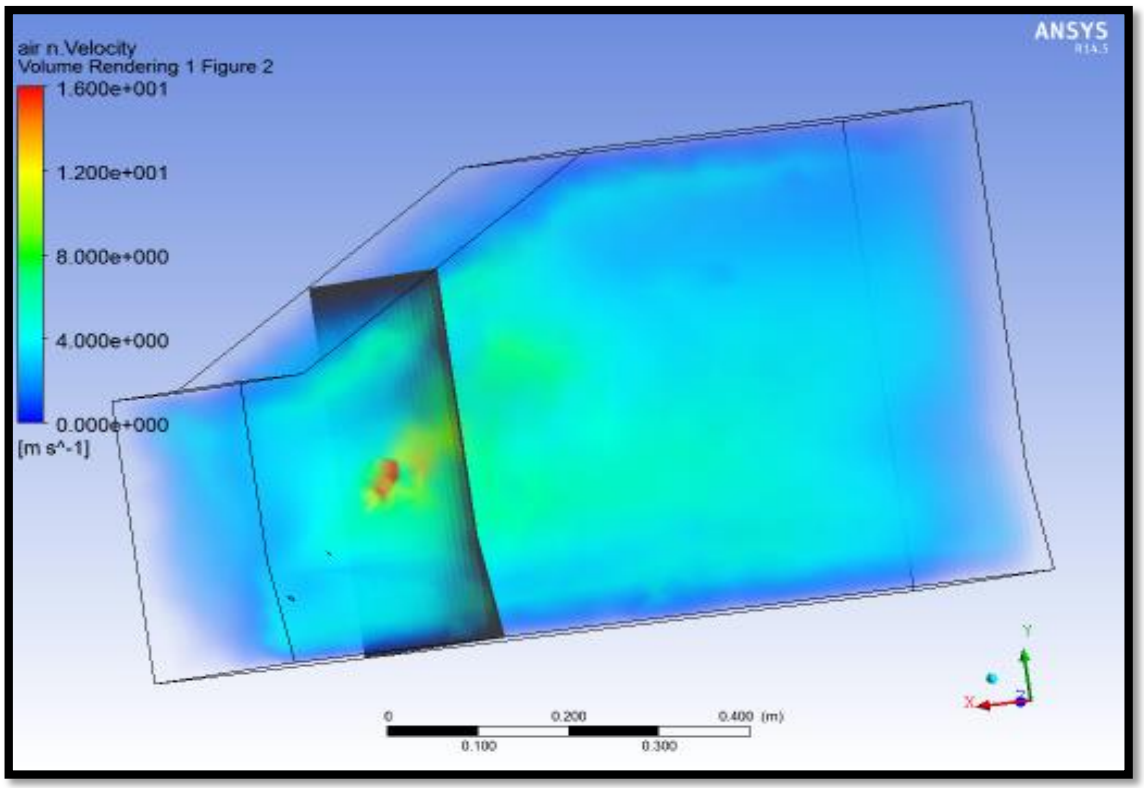

Fig. 3.29 : Velocity Distribution for Impinging Angle = 4^{o} & Outlet Dia. = 4 mm

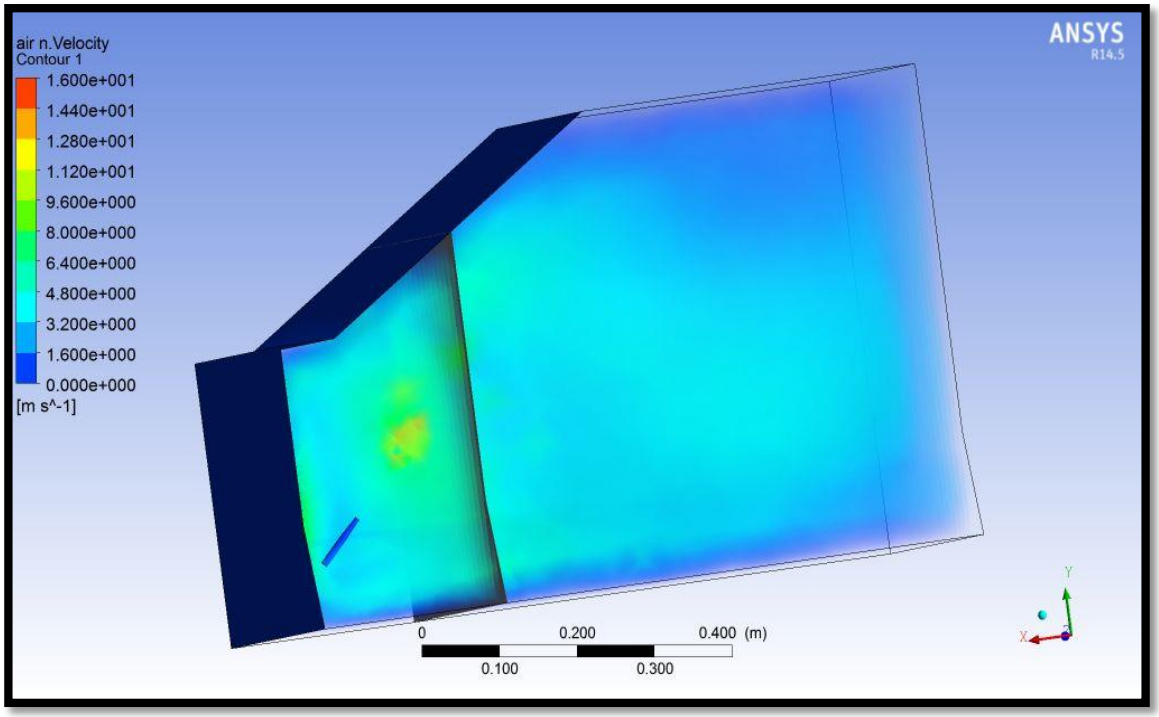

Fig. 3.30 : Velocity Distribution for Impinging Angle = 5^{o} & Outlet Dia. = 4 mm

3.5.5 Varying the impinging angle of the nozzle for outlet Diameter of 5 mm:

Table 3.5 : Varying the impinging angle for outlet diameter of 5mm

Experiment No.	Throat Length (mm)	Converging Section Length(mm)	Inlet Diameter(mm)	Outlet Diameter(mm)	Impinging Angle (degree)	Figure No.
1.	40	30	9	5	0	3.31
2.	40	30	9	5	1	3.32
3.	40	30	9	5	2	3.33
4.	40	30	9	5	3	3.34
5.	40	30	9	5	4	3.35
6.	40	30	9	5	5	3.36

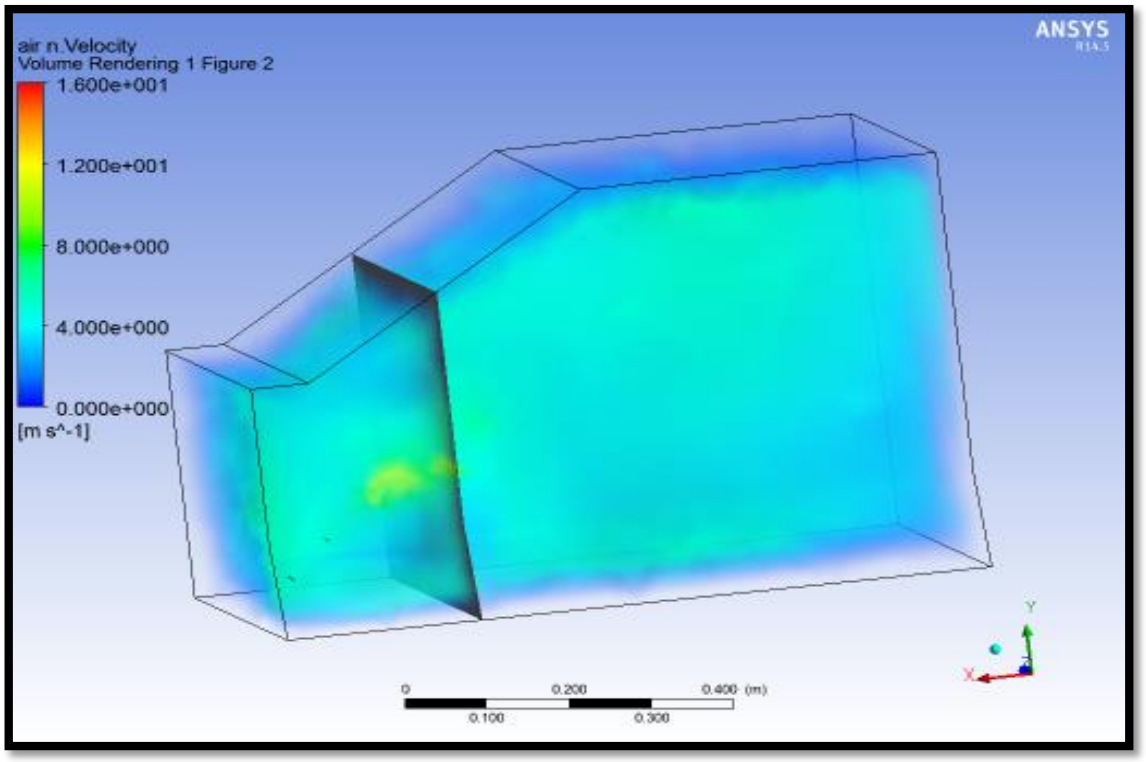

Fig. 3.31 : Velocity Distribution for Impinging Angle = 0^{o} & Outlet Dia. = 5 mm

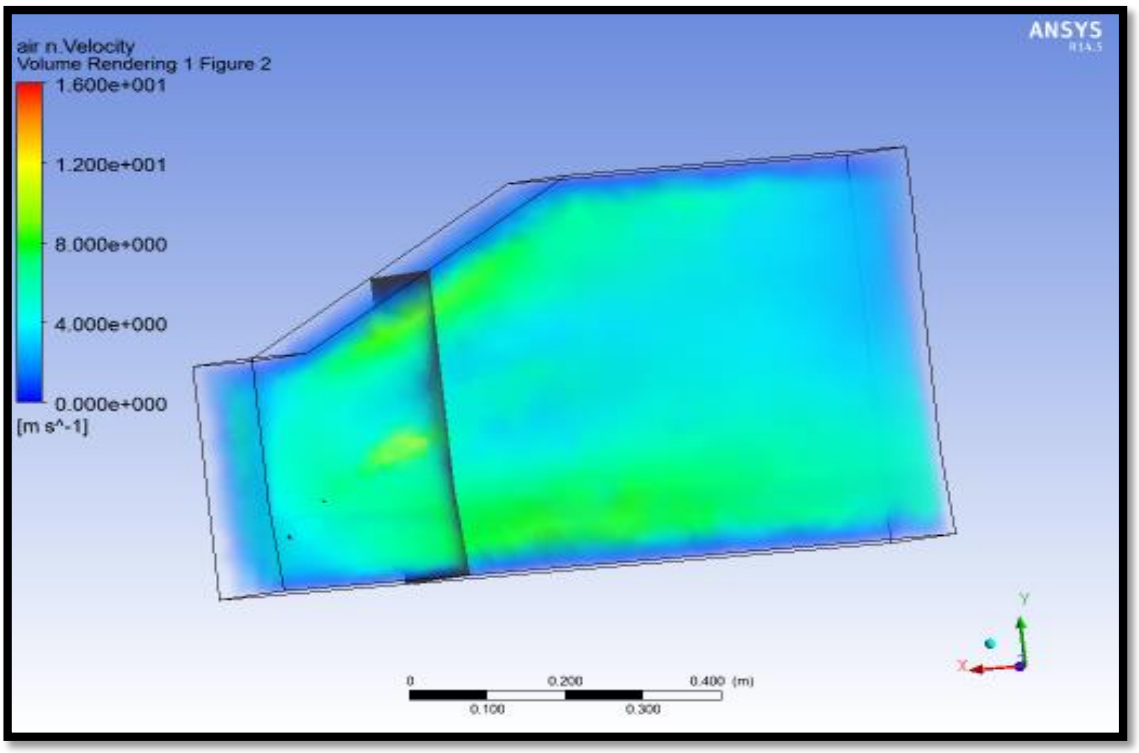

Fig. 3.32 : Velocity Distribution for Impinging Angle = 1^{o} & Outlet Dia. = 5 mm

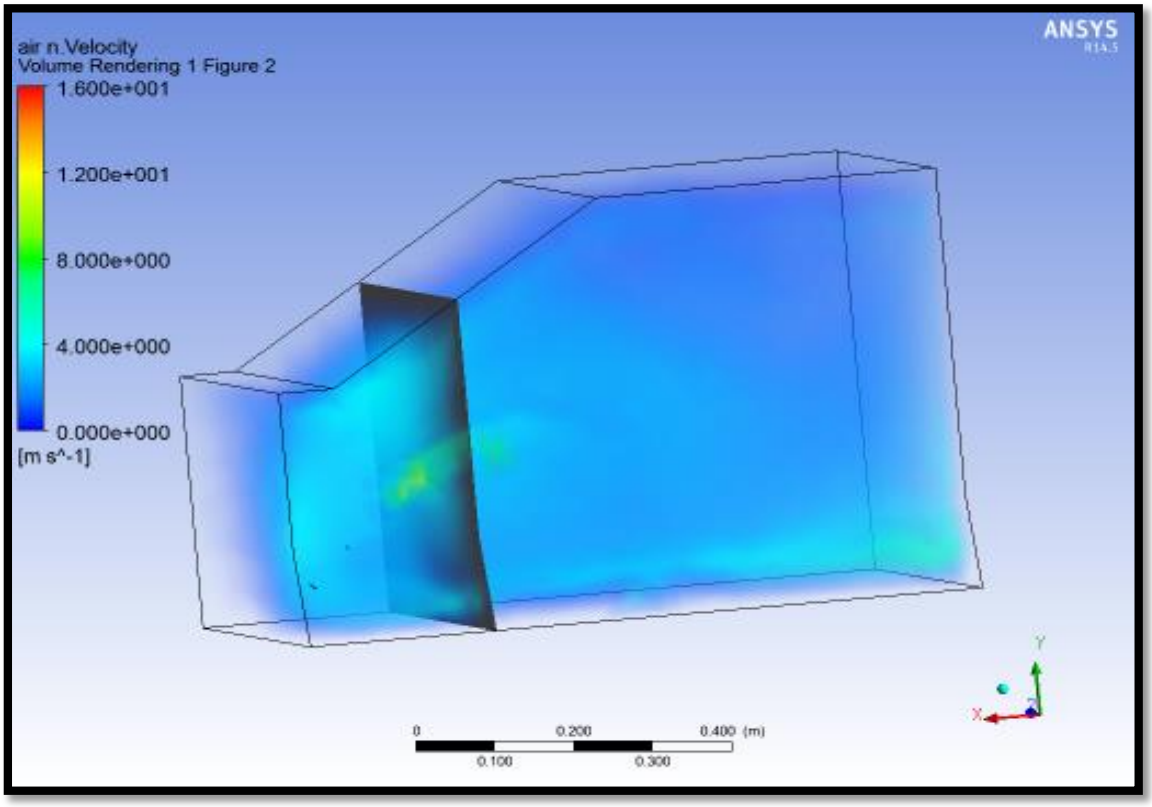

Fig. 3.33 : Velocity Distribution for Impinging Angle = 2^{o} & Outlet Dia. = 5 mm

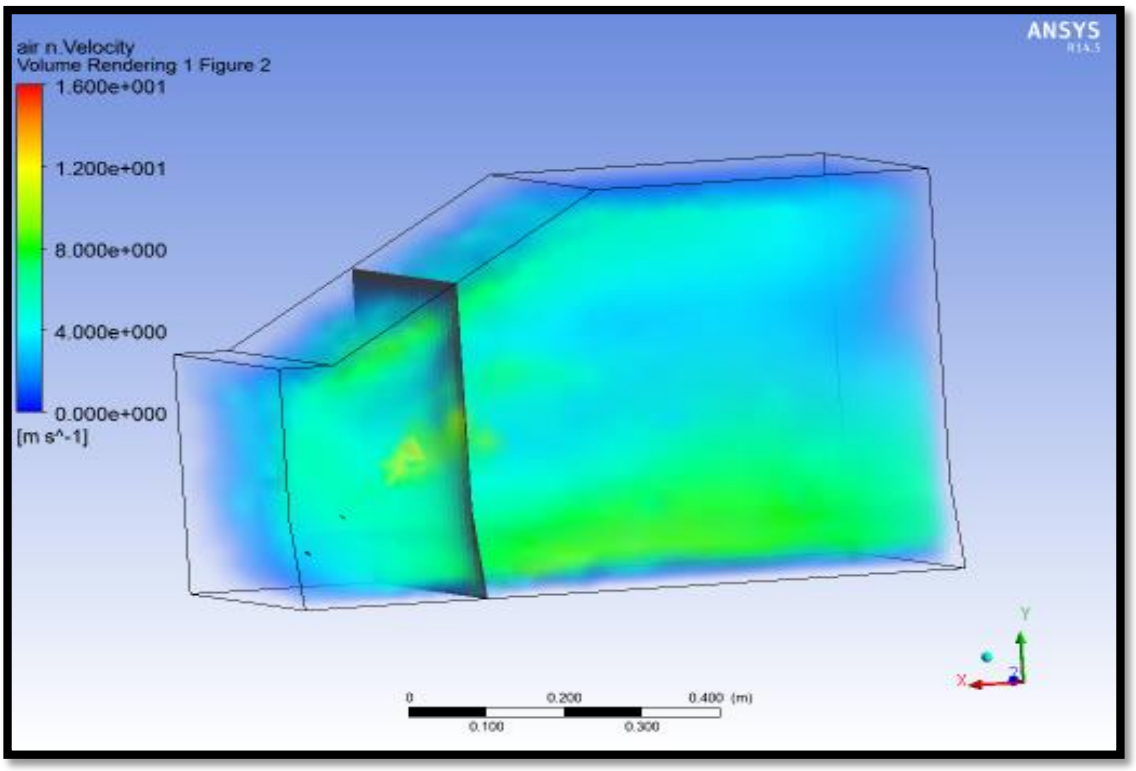

Fig. 3.34 : Velocity Distribution for Impinging Angle = 3° & Outlet Dia. = 5 mm

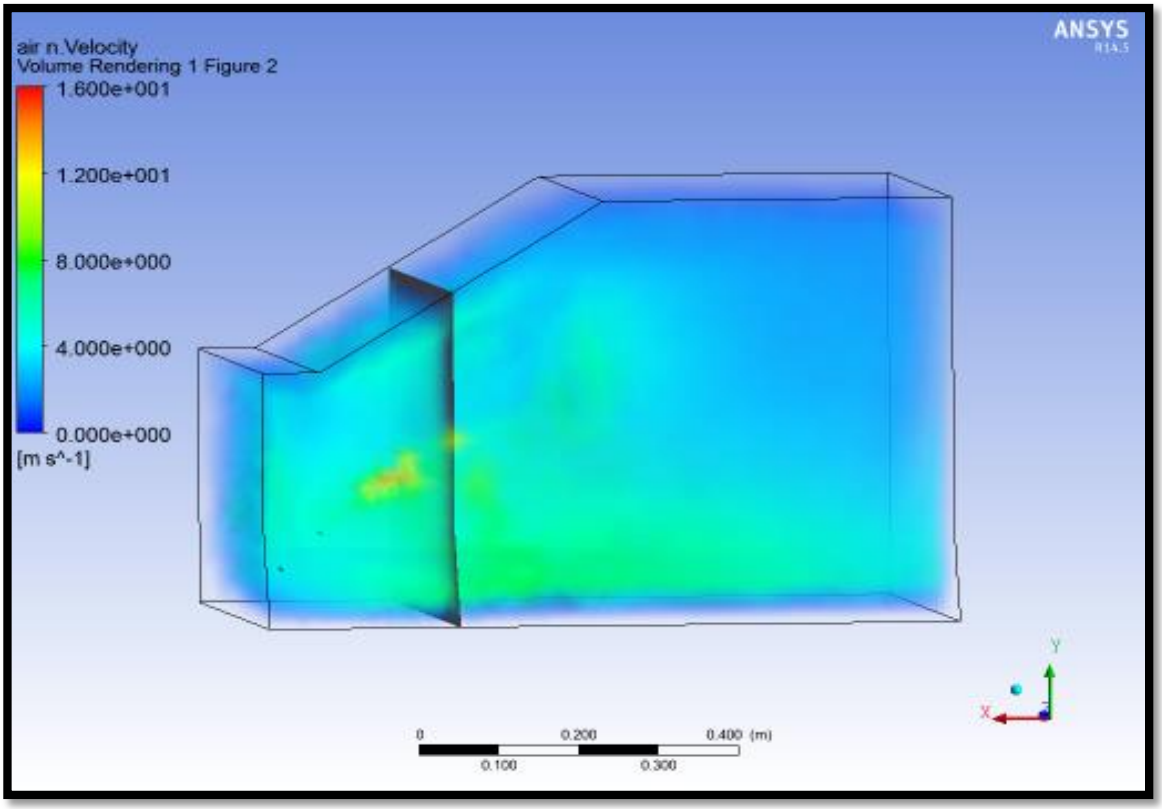

Fig. 3.35 : Velocity Distribution for Impinging Angle = 4° & Outlet Dia. = 5 mm

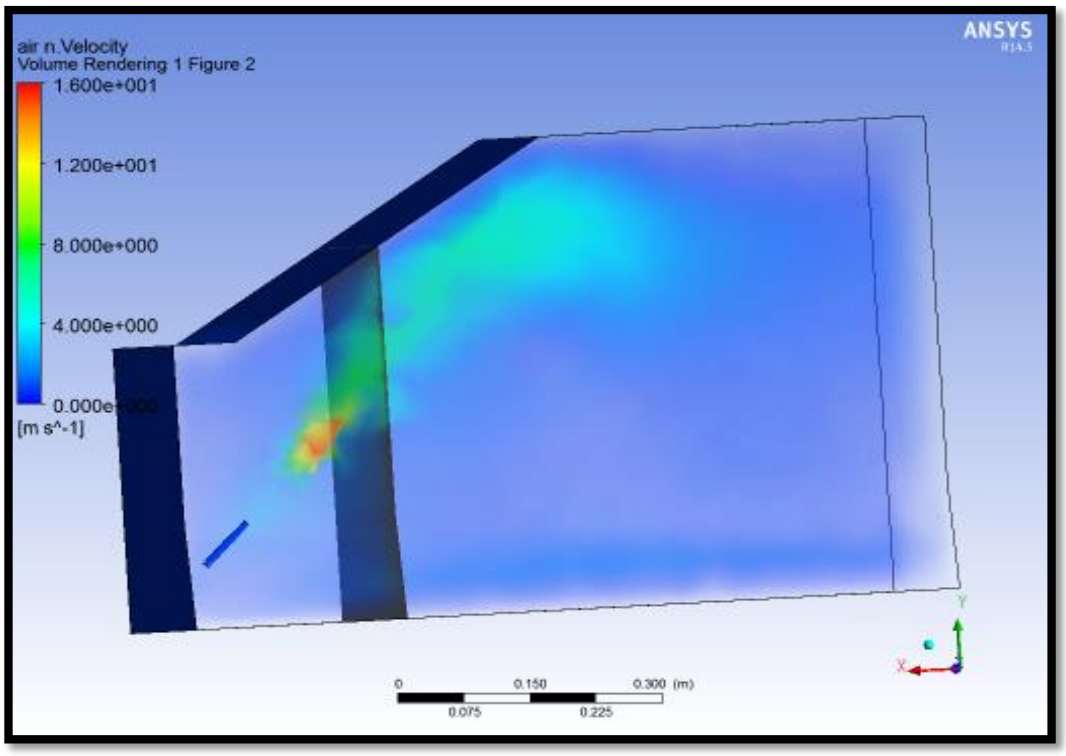

Fig. 3.36 : Velocity Distribution for Impinging Angle = 5^o & Outlet Dia. = 5 mm

Performing the above Velocity Distributions it can be made clear that nozzle with 1 mm of outlet Diameter and impinging angle of 0^o gives the best possible results. So fixing these two parameters and varying throat length following Velocity Distribution is performed.

3.5.6 Varying the throat length of the nozzle

Figures below demonstrate the varying throat lengths.

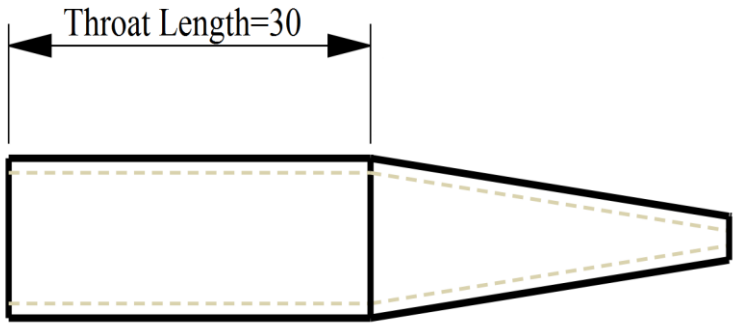

Fig. 3.37 : Nozzle with Throat Length of 30 mm

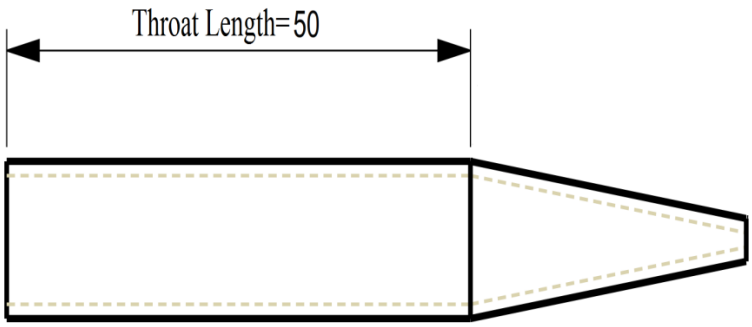

Fig. 3.38 : Nozzle with Throat Length of 50 mm

Fixed parameters are:

Impinging angle = 0^o

Outlet Diameter= 1 mm

Inlet Diameter= 9 mm

Converging section length = 30 mm

Table 3.6 : Varying the throat length of the nozzle

Experiment No.	Throat Length (mm)	Converging Section Length(mm)	Inlet Diameter(mm)	Outlet Diameter(mm)	Impinging Angle (degree)	Figure No.
1.	10	30	9	1	0	3.39
3.	30	30	9	1	0	3.40
4.	50	30	9	1	0	3.41

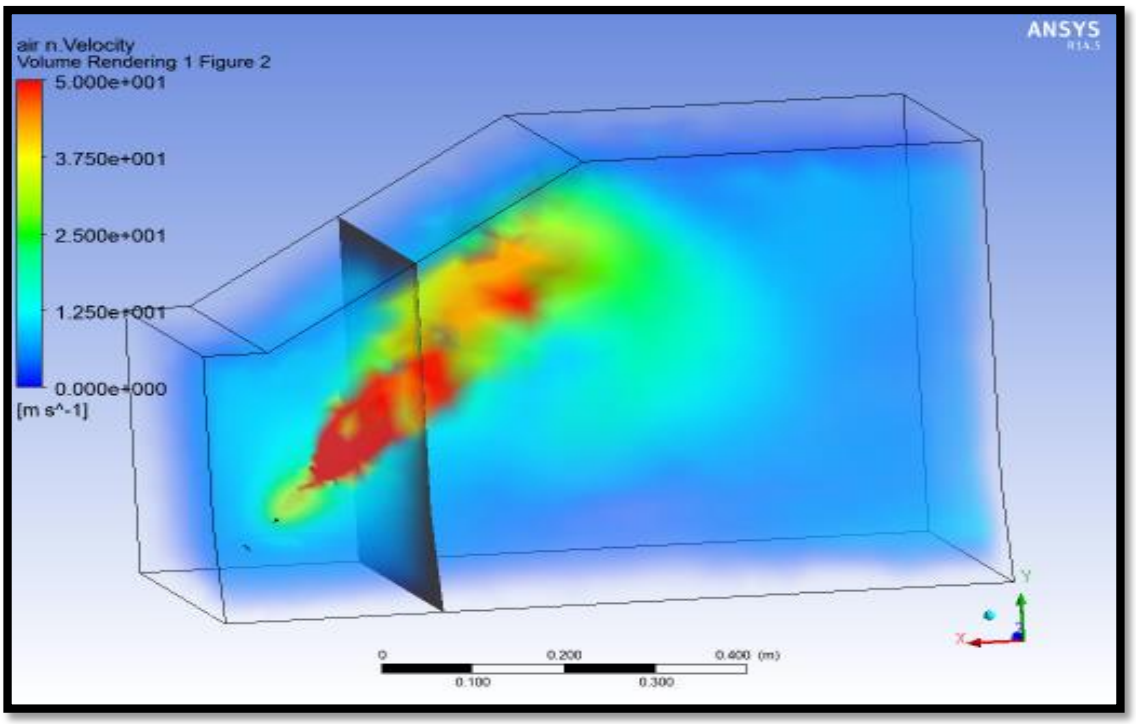

Fig. 3.39 : Velocity Distribution for Throat Length 10 mm

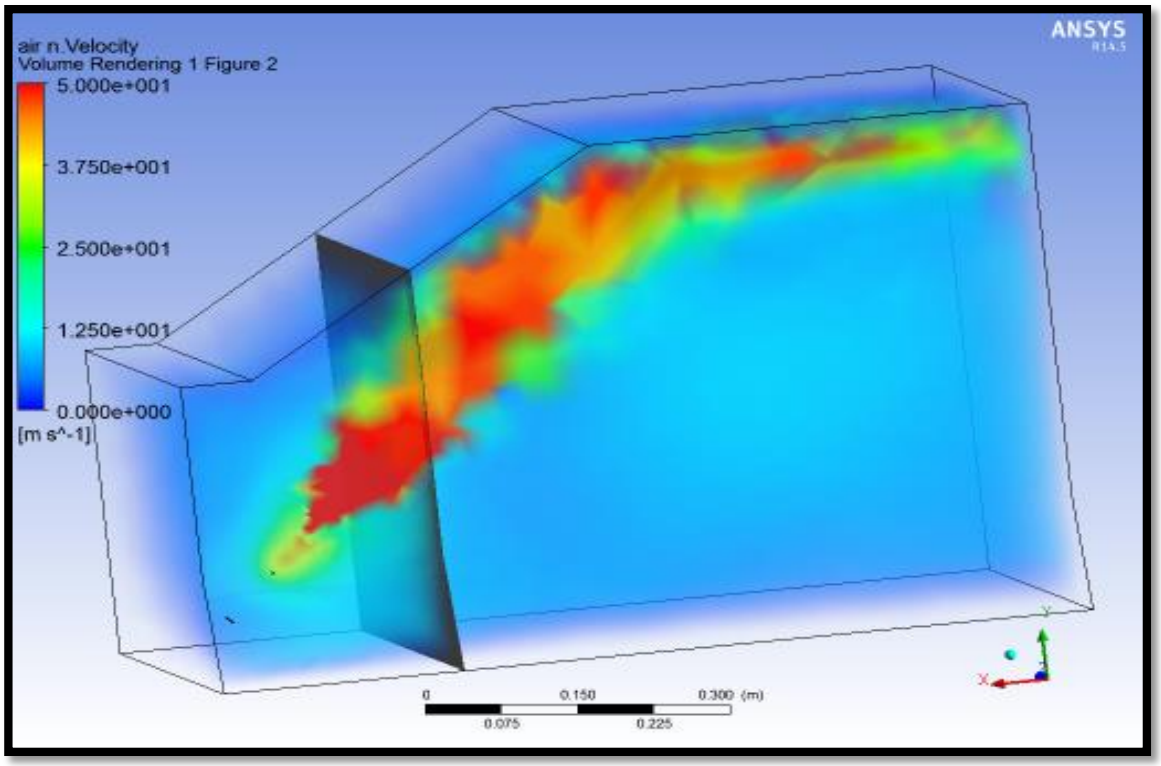

Fig. 3.40 : Velocity Distribution for Throat Length 30 mm

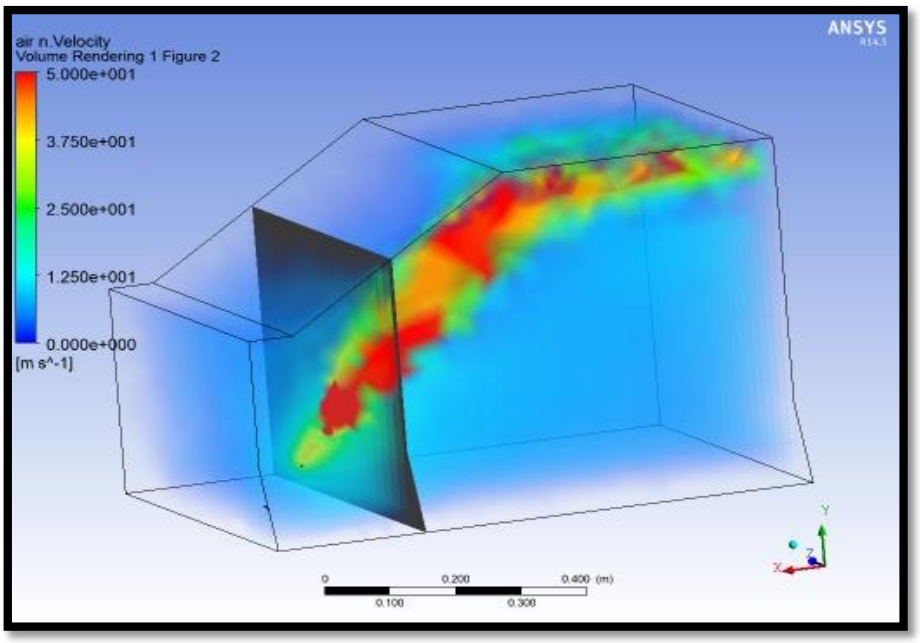

Fig. 3.41 : Velocity Distribution for Throat Length 50 mm

By analysing the above results the nozzle with the throat length of 30 mm seems to be effective as compare to nozzles with other throat lengths. So now the fixed parameters are:

Impinging angle = 0^{o}

Outlet Diameter= 1 mm

Throat Length = 30 mm

Now varying the converging length and inlet Diameter of the nozzle following Velocity Distributions are shown:

3.5.7 Varying the converging length of the nozzle for inlet Diameter of 5 mm:

Table 3.7 : Varying the converging length for inlet diameter of 5 mm

Experiment No.	Throat Length (mm)	Converging Section Length(mm)	Inlet Diameter(mm)	Outlet Diameter(mm)	Impinging Angle (degree)	Figure No.
1.	30	20	5	1	0	3.42
2.	30	30	5	1	0	3.43
3.	30	40	5	1	0	3.44
4.	30	50	5	1	0	3.45

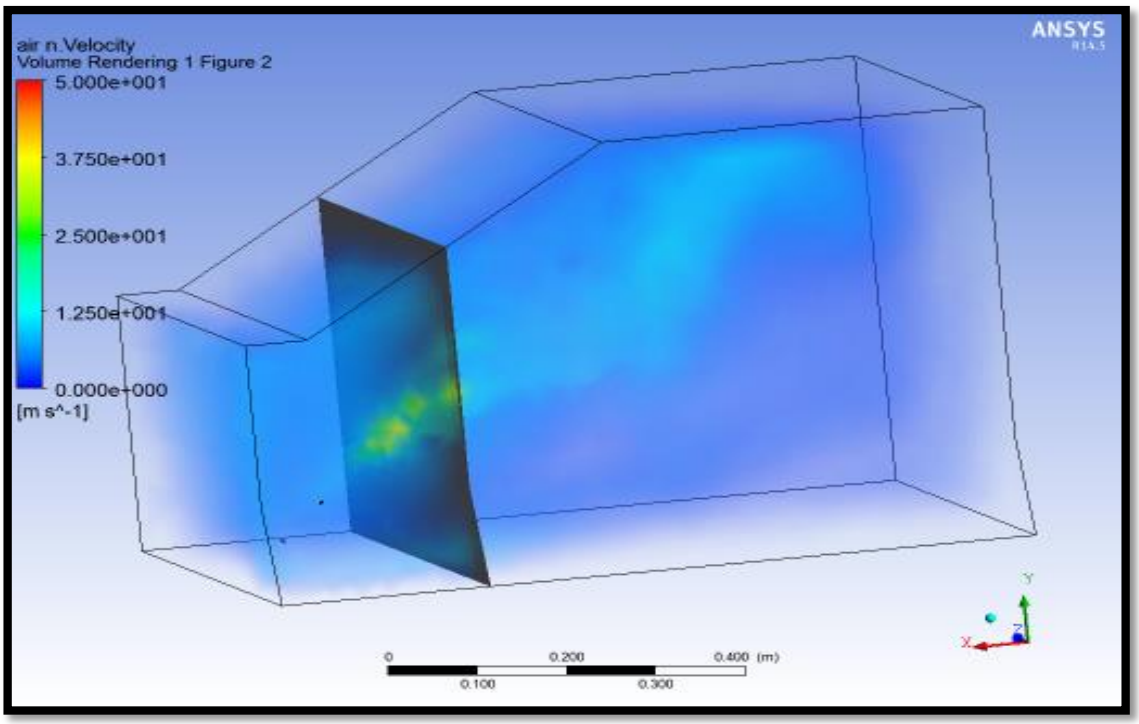

Fig. 3.42 : Velocity Distribution for Converging Length = 20 mm & Inlet Dia. = 5 mm

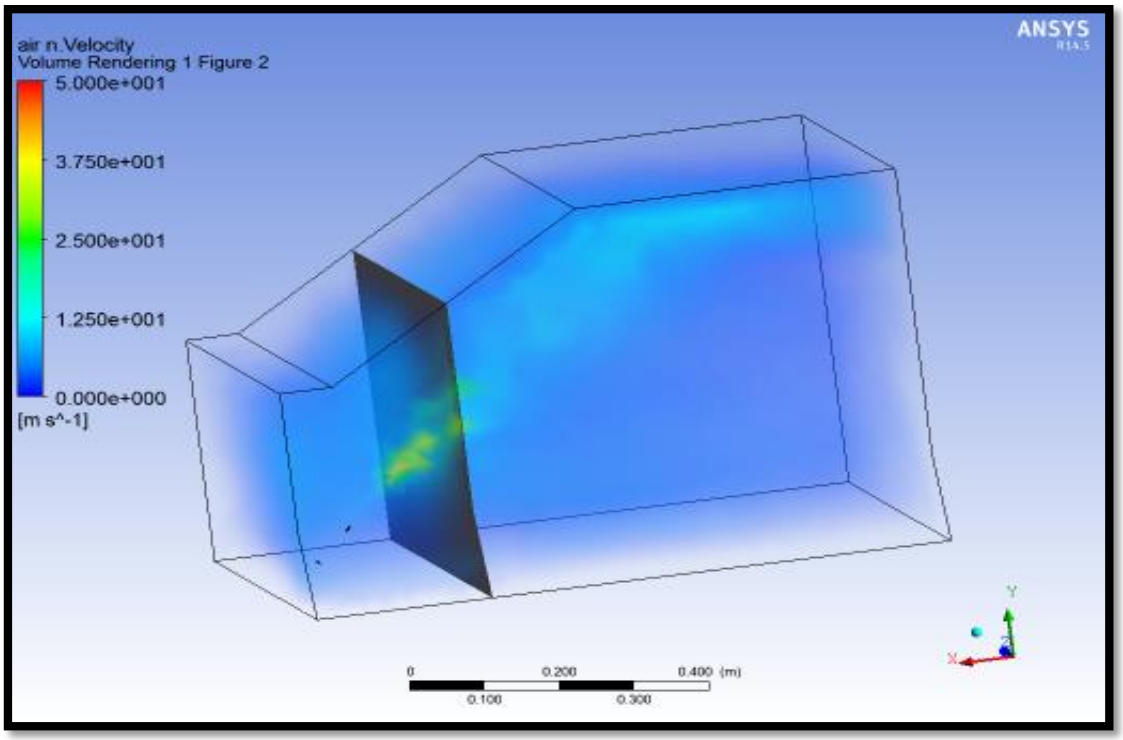

Fig. 3.43 : Velocity Distribution for Converging Length = 30 mm & Inlet Dia. = 5 mm

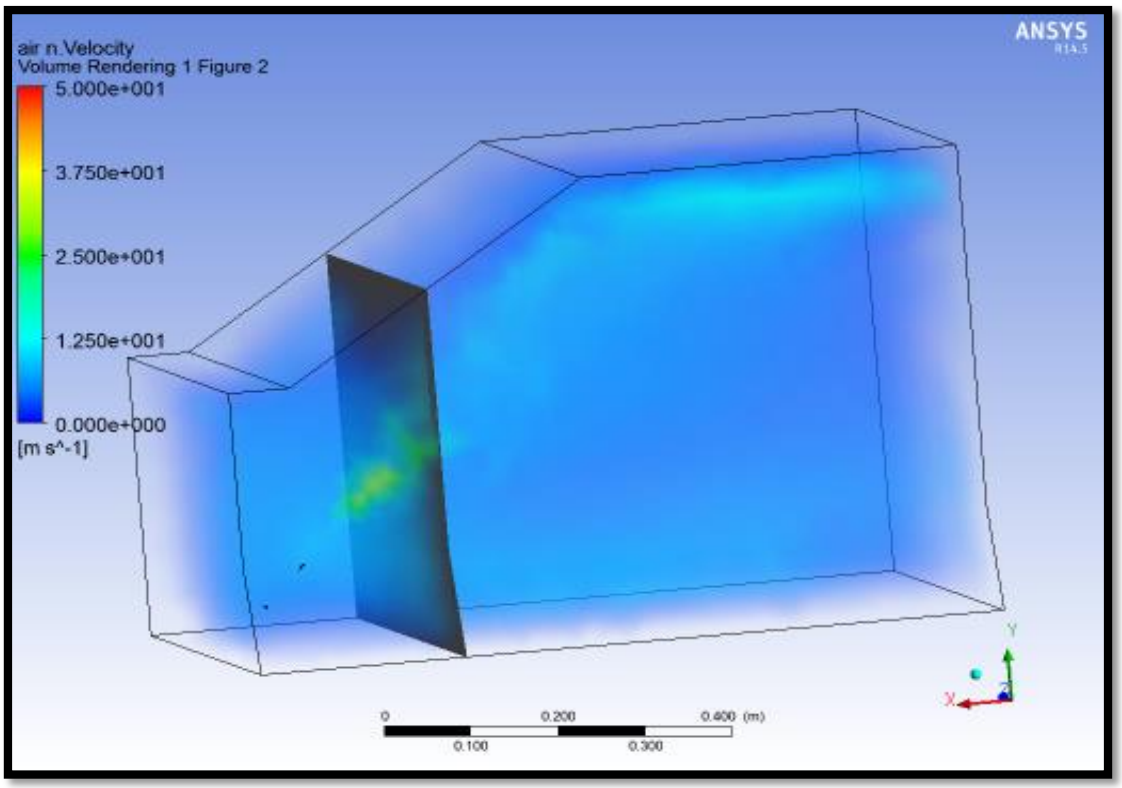

Fig. 3.44 : Velocity Distribution for Converging Length = 40 mm & Inlet Dia. = 5 mm

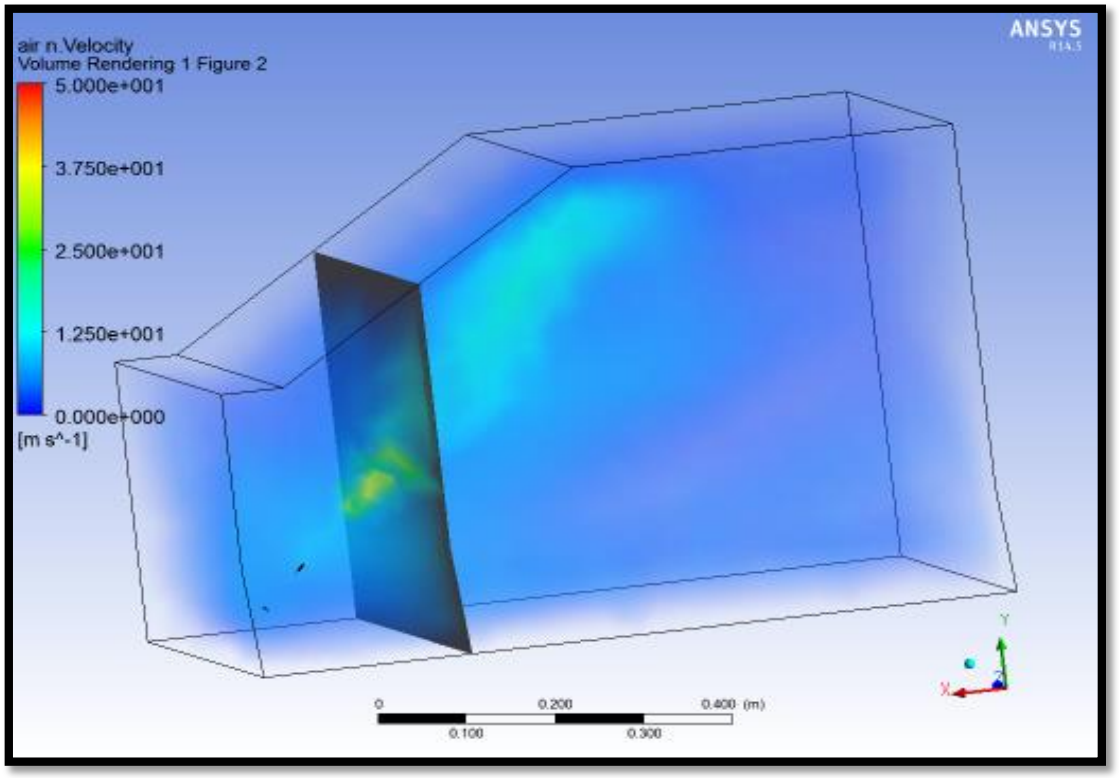

Fig. 3.45 : Velocity Distribution for Converging Length = 50 mm & Inlet Dia. = 5 mm

3.5.8 Varying the converging length of the nozzle for inlet Diameter of 6 mm:

Table 3.8 : Varying the converging length for inlet diameter of 6 mm

Experiment No.	Throat Length (mm)	Converging Section Length(mm)	Inlet Diameter(mm)	Outlet Diameter(mm)	Impinging Angle (degree)	Figure No.
1.	30	20	6	1	0	3.46
3.	30	40	6	1	0	3.47
4.	30	50	6	1	0	3.48

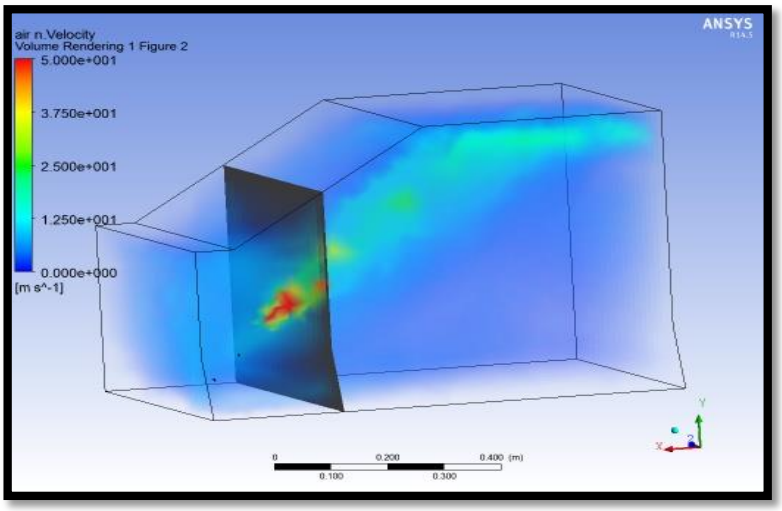

Fig. 3.46 : Velocity Distribution for Converging Length = 20 mm & Inlet Dia. = 6 mm

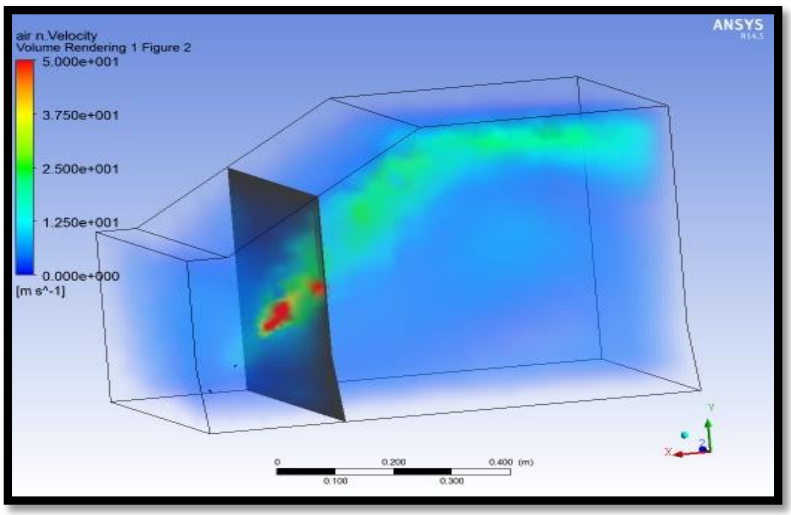

Fig. 3.47 : Velocity Distribution for Converging Length = 40 mm & Inlet Dia. = 6 mm

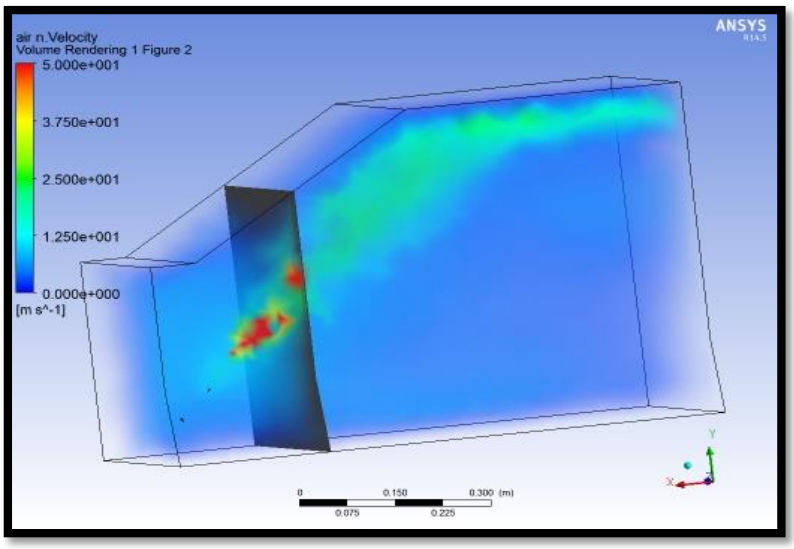

Fig. 3.48 : Velocity Distribution for Converging Length = 40 mm & Inlet Dia. = 6 mm

3.5.9 Varying the converging length of the nozzle for inlet Diameter of 7 mm:

Table 3.9 : Varying the converging length for inlet diameter of 7 mm

Experiment No.	Throat Length (mm)	Converging Section Length(mm)	Inlet Diameter(mm)	Outlet Diameter(mm)	Impinging Angle (degree)	Figure No.
4.	30	50	7	1	0	3.49

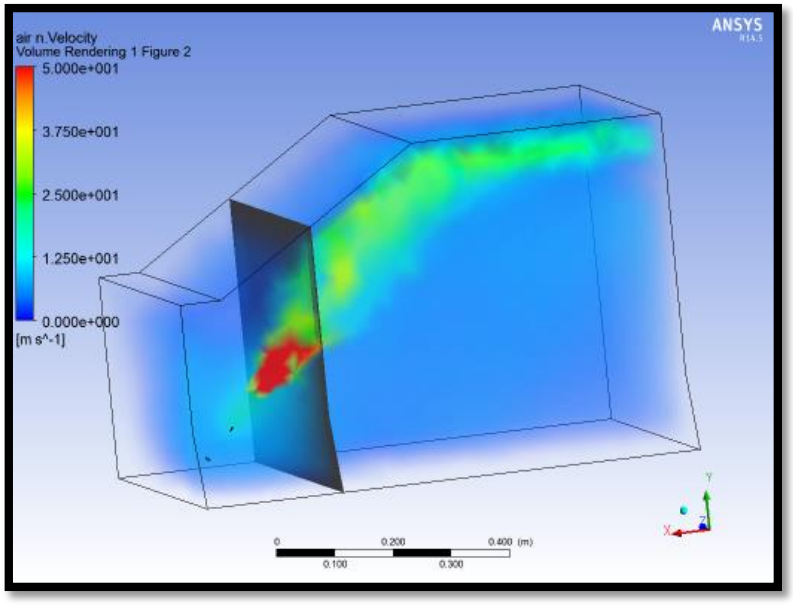

Fig. 3.49 : Velocity Distribution for Converging Length = 50 mm & Inlet Dia. = 7 mm

3.5.10 Varying the converging length of the nozzle for inlet Diameter of 8 mm:

Table 3.10 : Varying the converging length for inlet diameter of 8 mm

Experiment No.	Throat Length (mm)	Converging Section Length(mm)	Inlet Diameter(mm)	Outlet Diameter(mm)	Impinging Angle (degree)	Figure No.
4.	30	30	8	1	0	3.50

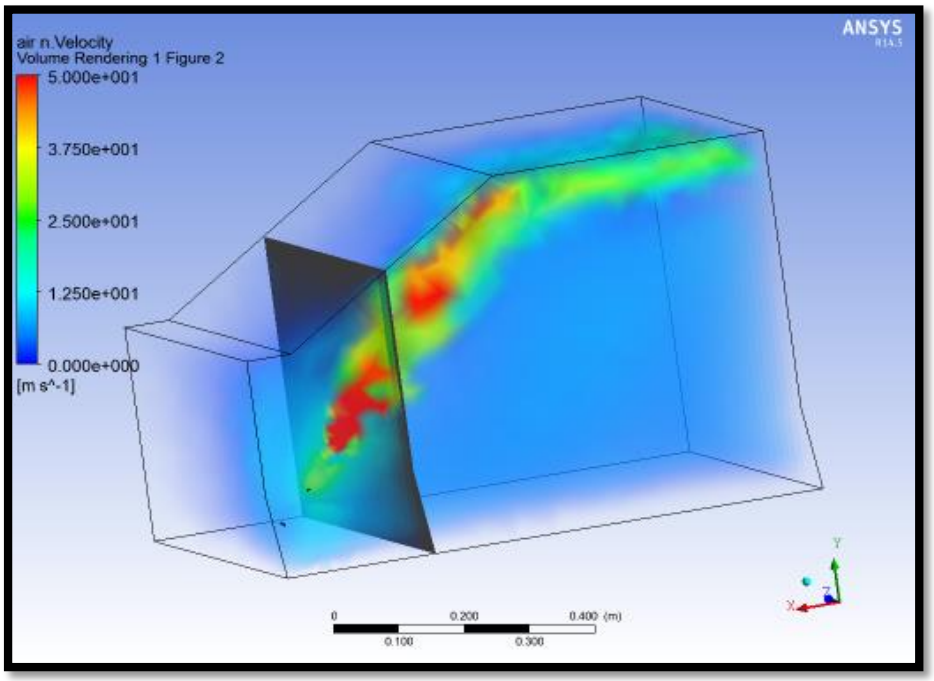

Fig. 3.50 : Velocity Distribution for Converging Length = 30 mm & Inlet Dia. = 8 mm

3.5.11 Varying the converging length of the nozzle for inlet Diameter of 9 mm:

Table 3.11 : Varying the converging length for inlet diameter of 9 mm

Experiment No.	Throat Length (mm)	Converging Section Length(mm)	Inlet Diameter(mm)	Outlet Diameter(mm)	Impinging Angle (degree)	Figure No.
1.	30	30	9	1	0	3.51
2.	30	40	9	1	0	3.52
3.	30	50	9	1	0	3.53

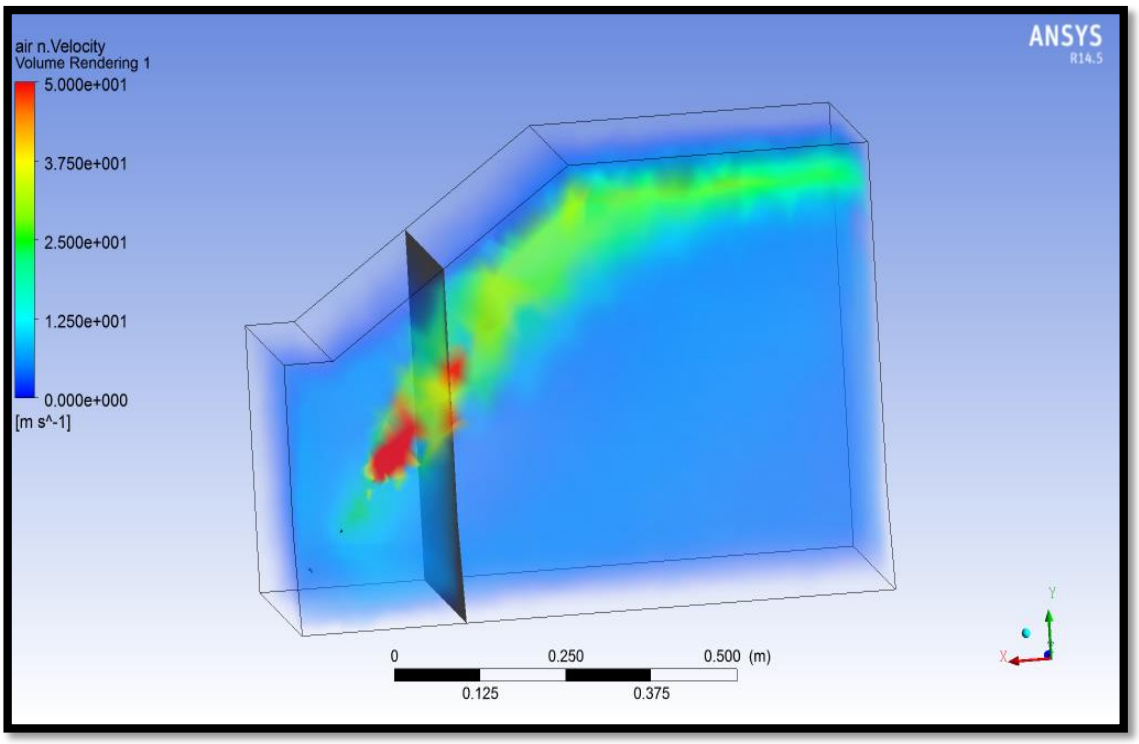

Fig. 3.51 : Velocity Distribution for Converging Length = 30 mm & Inlet Dia. = 9 mm

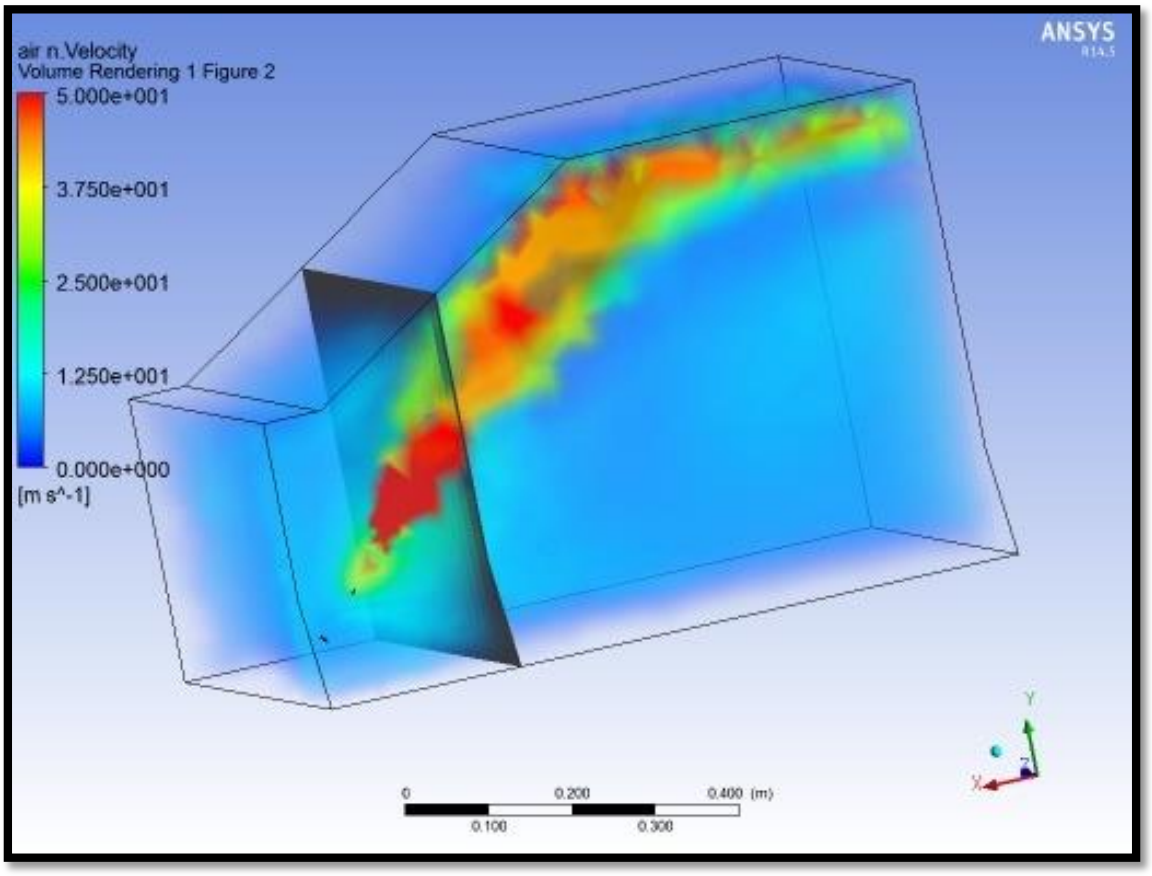

Fig. 3.52 : Velocity Distribution for Converging Length = 40 mm & Inlet Dia. = 9 mm

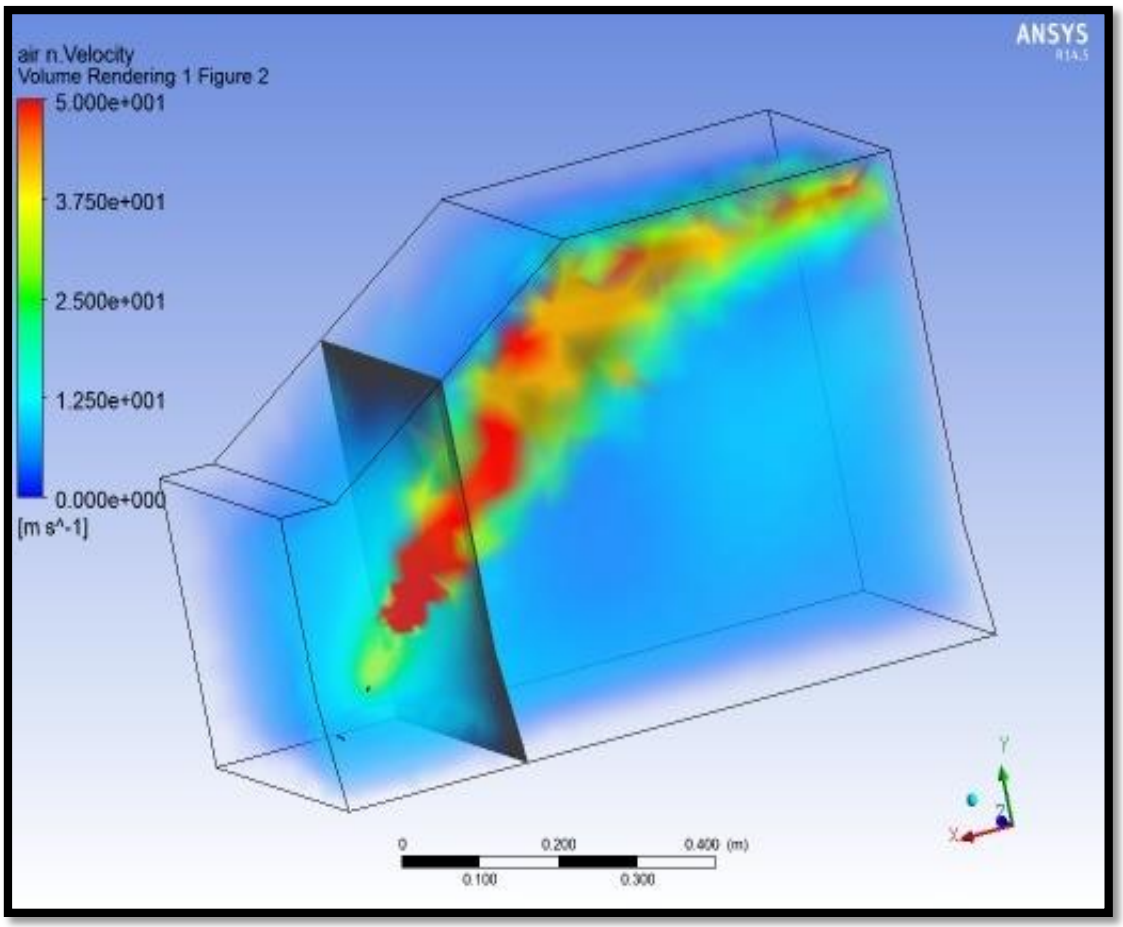

Fig. 3.53 : Velocity Distribution for Converging Length = 50 mm & Inlet Dia. = 9 mm

Analysing the above results it is clear that nozzle with the parameters shown below is the optimised nozzle:

Table 3.12 : Nozzle with optimised parameters

Throat Length (mm)	Converging Section Length(mm)	Inlet Diameter(mm)	Outlet Diameter(mm)	Impinging Angle (degree)
30	40	9	1	0

3.6 Velocity Distribution of Two Nozzles

The experimental set up for the two nozzles used is shown in figure below

Fig. 3.54 : Set up for two Nozzles

The figure above represents the arrangement of two nozzles for the experimental work.

Here the nozzles are mounted on the apparatus in such a way that their impinging angle can be changed by just tilting the set up. The axis of both the nozzles is at an angle to each other which is set to 30° as in the software. This is set in such a way to clear the maximum surface of the window glass to have a clear vision of the rear view mirror. Figure below makes it clearer.

Fig. 3.55 : Clear view of Angle between the Nozzles

For the velocity distribution fixed parameters of the nozzle are:

Table 3.13 : Nozzle Description

Experiment No.	Throat Length (mm)	Converging Section Length(mm)	Inlet Diameter(mm)	Outlet Diameter(mm)	Impinging Angle (degree)	Figure No.
1.	30	40	9	1	0	3.47

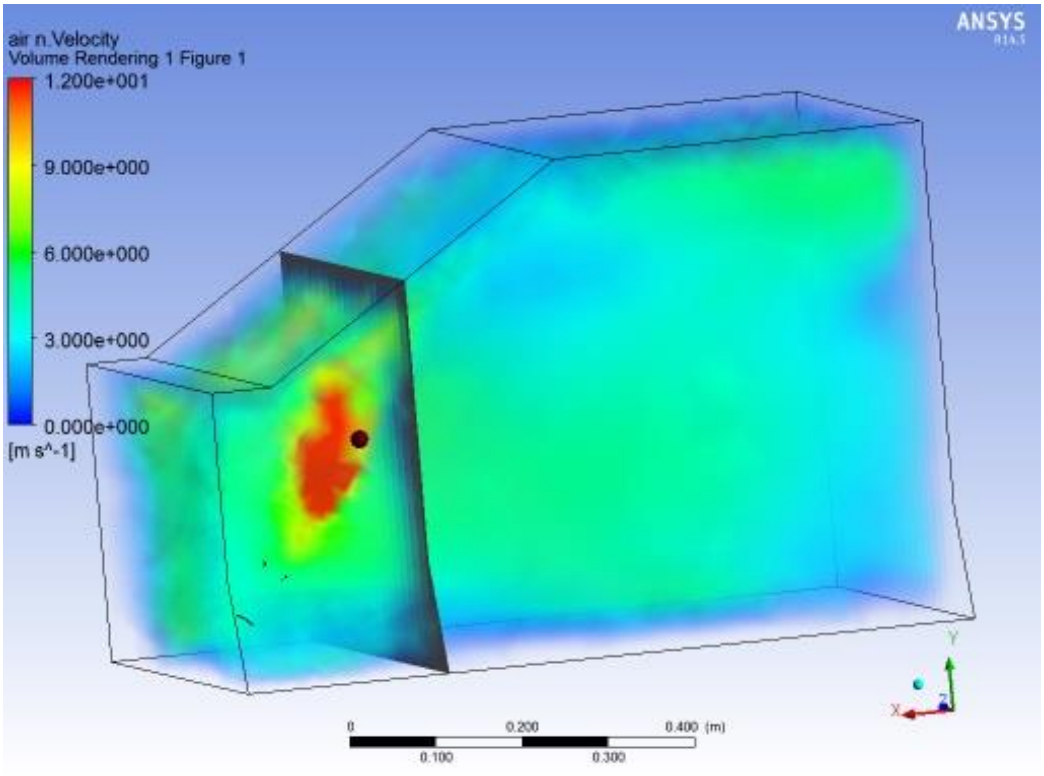

Fig. 3.56 : Velocity Distribution for two nozzles

In all the velocity distributions shown above the main region of concern is the red portion which represents the amount of air released from the nozzle. The more it spreads, the more effective is the nozzle and clears off the more area of the side window glass to make the visibility possible of the side view mirror to avoid accidents.

Chapter 4 Experimentation

This following section gives the details of different apparatus used for the experimentation of the present work.

4.1 Nozzle

Nozzle of following parameter was made final from the Velocity Distribution done in the previous chapter.

Table 4.1 : Optimised nozzle parameters

Experiment No.	Throat Length (mm)	Converging Section Length(mm)	Inlet Diameter(mm)	Outlet Diameter(mm)	Impinging Angle (degree)
1.	30	40	9	1	0

For the experimental work the nozzle with above parameters was manufactured with the help of rapid prototyping.

Rapid Prototyping

Rapid Prototyping (RP) can be defined as a group of techniques used to quickly fabricate a scale model of a part or assembly using three-dimensional computer aided design (CAD) data. Rapid Prototyping has also been referred to as solid free-form manufacturing; computer automated manufacturing, and layered manufacturing.

Methodology for Rapid Prototyping

The basic methodology for all current rapid prototyping techniques can be summarized as follows:

1. A CAD model is constructed, and then converted to STL format. The resolution can be set to minimize stair stepping.
2. The RP machine processes the STL file by creating sliced layers of the model.

3. The first layer of the physical model is created. The model is then lowered by the thickness of the next layer, and the process is repeated until completion of the model.
4. The model and any supports are removed. The surface of the model is then finished and cleaned.

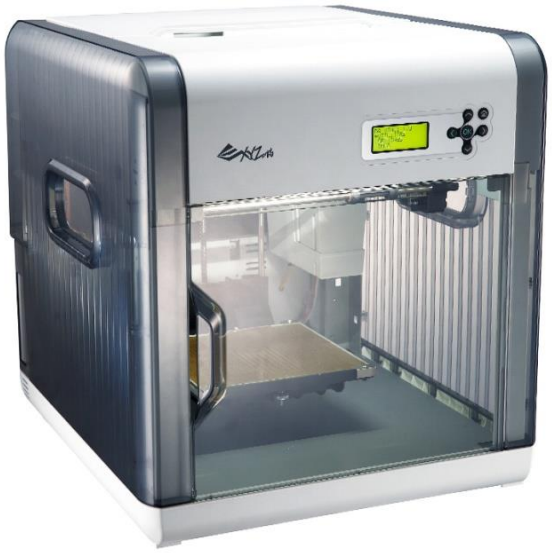

Fig. 4.1 **:** 3D Printer

4.2 Experimental Set up

Following set up was made for the testing:

Fig. 4.2 : Apparatus for Testing Mounted with Two Nozzles

Compressed air is used to remove the water droplets from the window glass

Compressed Air

The usage of compressed air is not limited only to industries, but they are also used in manufacturing, welding, constructions, power plants, ships, automobile plants, painting shops, and for filling breathing apparatus too. Thus there are so many types of air compressors used specifically for the above purposes.

An air compressor is a device that converts power (usually from an electric motor, a diesel engine or a gasoline engine) into kinetic energy by compressing and pressurizing air, which, on command, can be released in quick bursts.

Side Window Glass

Side glasses of an automobile are generally made up of tempered glass. The tempered glass has a property of not breaking into the sharp edges. Thus, it provides safety to the vehicle occupant if any accident occurs. The toughened glass is made by treating annealed glass with a thermal tempering process. A sheet of annealed glass is heated above 600° C i.e., above its annealing point, then its surfaces is rapidly cooled leaving the inner core hot. The different cooling rates between the surface and the core of the glass produce different physical properties, resulting in compressive stresses on the surface which is balanced by tensile stresses produced in the core of the glass.

Fig. 4.3 : Rear view From Side Mirror

Contribution of Thesis

The contribution of thesis is as follows:

- To model the nozzle of different parameters for the analyses purpose in Fluent.
- To analyse the effect of air through the nozzle on the side window glass in Fluent
- To compare the results obtained above and pick the best nozzle for the experimentation.
- To manufacture the nozzle for performing the experiment to check the efficiency of the analysed nozzle.
- To develop a set up made of wood on which a side window is mounted and this set up replicates the side window glass of a vehicle.
- To perform experiment on this set up by setting an arrangement at the corner of this set up to mount the nozzle for impinging an air jet.
- To measure the velocity of impinged air at different locations.
- To check whether required region is cleaned by the nozzle.

Experimental Set up

Fig. 4.4 : Experimental set up for testing the phenomenon of droplet cleaning mounted with single nozzle

Fig. 4.5 : Close View of Single Nozzle Set up

Here the window glass of Hyundai Santro is being used for the testing. The air for removing the water droplets from the surface of the window glass is supplied from the air compressor through the vent pipes. The air is being supplied with the velocity of 16m/s to remove the water droplets.

The settings for changing the angle of the nozzle can be done by twisting the arrangement fixed at the bottom right corner of the apparatus. The amount of the air supplied to the nozzle can be varied with the help of the valve provided in the air compressor. When the amount of air required at the nozzle is more, the valve can be opened to fulfil the demand of air and when the amount of air required at the nozzle is less, the valve can be closed to control the amount of air.

The velocity of air at the inlet and outlet of the air can be measured with the help of anemometer. Anemometer is the device used to measure the velocity of air. Hence the air at the desired velocity can be supplied to the nozzle for removing the water droplets from the surface of the window glass. In this way at different velocities the testing can be done for getting the iterations. Figure below depicts the anemometer used for the experimental work.

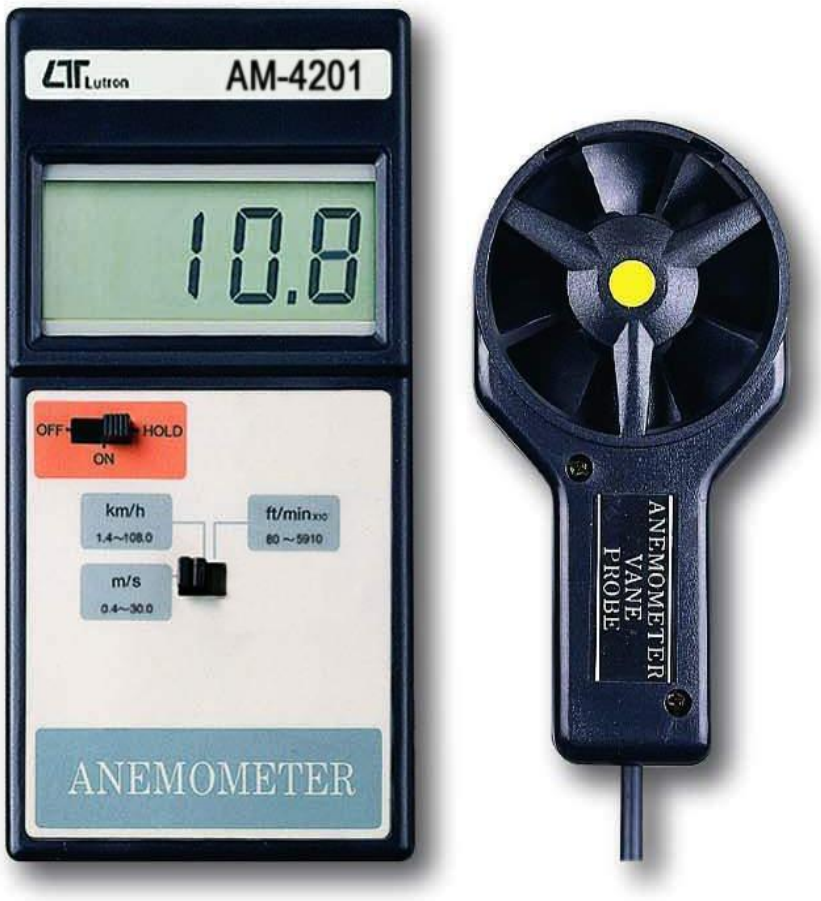

Fig. 4.6 : Anemometer

Anemometer can measure the velocity in m/s, km/h, ft/ min.

4.3 Experiments with single nozzle

While performing the experiments with single nozzle at different speeds and different angles following results were performed:

4.3.1 At an angle of 27^0

Table 4.2 : Data for Single Nozzle at 27^0 & outlet air velocity = 30 m/s

Speed (m/s)	Angle (degree)	Area Cleaned (mm^2)	Figure
30	27	190	4.7

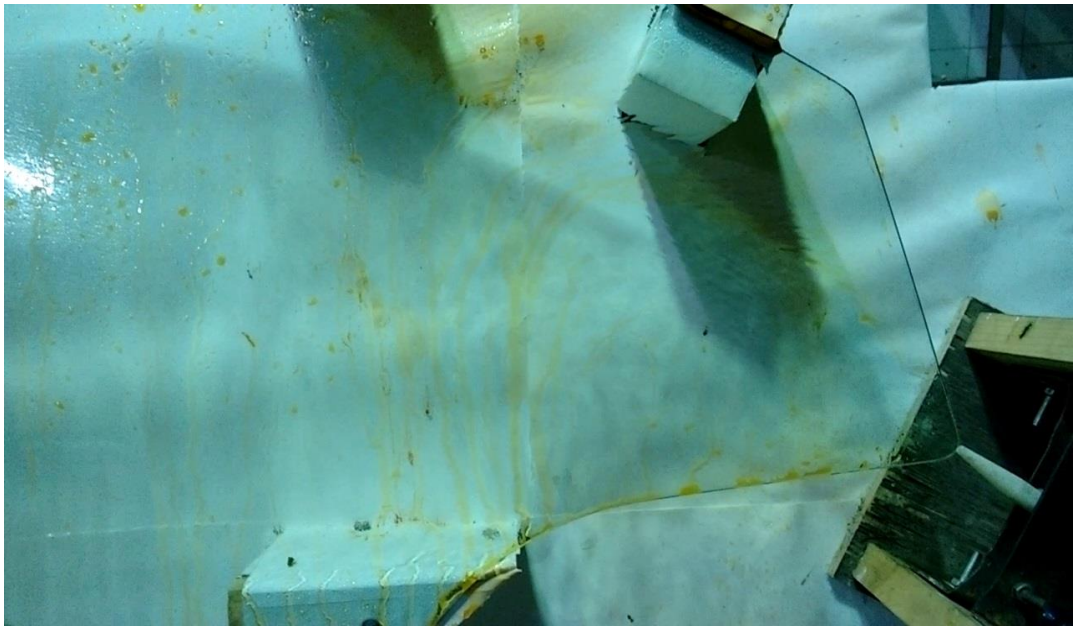

Fig. 4.7 : Area Cleaned 138 mm^2 at outlet air velocity = 30 m/s with Inlet Diameter=1 mm, Outlet Diameter=9 mm, Throat Length=30 mm, Converging Length=40 mm & Impinging Angle=0^0

Table 4.3 : Data for Single Nozzle at 27^0 & outlet air velocity = 35 m/s

Speed (m/s)	Angle (degree)	Area Cleaned (mm^2)	Figure
35	27	178	4.8

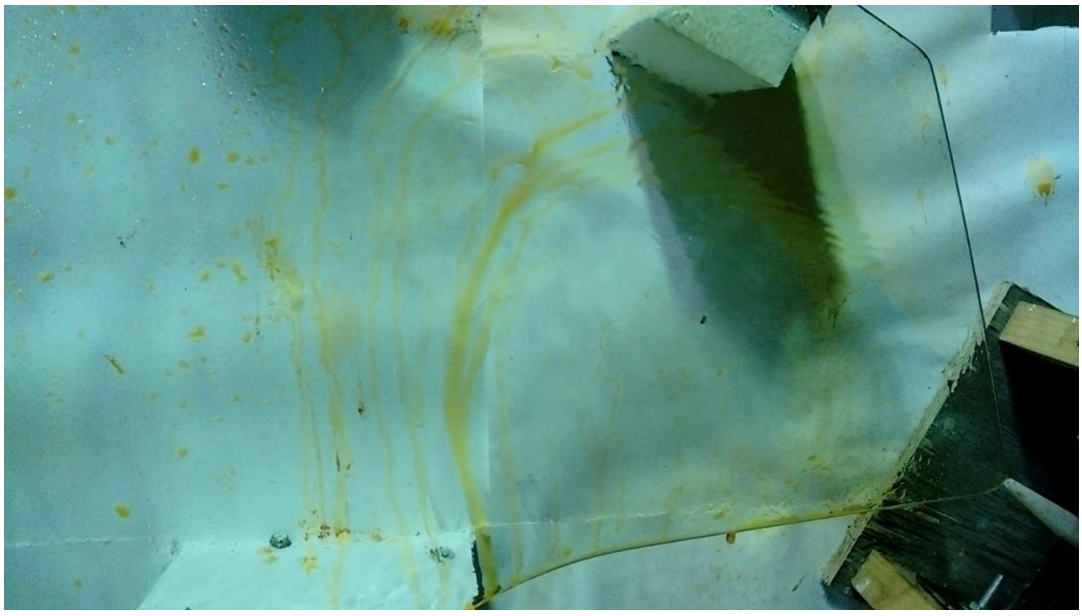

Fig. 4.8 : Area Cleaned 178 mm^2 at outlet air velocity = 35 m/s with Inlet Diameter=1 mm, Outlet Diameter=9 mm, Throat Length=30 mm, Converging Length=40 mm & Impinging Angle=0^0

Table 4.4 : Data for Single Nozzle at 27^0 & outlet air velocity = 40 m/s

Speed (m/s)	Angle (degree)	Area Cleaned (mm^2)	Figure
40	27	258	4.9

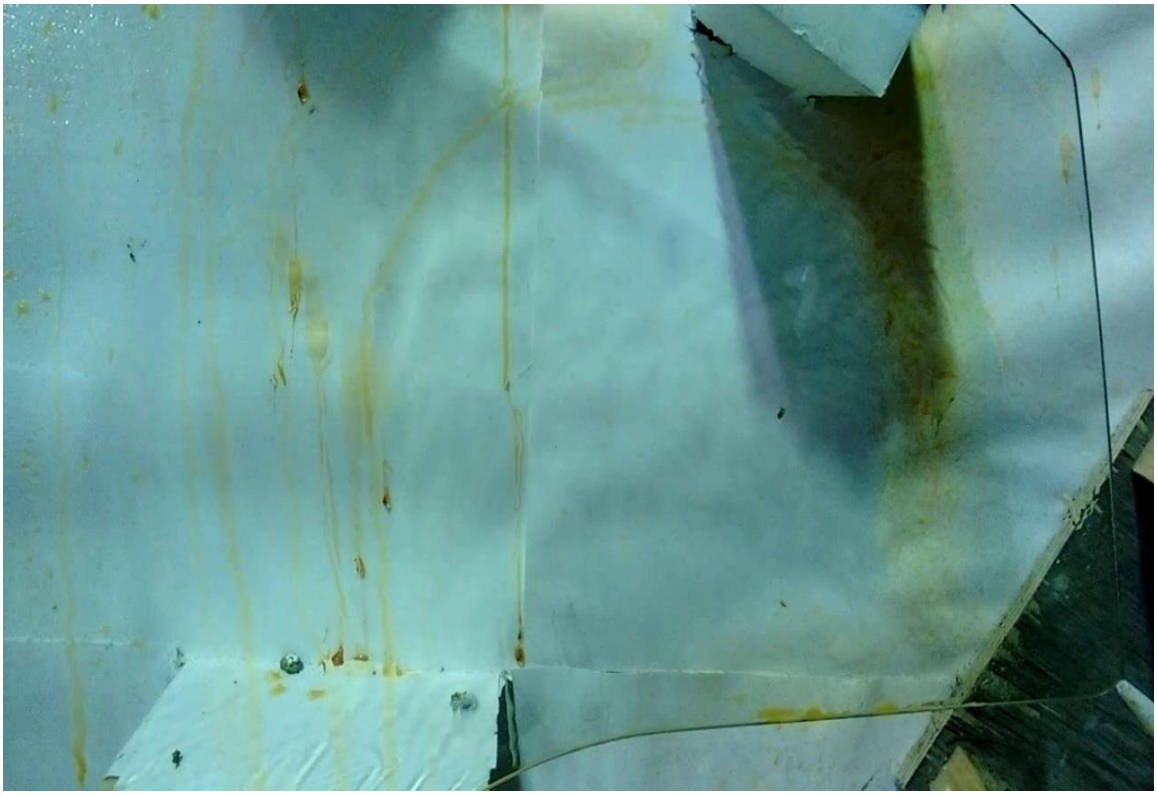

Fig. 4.9 : Area Cleaned 258 mm^2 at outlet air velocity = 40 m/s with Inlet Diameter=mm, Outlet Diameter=9 mm, Throat Length=30 mm, Converging Length=40 mm & Impinging Angle=0^0

4.3.2 At an angle of 21^0

Table 4.5 : Data for Single Nozzle at 21^0 & outlet air velocity = 30 m/s

Speed (m/s)	Angle (degree)	Area Cleaned (mm^2)	Figure
30	21	190	4.10

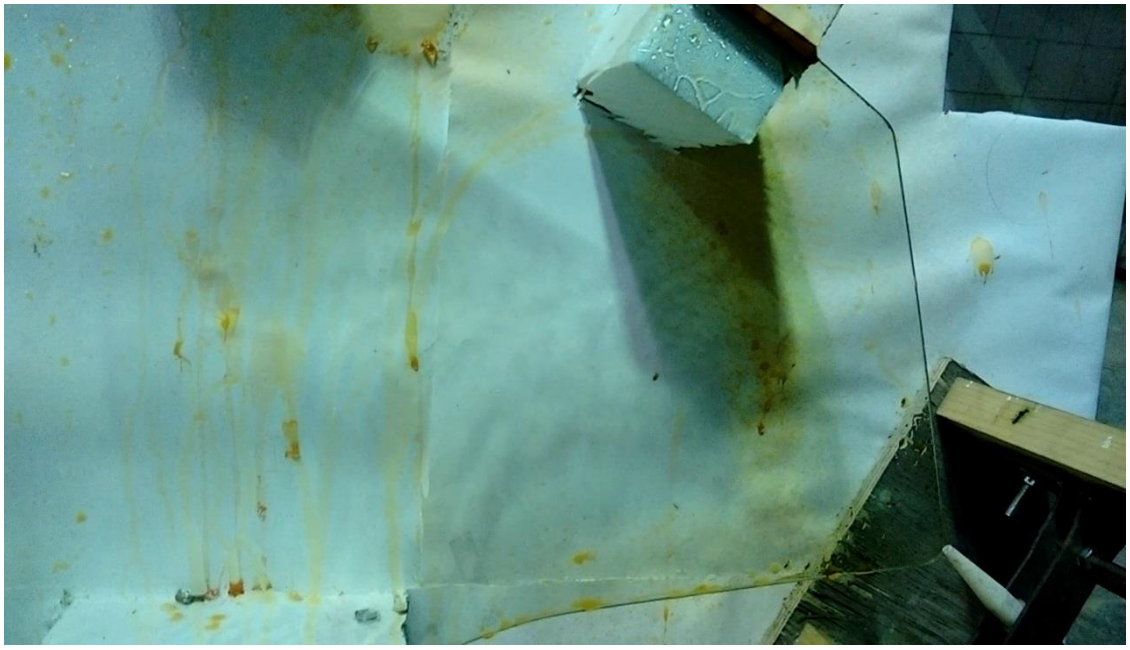

Fig. 4.10 : Area Cleaned 190 mm^2 at outlet air velocity = 30 m/s with Inlet Diameter=1 mm, Outlet Diameter=9 mm, Throat Length=30 mm, Converging Length=40 mm & Impinging Angle=0^0

Table 4.6 : Data for Single Nozzle at 21^0 outlet air velocity = 35 m/s

Speed (m/s)	Angle (degree)	Area Cleaned (mm^2)	Figure
35	21	198	4.11

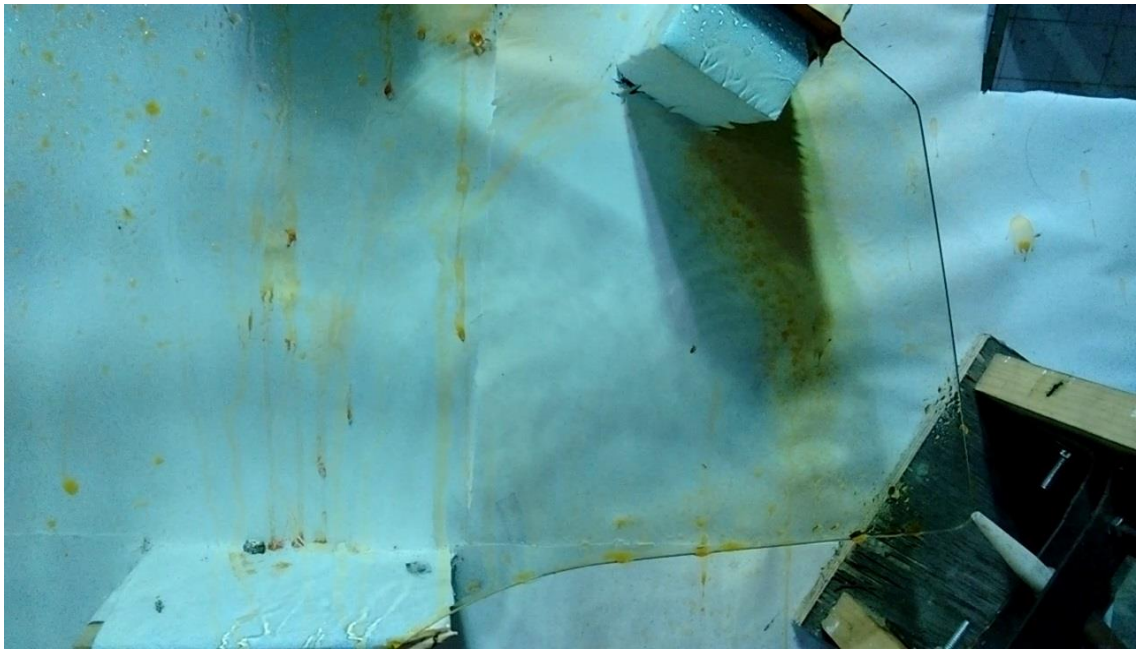

Fig. 4.11 : Area Cleaned 198 mm^2 at outlet air velocity = 35 m/s with Inlet Diameter=1 mm, Outlet Diameter=9 mm, Throat Length=30 mm, Converging Length=40 mm & Impinging Angle=0^0

Table 4.7 : Data for Single Nozzle at 21^0 & outlet air velocity = 40 m/s

Speed (m/s)	Angle (degree)	Area Cleaned (mm^2)	Figure
40	21	228	4.12

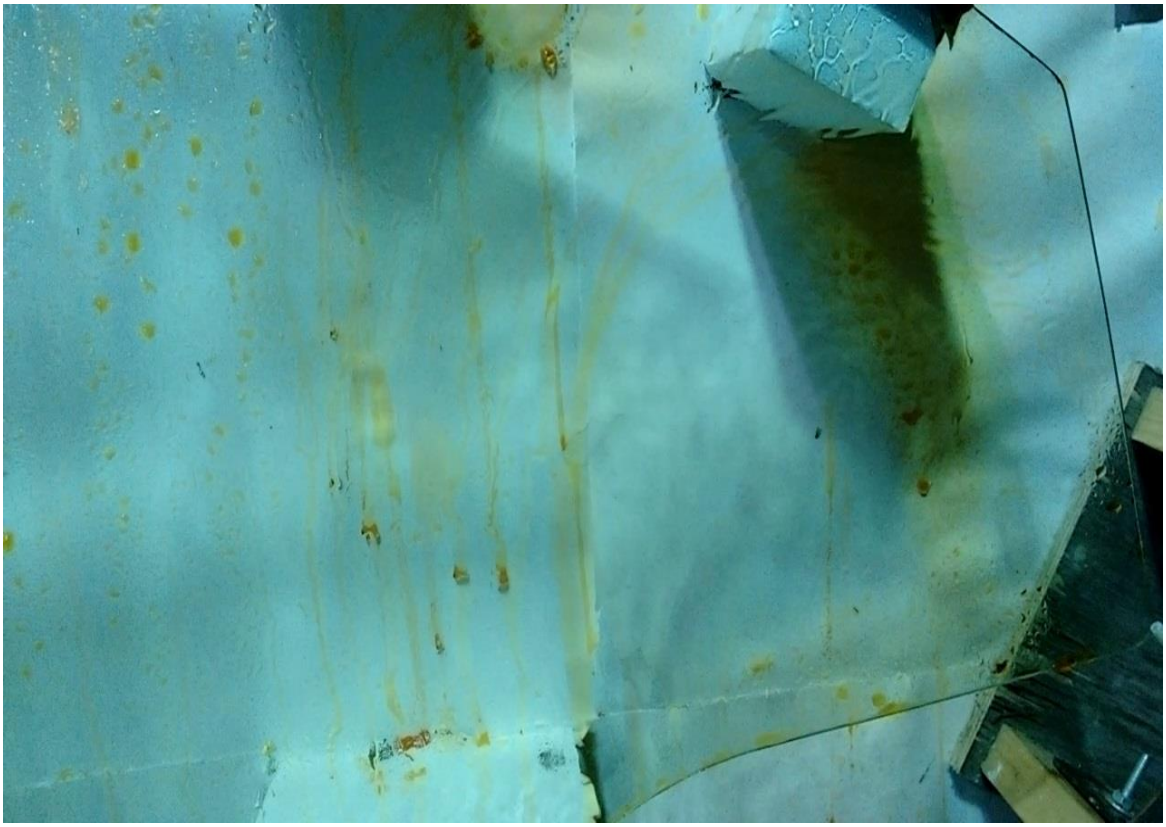

Fig. 4.12 : Area Cleaned 228 mm^2 at outlet air velocity = 40 m/s with Inlet Diameter=1 mm, Outlet Diameter=9 mm, Throat Length=30 mm, Converging Length=40 mm & Impinging Angle=0^0

4.3.3 At an angle of 48^0

Table 4.8 : Data for Single Nozzle at 48^0 outlet air velocity = 30 m/s

Speed (m/s)	Angle (degree)	Area Cleaned (mm^2)	Figure
30	48	158	4.13

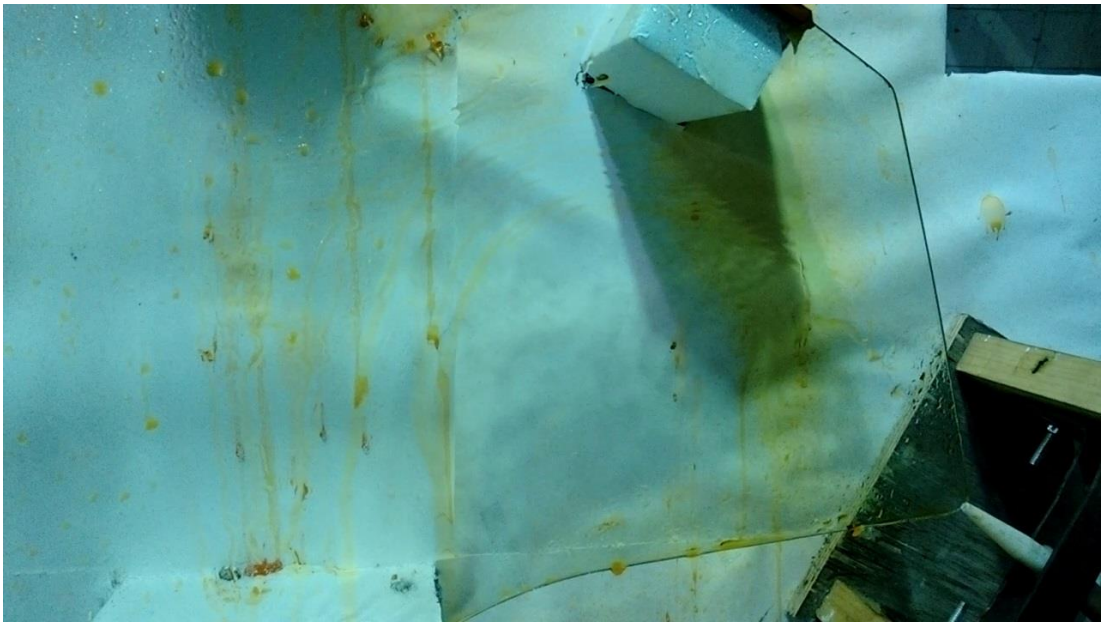

Fig. 4.13 : Area Cleaned 158 mm^2 at outlet air velocity = 30 m/s with Inlet Diameter=1 mm, Outlet Diameter=9 mm, Throat Length=30 mm, Converging Length=40 mm & Impinging Angle=0^0

Table 4.9 : Data for Single Nozzle at 48^0 & outlet air velocity = 35 m/s

Speed (m/s)	Angle (degree)	Area Cleaned (mm^2)	Figure
35	48	254	4.14

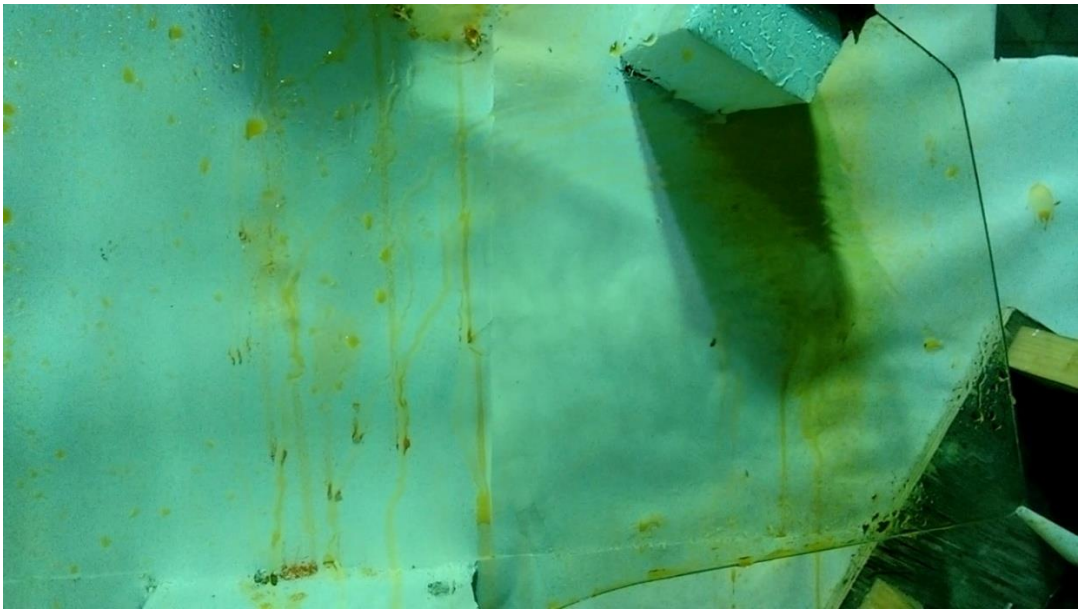

Fig. 4.14 : Area Cleaned 254 mm^2 at outlet air velocity = 35 m/s with Inlet Diameter=1 mm, Outlet Diameter=9 mm, Throat Length=30 mm, Converging Length=40 mm & Impinging Angle=0^0

Table 4.10 : Data for Single Nozzle at 48^0 & outlet air velocity = 40 m/s

Speed (m/s)	Angle (degree)	Area Cleaned (mm^2)	Figure
40	48	272	4.15

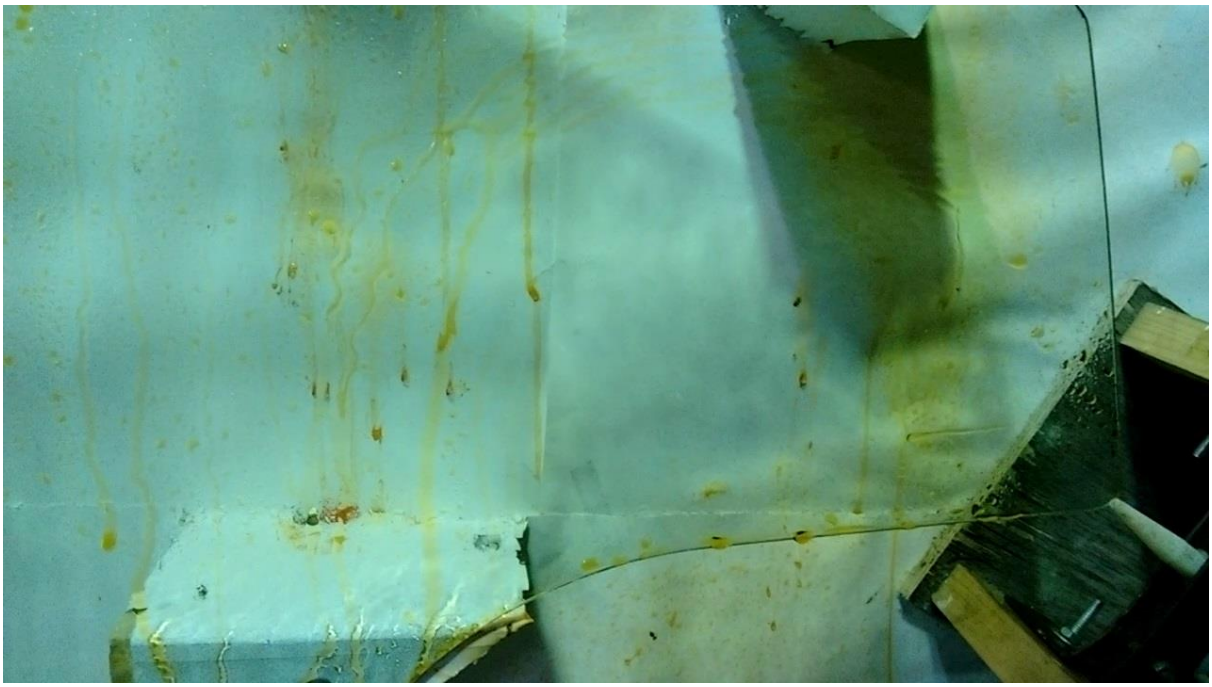

Fig. 4.15 : Area Cleaned 272 mm^2 at outlet air velocity = 40 m/s with Inlet Diameter=1 mm, Outlet Diameter=9 mm, Throat Length=30 mm, Converging Length=40 mm & Impinging Angle=0^0

4.4 Experiments with double nozzle

While performing the experiments with double nozzle at different speeds following results were performed:

4.4.1 Two Parallel Nozzles

Table 4.11 : Data for Two Parallel Nozzles at outlet air velocity = 30 m/s

Speed (m/s)	Area Cleaned (mm^2)	Figure
30	218	4.16

Fig. 4.16 : Area Cleaned 218 mm^2 at outlet air velocity = 30 m/s with Inlet Diameter=1 mm, Outlet Diameter=9 mm, Throat Length=30 mm, Converging Length=40 mm & Impinging Angle=0^0

Table 4.12 : Data for Two Parallel Nozzles at outlet air velocity = 35 m/s

Speed (m/s)	Area Cleaned (mm^2)	Figure
35	292	4.17

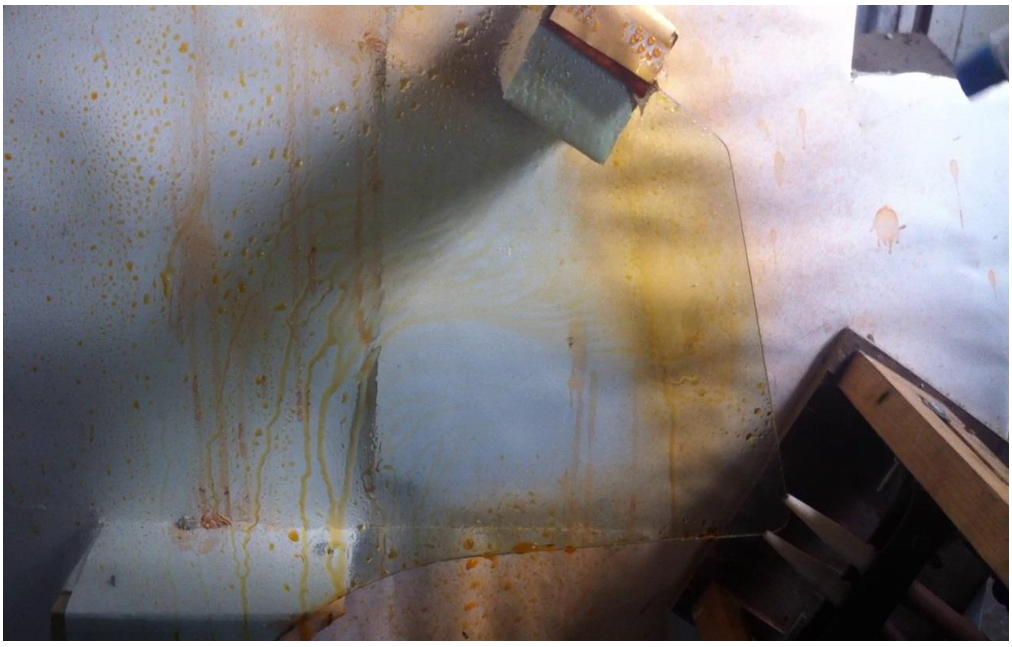

Fig. 4.17 : Area Cleaned 292 mm^2 at outlet air velocity = 35 m/s with Inlet Diameter=1 mm, Outlet Diameter=9 mm, Throat Length=30 mm, Converging Length=40 mm & Impinging Angle=0^0

Table 4.13 : Data for Two Parallel Nozzles at outlet air velocity = 40 m/s

Speed (m/s)	Area Cleaned (mm^2)	Figure
40	370	4.18

Fig. 4.18 : Area Cleaned 370 mm^2 at outlet air velocity = 40 m/s with Inlet Diameter=1 mm, Outlet Diameter=9 mm, Throat Length=30 mm, Converging Length=40 mm & Impinging Angle=0^0

4.4.2 Two Diverging Nozzles

While performing the experiments with two diverging nozzles at different speeds following results were performed:

Table 4.14 : Data for Two Diverging Nozzles at outlet air velocity = 30m/s

Speed (m/s)	Area Cleaned (mm^2)	Figure
30	100	4.19

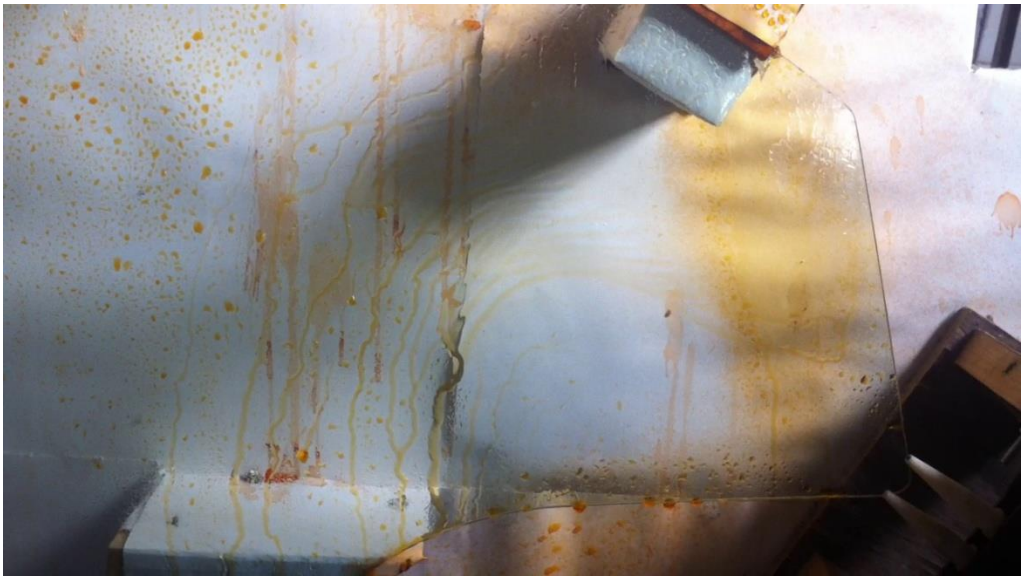

Fig. 4.19 : Area Cleaned 100 mm^2 at outlet air velocity = 30 m/s with Inlet Diameter=1 mm, Outlet Diameter=9 mm, Throat Length=30 mm, Converging Length=40 mm & Impinging Angle=0^0

Table 4.15 : Data for Two Diverging Nozzles at outlet air velocity = 35 m/s

Speed (m/s)	Area Cleaned (mm^2)	Figure
35	158	4.20

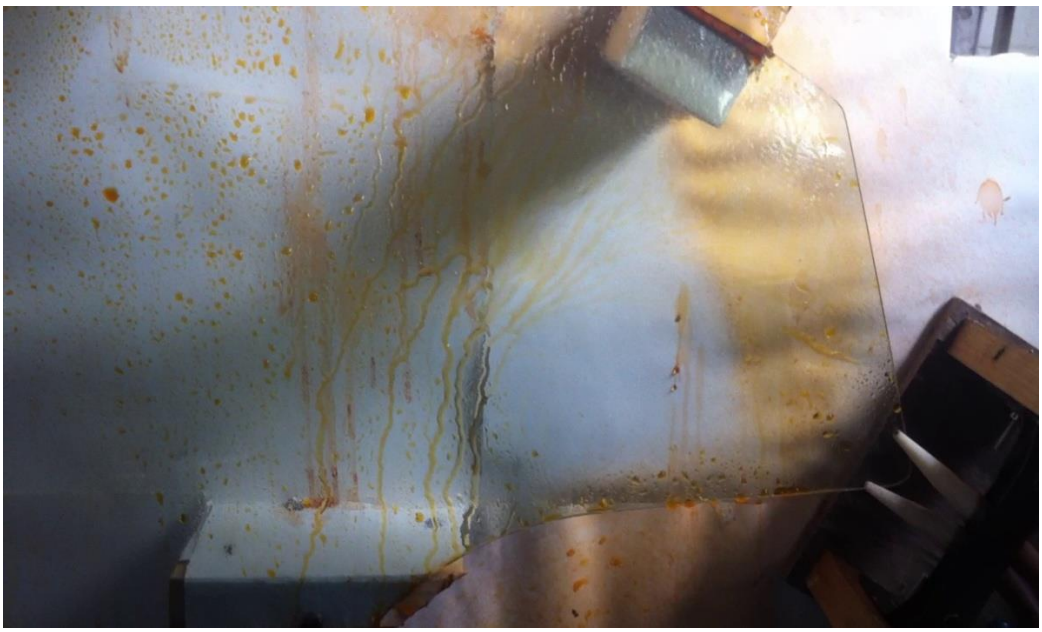

Fig. 4.20 : Area Cleaned 158 mm^2 at outlet air velocity = 35 m/s with Inlet Diameter=1 mm, Outlet Diameter=9 mm, Throat Length=30 mm, Converging Length=40 mm & Impinging Angle=0^0

Table 4.16 : Data for Two Diverging Nozzles at outlet air velocity = 40 m/s

Speed (m/s)	Area Cleaned (mm^2)	Figure
40	204	4.21

Fig. 4.21 : Area Cleaned 204 mm^2 at outlet air velocity = 40 m/s with Inlet Diameter=1 mm, Outlet Diameter=9 mm, Throat Length=30 mm, Converging Length=40 mm & Impinging Angle=0^0

4.4.3 Two Converging Nozzles

While performing the experiments with two converging nozzles at different speeds following results were performed:

Table 4.17 : Data for Two Converging Nozzles at outlet air velocity = 30 m/s

Speed (m/s)	Area Cleaned (mm^2)	Figure
30	146	4.22

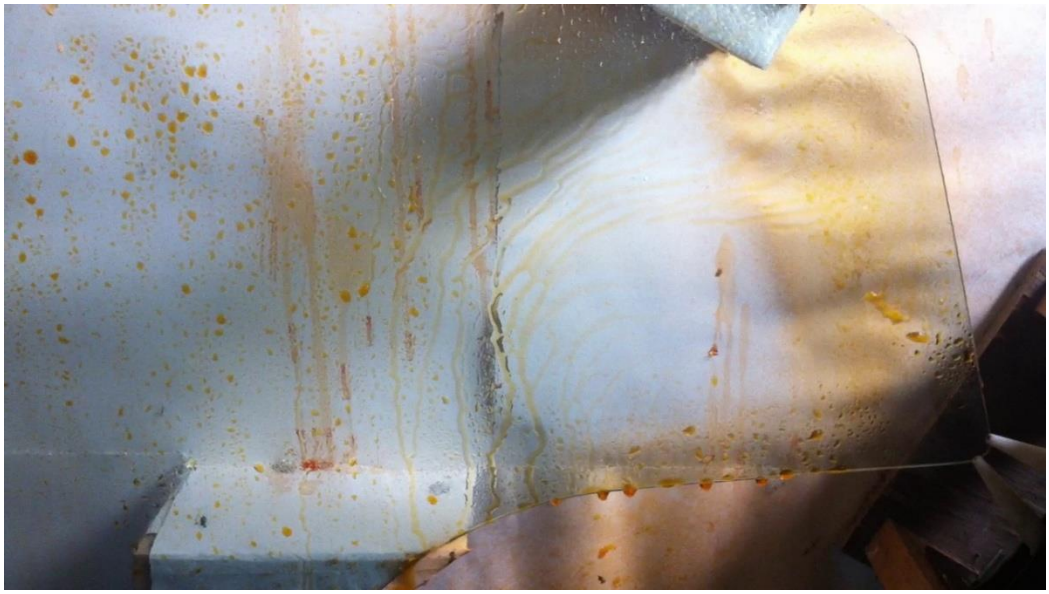

Fig. 4.22 : Area Cleaned 146 mm^2 at outlet air velocity = 30 m/s with Inlet Diameter=1 mm, Outlet Diameter=9 mm, Throat Length=30 mm, Converging Length=40 mm & Impinging Angle=0^0

Table 4.18 : Data for Two Converging Nozzles at outlet air velocity = 35 m/s

Speed (m/s)	Area Cleaned (mm^2)	Figure
35	186	4.23

Fig. 4.23 : Area Cleaned 186 mm^2 at outlet air velocity = 35 m/s with Inlet Diameter=1 mm, Outlet Diameter=9 mm, Throat Length=30 mm, Converging Length=40 mm & Impinging Angle=0^0

Table 4.19 : Data for Two Converging Nozzles at outlet air velocity = 40 m/s

Speed (m/s)	Area Cleaned (mm^2)	Figure
40	234	4.24

Fig. 4.24 : Area Cleaned 234 mm^2 at outlet air velocity = 40 m/s with Inlet Diameter=1 mm, Outlet Diameter=9 mm, Throat Length=30 mm, Converging Length=40 mm & Impinging Angle=0^0

5.1 Results of varying impinging angle for different outlet diameters

From the simulations performed for velocity distributions with different impinging angle and outlet diameter of the nozzle, the suitable impinging angle at which the nozzle must be mounted near the side window glass comes out to be 0^o. At this angle the air released from the nozzles gives us better velocity distribution over a large area and cover the maximum area which is an important objective of the work.

The velocity for droplet removal in each simulation was required as 16 m/s at a distance 170 mm from nozzle. The value of 16 m/s was obtained as an average value of five trials performed experimentally. It was obtained by performing the experiment with set up arranged for testing the nozzle. While performing the experiment it was observed that to clean the required region to view the rear view mirror from the side window glass during rain, minimum velocity required at the inlet of the nozzle is 17 m/s. Against this value, the velocity obtained at the outlet of the nozzle was 30 m/s. To have a proper view of the rear view mirror from the side window glass minimum area to be cleared was about 170 mm from the corner of the side window glass. With the velocity of 17 m/s at the inlet of the nozzle, the velocity of 16 m/s can be obtained at the plane of 170 mm from the corner of the side window glass. This is how the velocity was obtained.

Various simulations were performed to achieve the required nozzle by varying the different parameters of the nozzle. Initially velocity distributions were performed by varying the impinging angle at different outlet diameters. Best simulated results were obtained when the impinging angle was kept as 0^0 and outlet diameter as 1mm because the maximum amount of air is released from the nozzle with these parameters and dispersed well in the required region. After that more simulations were performed by fixing the impinging angle to 0^0 and outer diameter to 1 mm. Now throat length was varied and simulations were performed. The required result was obtained when the throat length was kept as 30 mm. To obtain the desired converging length and inlet diameter, above obtained parameters were fixed and simulations were performed by varying the converging length and inlet diameter. The desired results were obtained when the converging length was fixed to 40 mm and inlet diameter as 9 mm.

5.2 Best Simulated Results for Single Nozzle

Among all the probable parameters, the best results in terms of maximum amount of air is released from the nozzle and dispersed well in the required region were obtained with the parameters given below

Impinging Angle = 0^0

Outlet Diameter = 1 mm

Throat length = 40 mm

Converging Section Length = 30 mm

Inlet Diameter = 9 mm

Air velocity at inlet of the nozzle = 17 m/s

Air velocity at outlet of the nozzle = 30 m/s

Area cleaned = 190 mm^2

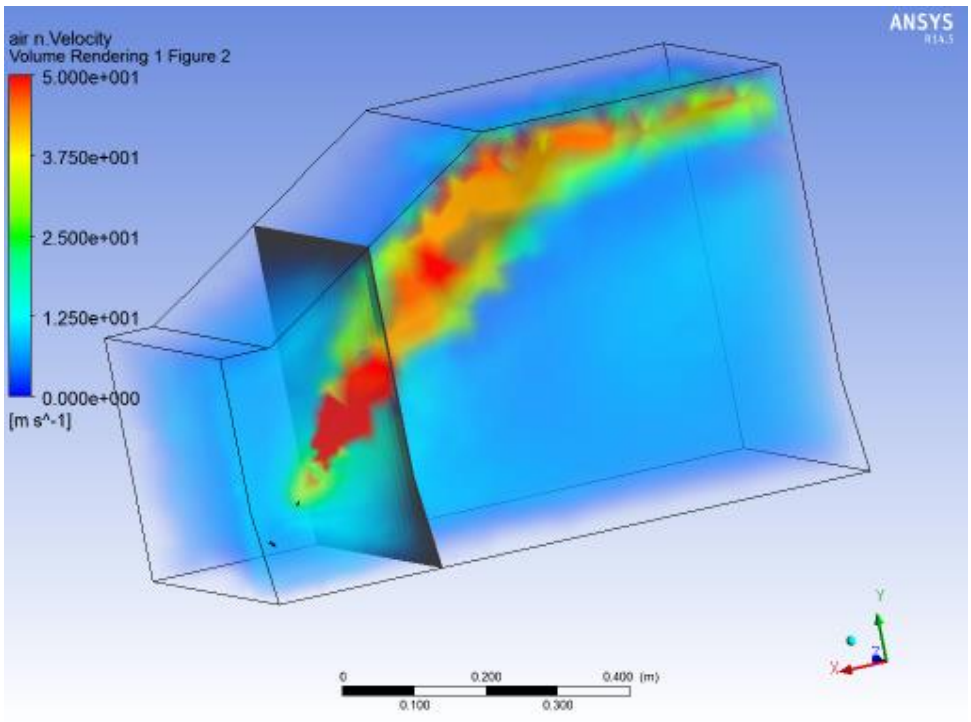

Fig. 5.1 : Best Simulated Result for Single Nozzle

In the Velocity Distribution shown above the main region of concern is the red portion which represents the amount of air released from the nozzle. The more it spreads, the more effective

is the nozzle and clears off the more area of the side window glass to make the visibility possible of the side view mirror to avoid accidents.

5.3 Best Simulated Results for Double Nozzle

Parameters of the nozzle are:

Throat Length = 30 mm

Converging Section Length = 40 mm

Inlet Diameter of the nozzle = 9 mm

Outlet Diameter of the nozzle = 1mm

Impinging angle = 0^{o}

Air velocity at inlet of the nozzle = 17 m/s

Air velocity at outlet of the nozzle = 30 m/s

Area cleaned = 218 mm^2

Using the nozzle with the above parameters the results of the Velocity Distribution done when two nozzles are mounted simultaneously is shown below:

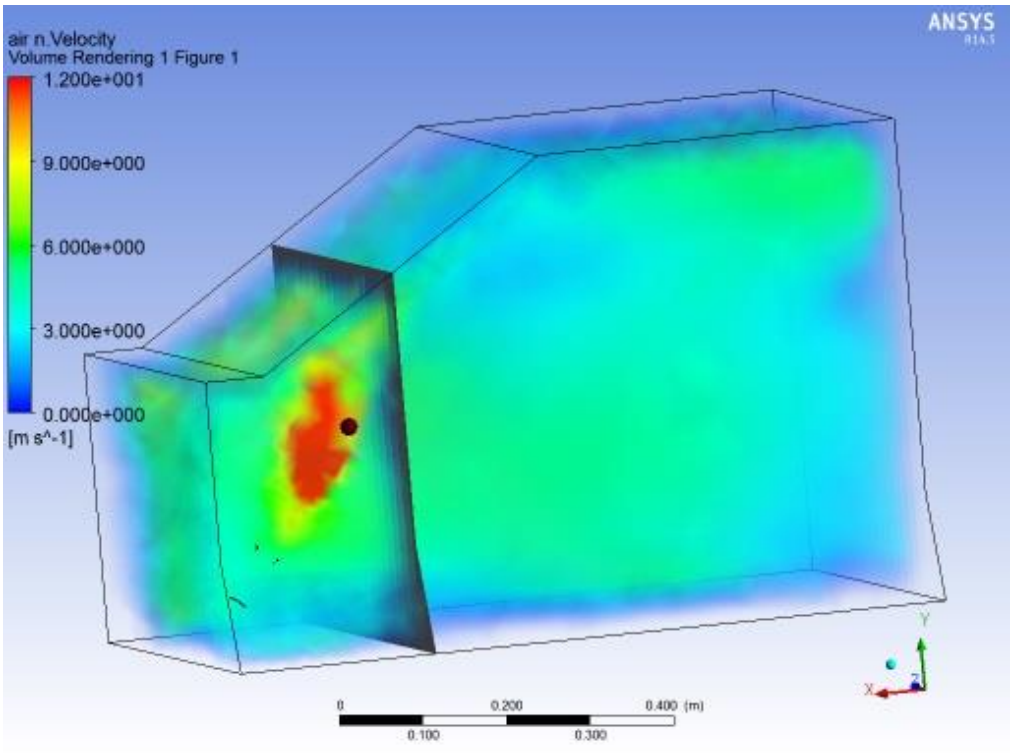

Fig. 5.2 : Best Simulated Result for two nozzles

5.4 Best Experimental Results for Single Nozzle

The best obtained result is as shown in figure below:

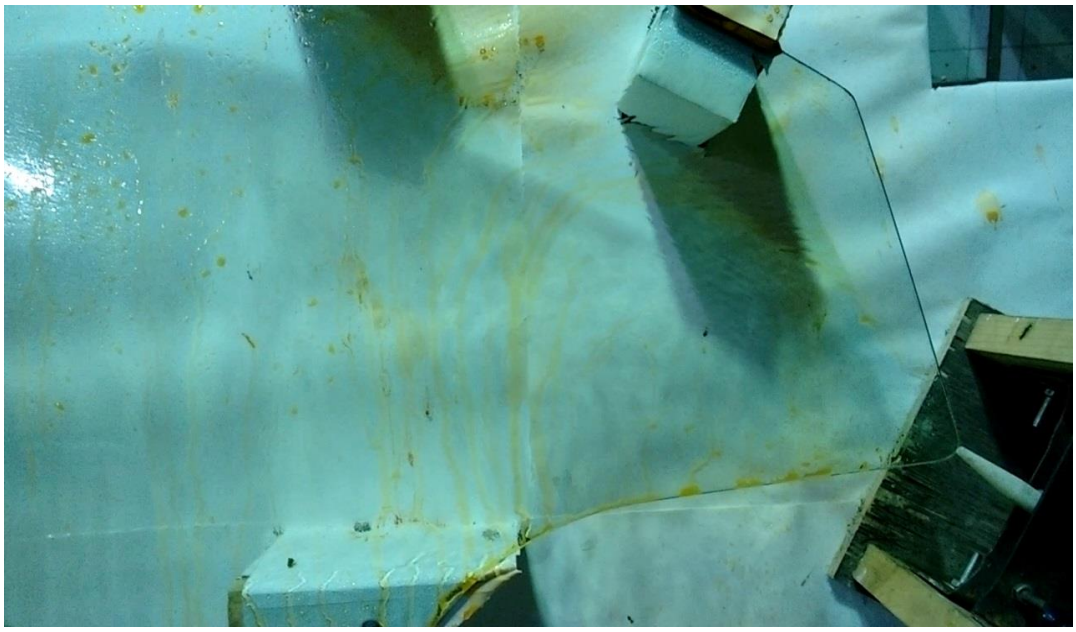

Fig. 5.3 : Best Experimental Result for Single Nozzle

Parameters of the nozzle used in the above experiment are:

Throat Length = 30 mm

Converging Section Length = 40 mm

Inlet Diameter of the nozzle = 9 mm

Outlet Diameter of the nozzle = 1mm

Impinging angle = 0^{o}

Air velocity at inlet of the nozzle = 17 m/s

Air velocity at outlet of the nozzle = 30 m/s

Area Cleaned = 190 mm^2

5.5 Best Experimental Results for Double Nozzle

The suitable results were obtained when both the nozzles are kept parallel to each other and other parameters are:

Throat Length = 30 mm

Converging Section Length = 40 mm

Inlet Diameter of the nozzle = 9 mm

Outlet Diameter of the nozzle = 1mm

Impinging angle = 0^{o}

Air velocity at inlet of the nozzle = 17 m/s

Air velocity at outlet of the nozzle = 30 m/s

Area Cleaned = 218 mm^2

Fig. 5.4 : Best Experimental Result for Double Nozzle

6.1 Conclusion

In present study, the nozzle at different impinging angles, different outlet diameters and inlet diameters, throat length and converging section length have been investigated with the help of a CFD solver- Fluent. The major focus of the study was to analyse the droplet cleaning action of air jet by varying different parameters and to evaluate the nozzle with the effective specifications, which can spread over the maximum possible area on the side window glass. Proposed system will help to overcome the short comings of the previous inventions. It provides an air jet clearing system for a vehicle which facilitates improved visibility through the windows and the external rear view mirrors of that vehicle in the different weather conditions (rain, snow and fog). According to the results obtained, the proposed system is capable of blowing compressed air onto the surface of the windows to be cleared. The main components of the system are small enough, which can fit inside the cavity provided for external mirror housing. They can be mounted universally as an add-on component onto a variety of existing vehicles having mirrors and windows of different designs and sizes.

Based on the experimental and simulated data, it has been observed that experimental results are in good agreement with the results obtained from the computer simulation. After comparing all the results and their experimental verification it is found that the best cleaning action with maximum coverage area using minimum inlet velocity is obtained with below mentioned parameters.

Nozzle Throat Length = 30 mm

Nozzle Converging Section Length = 40 mm

Inlet Diameter of the nozzle = 9 mm

Outlet Diameter of the nozzle = 1 mm

Impinging angle = 0^o

The area cleaned by single nozzle is 190 mm^2 and by two nozzles is 218 mm^2. Although the area cleaned by set up using two nozzles is more as compare to single nozzle. But quantity of air required to clean the desired area is nearly double than that of the volume of air required

for single nozzle. The area cleaned by double nozzles is not significantly high than the area cleaned by the single nozzle. Keeping in mind the physical set up required for the proposed work will be more bulky and need more space while using double nozzle. Hence single nozzle is preferred over double nozzle arrangement.

6.2 Future Scope

The present study is the preliminary investigation of the new concept for improving the visibility. The parameters of the nozzle can be optimised using different manufacturing material and improved methods of manufacturing to getting low friction nozzles. The proposed model can be used to produce a prototype using real car in production.

References

[1] Vandale A.J., Vandale M.E.,"Exterior side view mirror and window defogger system", Patent No. US 6267664 B1, 2001.

[2] Wang Mingyu, Urbank T. M. And Sangwan K. V.,**"**Clear vision automatic windshield defogging system", 2004.

[3] Urbank, T. M., Kelly, S. M., King, T. O. and Archibald, C. A., "Development and Application of an Integrated Dew Point Temperature Sensor", SAE Paper 2001-01-0585, Detroit, Michigan, 2001.

[4] Peters, A. R., "Interior Window Fogging- An Velocity Distribution of the Parameters Involved", SAE Paper 720503, Detroit, Michigan, 1972.

[5] Cole, J. and Passmore, M., "An Experimental Study of Automotive Glass Demisting", Proceedings of the 2nd MIRA Intl. Conf. On Vehicle Aerodynamics, Convertry, UK, pp. 1-9, October, 1998.

[6] Jefferson. J. B., Jr., Jefferson F., "Vehicle glass clearing system", Patent No. 6100500, 2000.

[7] Berzin Leonid, "Universal clearing air system for windows and external mirrors of the vehicle", Patent No. US 6290361 B1, 2001.

[8] Troy, Sharma Rajeev, MI,"A/C system side view mirror and side glass de-icer", Patent No. US 7798658 B2, 2001.

[9] Lee J. H., Oh S. H., Oh S. W.,Kim K. S. And Kim S. H.," An Effective Control of Auto Defog System to Keep Automobile Windshield Glass Clear", International Conference on Control, Automation and Systems 2010 (922-923).

[10] L. I. Davis, G. A. Dage and J. D. Hoeschele, "Conditions for Incipient Windshield Fogging and Anti-Fog Strategy for Automatic Climate Control," *SAE paper 2001-01-0583,* Detroit, Michigan, 2001.